Improving Load Shedding Schemes for Critical System Conditions

Optimising Frequency Defence for the Future Power System

MSc. Sustainable Energy Technology

Padraig Buckley

Delft University of Technology

TU Delft

Improving Load Shedding Schemes for Critical System Conditions

Optimising Frequency Defence for the Future Power System

by

Padraig Buckley

to obtain the degree of Master of Science
at the Delft University of Technology,
to be defended publicly on Wednesday August 23, 2023 at 11:00 AM.

Student number:	5623847	
Project duration:	December 8, 2022 – August 23, 2023	
Thesis committee:	Prof. M. Popov,	Professor TU Delft, Primary Supervisor
	Dr. Aleksandra Lekic	Assistant Professor TU, Delft
	Dr. M. Ghaffarian Niasar	Assistant Professor, TU Delft
	A. Boričić,	TU Delft / TenneT, Daily Supervisor

This thesis is confidential and cannot be made public until December 31, 2024.

Cover: Power lines sunset - Photo by Elena Shen, 2017
Style: TU Delft Report Style, with modifications by Daan Zwaneveld

TU Delft

Preface

It is difficult to condense two years' worth of experiences and learning into a few paragraphs but, as I write this now, my overwhelming emotions are ones of gratitude and contentment at having chosen to embark on this journey at TU Delft. I will be concluding this chapter of my life with very few regrets, a lot of new learnings and countless memories which I look back on fondly.

Coming to Delft and completing this masters in Sustainable Energy Technology has allowed me to gain a more comprehensive understanding of the challenges and solutions to the greatest trial facing humanity in this generation. I am grateful for the exposure to industry leading experts in all of the courses I followed during my time here and I am glad to have improved my skills in developing system integration strategies for renewable energy, both here and abroad. I look forward putting this newly gained knowledge to good use and making some positive impacts in the world of sustainable energy.

I would like to formally thank Reddyn for their support of this project throughout its duration and for giving me the opportunity to pursue such an engaging research topic. Successful completion of this thesis project, a collaboration between TU Delft and industrial partners, would not have been possible without the input of numerous mentors, supervisors and external experts. My most sincere thanks must go to my daily supervisor, Aleksandar Boričić for generously giving his time to have regular meetings, provide feedback and engage in fun discussions about directions we could go in the project, even when dealing with the transition to a new job position. I would sincerely like to thank the project team at Alliander for welcoming me to the group and in particular, Martijn Janssen and Timothy Plevier for their continued support and the positive environment they created during all of our interactions, it was a pleasure to work with you. Thank you also to Professor Marjan Popov, my primary supervisor who gave me the chance to complete this rewarding project and has been enthusiastic and supportive during all discussions.

The last two years has been filled with countless new experiences, both in the Netherlands and abroad, but these experiences would never have been the same without the incredible people I got to share them with. I can happily say that I have been lucky to meet some of the kindest, most intelligent, funniest and most supportive people during my time here and I will be closing the door on this chapter with more happy memories than I can possibly count. In this place I have felt encouraged to be entirely myself and there is no stronger sign of friendship to me than that, I will always feel their hand on my shoulder. I look back with a smile on the Saturday 6am train rides, fantasy novel debrief sessions and feel particularly satisfied that everyone now knows to split the G on their pint of Guinness.

Finally, I would like to thank my family and my friends back home for supporting me on this adventure and always welcoming me with open arms whenever I did manage to make it home or follow up on video calls. None of this would have been possible without them and I can't wait to share more experiences with you all in the future.

Padraig Buckley
Delft, August 2023

Summary

As the electricity sector transitions towards a low-carbon future, an increasing proportion of synchronous generation in the power system is replaced with inverter-based resources (IBRs). The result is a reduction in the available rotational inertia in the grid, depleting its ability to withstand and arrest frequency changes following disturbances. Consequently, disturbances such as a loss of generation or load have an increasingly larger impact on the system, resulting in higher frequency deviations and increased rate of change of frequency (ROCOF).

On two occasions in 2021, the Continental Europe Synchronous Area (CESA) experienced system splitting events caused by cascading trips of several transmission system elements. In both cases, system defence plans were activated in order to preserve the integrity of the overall system. The amount of disconnected load was limited on both occasions, however, should similar events occur in the future with even lower rotational inertia in the grid, the impact could be more severe. This raises the question of whether the existing defence measures are sufficient to maintain system integrity and stable system operation.

Currently in CESA, containment of system frequency excursions following a severe loss of generation is achieved through low-frequency demand disconnection (LFDD) at a frequency below 49Hz. Due to the reduction in traditional synchronous generation and system inertia, the frequency stability of the system is expected to deteriorate, leading to an elevated impact of major disturbances, a rising probability of forced disconnections at frequencies below 49 Hz, and the potential for cascading loss of generation and blackout events.

The objective of this research is to explore the potential impact of reduced system inertia and increased penetration of renewable generation on the performance of the traditional LFDD scheme. In conjunction, additional proactive measures are proposed and investigated with the aim to reduce the probability of LFDD disconnections, by taking actions at frequency thresholds between 50 and 49Hz, as well as to improve the performance of the LFDD scheme in the event that disconnections are required. As a test case, the LFDD scheme as currently applied by one of the distribution system operators in the Netherlands is considered.

This project is therefore categorised in two primary research directions: (i) improving selection criteria for LFDD load shedding locations, and (ii) improving LFDD performance using alternative load shedding schemes.

Key topics explored in this research include: (i) the use of system strength and real-time DER generation as input parameters to load bus selection criteria for LFDD, and (ii) proactive RoCoF-based disconnection of pre-determined consumers above 49Hz. The findings of this study indicate that adapting the current LFDD implementation based on the local system strength and the level of active DER generation at LFDD buses can improve frequency response and reduce instability following LFDD switching operations. Furthermore, proactive ROCOF-based demand side load management techniques above 49Hz prove effective in reducing frequency deviation during the most severe events while avoiding LFDD over-shedding for smaller contingencies.

This research provides insights for power grid operators and policymakers in Continental Europe. It aims to enhance grid resilience and reduce the risk of potential blackouts amid the increasing integration of inverter-based generation. Through further investigation, validation and implementation of these strategies, IBR-dominated power systems are expected to better cope with disturbances.

Contents

List of Figures

List of Tables

Nomenclature

Abbreviations

Abbreviation	Definition
CESA	Central European Synchronous Area
COI	Centre of Inertia
DSO	Distribution System Operator
DER	Distributed Energy Resource
EPS	Electrical Power System
IBR	Inverter Based Resource
IEA	International Energy Agency
IPCC	International Panel on Climate Change
IRENA	International Renewable Energy Agency
LFDD	Low Frequency Demand Disconnection
PMU	Phasor Measurement Unit
RES	Renewable Energy Sources
ROCOF	Rate of Change of Frequency
SNSP	System Non-Synchronous Penetration
TSO	Transmission System Operator
UFLS	Underfrequency Load Shedding

Symbols

Symbol	Definition	Unit
f_{coi}	Frequency at Centre of Inertia	[Hz]
H_i	Generator Inertia	[s]
H_{synch}^{gen}	Cumulative inertia of all synchronous generators	[s]
I_i	Generator inertia time constant	[s]
J	Inertia	[GWs]
m_0	Initial ROCOF Following Event	[Hz/s]
P_{imb}	Power Imbalance	[MW]
P_{LFDD}	Load Available for LFDD	[MW]
P_{LOAD}	Cumulative Load Active power	[MW]
s_i	Motor Rotational Speed	[rad/s]
$S_{G,i}$	Generator Rated Power	[MVA]
T_e	Electrical Torque on System	[Nm]
T_m	Mechanical Torque of Rotating Machines	[Nm]
T_{Start}	Load Shedding Start Time	[s]
α	LFDD Scaling Factor	N/A
Λ	Imbalance Factor	N/A
Ω	Angular Speed of Rotating Machines	[rad/s]

1 Introduction

Climate change has emerged as one of the greatest challenges facing the human population in our time. Without drastic action, rapid increase in global temperature, coupled with increased emission of greenhouse gases and depletion of the Earth's natural resources, will continue to have devastating effects on global ecosystems [1]. According to the intergovernmental panel on climate change, rapid and sustained mitigation measures and accelerated implementation of policy and technical adaptation actions in this decade would reduce the projected damages for both humans and ecosystems [2].

One strategy to combat climate change is through the reduction of fossil fuels used in the generation of electricity. According to the "Roadmap to 2050" released by the International Renewable Energy Agency (IRENA), electrification of the power system with renewable generation sources, such as wind and solar, can reduce carbon dioxide emissions immediately and substantially [3]. In order to realise this future carbon-neutral power system, innovation and advancement are required in many areas such as power system control, infrastructure, defence and restoration.

1.1. Renewable Energy Trends

The global effort to reduce reliance on fossil fuels and adopt sustainable approaches for various human activities is well-documented. In the realm of power generation, there has been a remarkable surge in the utilization of renewable energy sources, particularly solar and wind power. Governments and nations are increasingly striving to accelerate the transition towards cleaner energy alternatives, aiming to mitigate the detrimental impacts associated with global warming [4].

Recent worldwide events have expedited strategies aimed at diminishing dependence on imported fossil fuels in Europe, such as natural gas. Instead, the focus is shifting toward the integration of renewable energy sources within domestic energy grids. The 2022 IEA Renewables report discusses the influence of the ongoing conflict in Ukraine on renewable energy patterns in Europe and globally [5]. These unfolding events have prompted an unexpected 30% surge in growth estimates for renewable energy. According to the report, a substantial 2500GW surge in renewable energy capacity is anticipated between 2022 and 2027, marking an 85% increase compared to the previous five-year period. The report predicts that renewable energy might emerge as the primary global energy source by the beginning of 2025.

Europe is projected to be the second-largest contributor to the global upswing in renewable energy adoption by 2027, trailing closely behind China. Three quarters of this surge will be concentrated in seven key countries, among them the Netherlands. Forecasts indicate that renewable energy generation across Europe will soar by 60% from the 2022 benchmarks, reaching 12400 TWh by 2027. In the Netherlands, plans entail the addition of 30GW in renewable energy capacity by 2027. This augmentation will predominantly arise from the establishment of expansive utility-scale solar installations, alongside the construction of onshore and offshore wind farms. The capacity for both utility-scale solar installations and decentralized photovoltaic generation is poised to increase by 17 GW in the period

2022- 2027.
The increasing penetration of renewable energy sources poses a number of technical challenges for the design and operation of the power grid. According to a 2022 ENTSO-E report which outlines the innovations needed to create a carbon-neutral power system, increasing the share of renewable generation requires innovation in the areas of system flexibility, system operation, energy infrastructure, and market design [6]. Preparing and operating a power system with a rapidly increasing number of actors, changes in the direction of power flow and varying demand side constraints is both a technical and a political challenge. The primary technical challenges associated with the future power system can be broken into three categories: Affordability, Sustainability, and Resilience [6].

1.2. Effects of Increased RES on Inertia & Power System Stability

The predicted growth in penetration of renewable energy sources (RES) and inverter-based resources (IBRs) on the power grid is set to have an increasing effect on power system dynamics [7]. Traditional power systems with large amounts of synchronous machines connected both on the generation side and load side of the transmission grid are now transitioning to systems with increasingly large amounts of non-synchronous generation and load. The effects of this change can be seen in many areas of power system dynamics such as voltage control, system protection, congestion management, grid stability, and system inertia [8, 9, 10].

In a traditional power system, control of frequency and voltage is provided by the synchronous generation units connected to the network [11]. Grid-forming inverters, capable of providing the reference voltage and frequency needed to create a stable network, are being developed but have yet to be implemented on a large scale in the European power grid. As a result, the dominant share of IBRs is connected to the grid through grid-following inverters which do not provide the same voltage and frequency control as traditional synchronous generators [12].

1.2.1. Inertia and Stability in Power Systems

Inertia in a power system is directly related to the kinetic energy of the rotating masses connected to the system [11]. Rotational inertia acts as a buffer to aid the system in the immediate moments following a disturbance, such as loss of generation [13]. As described in Equation 1.1 inertia (J) is a phenomenon related to the relationship between the mechanical torque of the rotating machines and the electrical torque of the system [11]. Inertia response is an instant system response based on inherent characteristics of the system. In contrast, other system responses such as secondary and tertiary control require measurements and then provide subsequent reactions, hence their response following a disturbance is delayed.

$$T_m(t) - T_e(t) = J.\frac{d\Omega}{dt} \tag{1.1}$$

Equation 1.1 describes the relationship between the mechanical torque of rotating machines $T_m(t)$, the electrical torque of the system $T_e(t)$ and the angular speed of rotating machines $\frac{d\Omega}{dt}$. The left side of the equation represents the balance between the mechanical torque expressed on the rotating mass and the electrical torque of the system. When this balance is non-zero, such as during a system disturbance, this causes an angular speed deviation. Inertia reduces the frequency deviation in the immediate moments following a system imbalance by providing a limited power source which can help to maintain supply to the load. This occurs due to the immediate deployment of kinetic energy stored in the rotating masses connected to the system and does not involve any control mechanisms. It is clear from the equation that a system with higher inertia can expect to experience a smaller angular speed deviation, and therefore higher frequency stability margins, for a given imbalance, than a low inertia system.

1.2.2. Effect of lower inertia system on system stability

Rapid growth in the share of renewable energy generation creates numerous stability challenges for the power grid. Most RES are connected to the network via power electronics components such as inverters. There is no rotating mass associated with these renewable generators to provide the inertia required to maintain frequency stability following a disturbance. It is expected that a higher frequency deviation and rate of change of frequency (ROCOF) values will be seen for low inertia systems in response to an imbalance in comparison with a traditional system [14]. As a result of higher ROCOF values following a disturbance, the system frequency is more likely to breach safe thresholds before control measures can react and restore balance [15]. A visual representation of the effect of lower inertia on frequency response to a contingency event is shown in Figure 1.1.

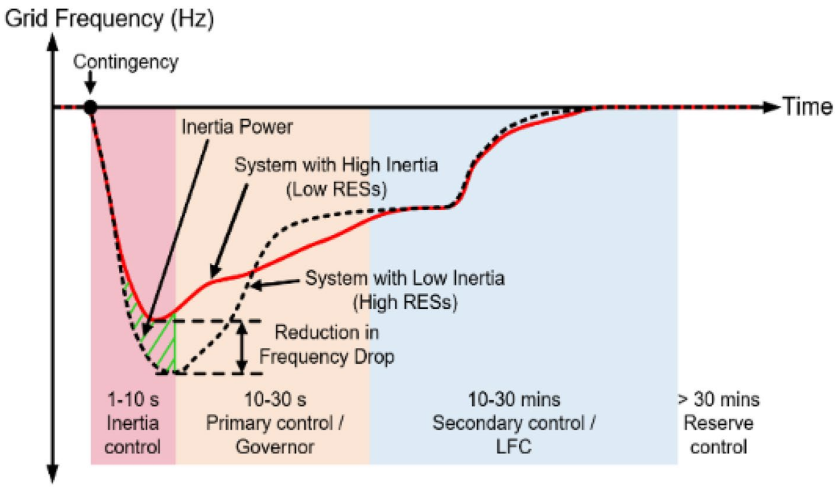

Figure 1.1: Frequency Response - Low vs High Inertia System [16].

It is evident from Figure 1.1 that systems with lower inertia can expect higher frequency deviations in comparison to a traditional power system, for a given disturbance size. Higher ROCOF values associated with inertia systems can also pose challenges for equipment as there is a danger of disconnection of synchronous generators and IBRs should ROCOF values exceed 2Hz/s [17]. The shift to non-synchronous generation can also affect short circuit levels and voltage stability in a power grid. According to the 2020 ENTSO-E paper on grid stability, a synchronous machine can inject 3-5 times its nominal current instantaneously following a disturbance [11]. This is a reactive power injection in the grid that helps to maintain the voltage immediately after an event and thus improves grid stability. IBRs cannot inject this level of current into the system following an event. Typically, IBRs can inject current up to 1.2 pu, which may be insufficient to maintain the voltage stability following an event. The reduced fault levels associated with the high (low) penetration of RES (synchronous) generation is one of the primary causes of reduced system strength expected in the future. This topic is, however, out of the scope of this research, and is discussed in more detail in [18, 19, 20, 21].

1.2.3. Frequency Defence Measures - Load Shedding

During severe frequency deviation events, the most appropriate method to prevent system collapse is the disconnection of certain loads to restore power balance on the system [22]. Underfrequency operation could be a huge threat to safe and stable operation of a power system, therefore, power balance should be restored by shedding the appropriate amount of load as quickly as possible following a contingency event. This method of frequency defence is called Underfrequency Load Shedding (UFLS). The focus of this thesis is on the UFLS schemes employed in the CESA, particularly in the Netherlands. In the CESA, load shedding for frequency defence is referred to as Low Frequency Demand Disconnection (LFDD) and operated based on the same principle as UFLS [23]. Further details on the state of the art of UFLS schemes are presented in chapter 2.

1.2.4. System Splitting Events - Continental European Synchronous Area

Historically, power systems around the globe have remained relatively stable due to the dominant share of electricity coming from synchronous generators and the resulting abundance of rotational inertia on the grid [24]. As discussed previously, the increased share of renewable generation is expected to cause the stability of power systems to deteriorate as synchronous generation provides a decreasing proportion of electricity. There have been few major contingency events in the CESA in recent years, data from some of these contingency events is available and may be useful in designing emergency defence and restoration procedures for the future CESA system.

In 2021, the CESA experienced two system-splitting contingency events due to cascading trips of several transmission network elements. In both cases, emergency defence measures were activated and the system was successfully restored to normal operation. Due to the rapid and effective response, no major damages were observed in the power system in either case.

On January 8, 2021, a contingency event was caused by the tripping of overcurrent protection in the busbar coupler of a substation in Croatia [25]. The cause of the overcurrent trip was increased power flows in the region of the substation due to unexpected weather patterns in Europe which affected the day-ahead predictions for energy usage in the region. The subsequent redirection of power flows following this initial trip caused further cascading trips in the protection systems of nearby substations. The initial substation trips resulted in widespread cascading trips of transmission lines within 20 seconds due to transmission system protection. As a consequence of these disconnections, the system was split into two separate synchronous areas. One of these synchronous areas had a surplus of generation, and therefore an increasing frequency, while the other had a surplus of load, and therefore a decreasing frequency. In both cases, the system response mechanisms were effective in restoring power balance without any additional loss of supply.

The second CESA system splitting event occurred on 24 July 2021 [26], when the Iberian peninsula was separated from the rest of the CESA due to cascading trips of transmission system elements. In this case, the tripping of an interconnecting transmission line between France and Spain was initially caused by a fire in Southern France in an area through which two 400kV transmission lines passed. The loss of supply from one of the Spanish-French interconnectors caused the other two interconnectors between these areas to become overloaded resulting in further tripping and a complete loss of synchronisation between the French and Spanish Power systems. To restore frequency in some areas, emergency response measures were activated and emergency shedding of certain load elements took place. Load shedding occurred in both the Spanish and Portuguese grids due to the power imbalance and generation deficit caused by the loss of power from the interconnectors. Following emergency defence and restoration procedures, normal operation was restored to the system.

1.3. Research Outline & Justification

Given the anticipated increase in inverter-based resources in the CESA and the subsequent reduction in rotational inertia and inherent stability of the future power system, it is possible that existing system defence measures may be insufficient to arrest frequency decline should a severe contingency occur in the future. Consequently, the purpose of this research is to investigate, firstly, the effect of increased penetration of renewable energy on post-contingency power system dynamics and, subsequently, the corresponding effect on the performance of the existing underfrequency system defence measures. Findings from this initial research phase are then used to guide investigation into potential improvements to existing defence measures to enable a more robust response to contingency events and reduce the risk of cascading disconnections and blackouts in the future power system. These goals have led to the following research questions:

1. *How does the increased penetration of inverter-based resources influence power system frequency trajectory during large-scale disturbances, such as generation loss?*

2. *To what extent does the increased proliferation of renewable generation affect the efficacy of current frequency defence measures implemented on the grid?*

3. *What strategies can be adopted to enhance the performance of the existing frequency defence mechanisms in a lower inertia power system?*

4. *What are some alternative approaches to frequency defence that could be implemented outside of existing measures? Do these exhibit enhanced performance within the future power system?*

5. *Among the proposed enhancements and alternatives to current system defence mechanisms, which solutions are the most applicable for implementation within the Continental European Synchronous Area?*

1.3.1. Research Method and Structure

This research is focused on the analysis and improvement of system defence procedures, specifically shedding of load to restore power balance following a loss of generation event. In the CESA, emergency and restoration grid code, this procedure is known as Low-Frequency Demand Disconnection (LFDD). The project can be broken into two research phases:

- **Phase 1:** Modelling and Analysis of existing Dutch LFDD scheme.
- **Phase 2:** Conception, analysis and validation of proposed improvements to LFDD.

This research is carried out through analysis of the frequency response of a grid network, with varying levels of rotational inertia, to loss of generation contingency events. The analysis is achieved using a test grid network and by creating multiple scenarios based on different contingency event sizes and penetration levels of renewable generation. The primary focus is placed on the ability of defence measures to arrest frequency decline following a contingency event while minimising load shedding amount. Emphasis is also placed on the stability of frequency in the moments immediately following load-shedding switching actions. Longer-term measures to restore nominal operating conditions, such as secondary and tertiary control, are not included in this research. As this research is a joint venture between TU Delft and industry partners from the Dutch power grid, emphasis is placed on the relevance and suitability of proposed methods to the technical and legislative possibilities of the Dutch power system.

The research presented in this report is structured as follows:
An overview of the start of the art of underfrequency load-shedding schemes is presented in chapter 2.
The methodology for phase 1 of this research, the analysis of the existing Dutch LFDD scheme, is described in chapter 3.
Corresponding results and discussion on the performance of the existing Dutch LFDD scheme are shown in chapter 4.
Methodology for phase 2 of this work, evaluation of proposed improvements to LFDD, is outlined in chapter 5.
Results and analysis of the performance of each proposed improvement are presented in chapter 6.
An overview and consolidation of all proposed improvements to LFDD, including performance benefits and challenges from a technical, legislative, and implementation perspective, is provided in chapter 7.
Finally, conclusions drawn from this work and answers to research questions are presented in chapter 8 while recommendations for continuation of this research are provided in chapter 9.

2
State of the Art - Underfrequency Load Shedding

In this section, literature research is presented in the area of underfrequency load shedding. In some circumstances, when the magnitude of frequency deviation reaches unsafe levels following an event, there is a risk of cascading disconnection of generators and possible blackout [27]. One method taken to prevent this occurrence is called Underfrequency Load Shedding (UFLS), referred to as Low-Frequency Demand Disconnection (LFDD) in the CESA. UFLS is the principal measure to prevent successive frequency declination and blackouts following massive loss of generation [28]. The purpose of UFLS is to disconnect a certain amount of load to restore power balance and therefore allow the frequency to recover and normal operating conditions to be restored on the network. There are a number of methods that can be used to design a load-shedding scheme. These vary in complexity, performance, speed of response and versatility.

UFLS schemes can broadly be grouped into three separate categories: traditional, adaptive, and semi-adaptive methods [29]. These schemes can vary in terms of the method used to determine load shedding amount, speed of response to an event, complexity and robustness [29]. Traditional UFLS schemes, common in large-scale power systems, are described in section 2.1. Modern, adaptive UFLS schemes which may include complex calculation or wide area monitoring are explained in section 2.2. Finally, in section 2.3 semi-adaptive UFLS schemes, a combination of the other two load-shedding methods, is explored.

2.1. Traditional UFLS Schemes

Historically, the dominant portion of electricity generation has come from synchronous generation sources. As a result, these systems were robust, and large frequency deviation and cascading disconnections were largely uncommon. Consequently, traditional UFLS schemes have been the most commonly implemented in industry and remain the most prevalent measure to arrest severe frequency deviations in large power systems such as the Continental European Synchronous Area (CESA) [24]. These schemes operate on a stage-by-stage basis in which a predefined amount of load is shed as the frequency crosses a specific threshold value. The setting of each stage involves:

1. Amount of disconnected load per stage

2. Frequency threshold at which the stage is to be activated

As different electrical power systems (EPSs) vary in terms of power flow magnitude and direction, RES penetration, and network strength, load-shedding schemes of this type vary from one network to another [30]. Typically, traditional UFLS schemes are set with 0.2-0.25Hz between thresholds and a total of 5-8 thresholds set depending on the system characteristics and the total load shedding amount required. Traditional load shedding schemes make the decision on how much load to shed independently of other parameters in the system such as voltage level or system inertia [31]. The operation of a typical traditional UFLS scheme is described in Figure 2.1.

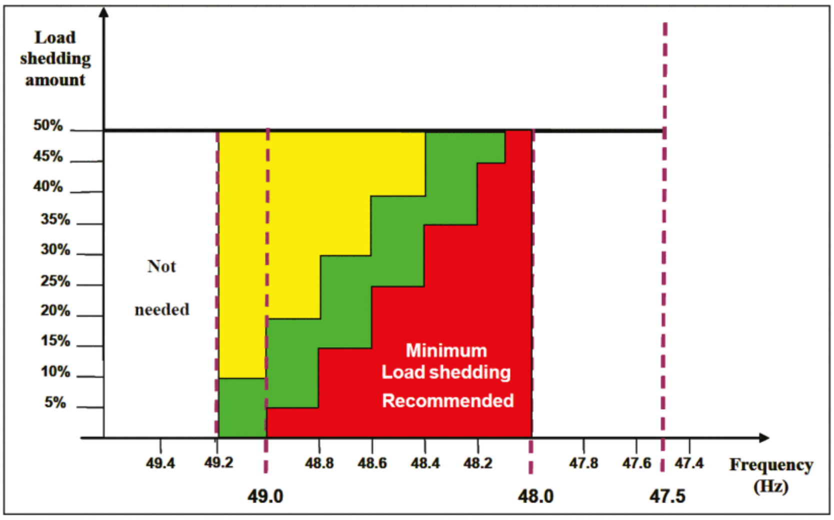

Figure 2.1: Diagram of operation of Traditional UFLS scheme [32].

As shown in the above figure, traditional load shedding schemes operate by disconnecting a pre-defined portion of load at certain frequency thresholds. Typically, a minimum and maximum load-shedding amount for each frequency threshold is described in the grid code for the appropriate region. In the CESA, ENTSO-E recommends no less than 5% of peak load be shed in any one step, with the maximum load shedding per step capped at 10% [7]. Frequency measurement for traditional load-shedding schemes occurs at the substation level (i.e. at the location of individual UFLS relays). This is known as a local UFLS. Local UFLS schemes are desirable for their security and simplicity as no real-time communication between devices, or between relays and a central controller, is required for the scheme to operate [30]. Traditional UFLS schemes are suitable for systems with high levels of synchronous generation with large inherent stability to withstand disturbances. In converter-dominated systems, traditional load-shedding schemes are limited by their inability to provide the optimum load-shedding amount. The Dutch LFDD scheme, which is the focus of analysis in phase 1 of this research, is a traditional scheme designed based on CESA grid code requirements. Further information regarding the design and operation of this scheme is presented in chapter 3.

2.2. Adaptive UFLS Schemes

As the penetration of RES increases, system defence measures are required to become more advanced due to more challenging system dynamics and a lack of inherent stability. A body of research has been carried out into more complex UFLS schemes which are not bound by fixed thresholds and predetermined load shedding amounts[30]. Although these schemes have received increasing attention in the past decade, adaptive methods of load shedding have been discussed in literature as early as 1992 [33]. Adaptive UFLS schemes involve online calculation of the load shedding amount following a contingency event such as loss of generation. This is typically carried out by using the rate of change of frequency (ROCOF) at the centre of inertia (COI) of the system [28]. The power imbalance in the system is typically calculated using the system inertia and maximum ROCOF following an event. The estimated power imbalance is then used to calculate the required load-shedding amount to prevent the frequency from reaching unsustainable levels [28]. A flowchart describing the operation of a typical adaptive load shedding scheme is shown in Figure 2.2.

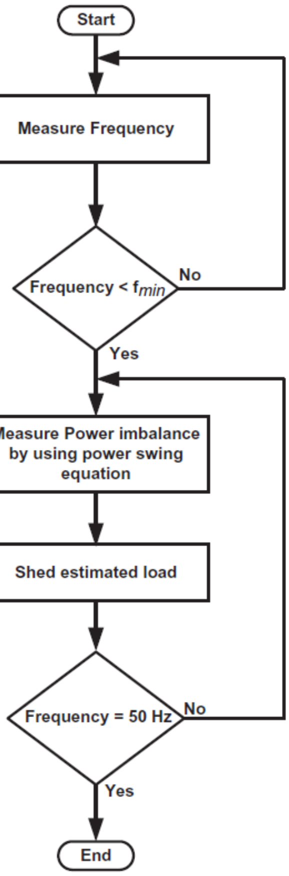

Figure 2.2: Flow diagram of a conventional adaptive load shedding scheme [34].

In a conventional adaptive UFLS scheme, real-time measurements, possibly from phasor measurement units (PMUs), are used to estimate the power imbalance in the system. This power imbalance estimate is then used to decide the appropriate load-shedding amount and number of load-shedding steps. The calculation of load shedding amount can be completed based on a number of parameters such as system inertia, available reserves, estimated minimum frequency or voltage stability in the system. Following the decision on the load-shedding amount and the location of loads to be shed, commands are delivered to the appropriate UFLS relays to disconnect the desired loads. The frequency trajectory following load-shedding actions is monitored to determine whether more shedding steps are required to restore frequency to nominal values. As EPSs become increasingly complex, online calculation of power imbalance becomes more difficult, in part because system inertia is more difficult to predict at a given moment due to variability in renewable generation, load consumption and power flow. Similarly, there is some debate in the literature regarding the correct method to calculate or measure the maximum ROCOF as it is difficult to determine the exact moment at which this maximum ROCOF occurs [14].

Adaptive schemes are widely discussed in the literature, these schemes commonly require wide-area measurements and communication between UFLS relays and the central controller [35]. These schemes can be highly effective in arresting frequency decline following a disturbance and alleviating under and overshedding concerns by computing the ideal load-shedding amount for each contingency event and system inertia level. Due to the computational and operational complexity of these schemes including power deficit estimation, hardware (PMUs) dispersion in the system, and communication between relays and controllers, adaptive load shedding schemes have not yet been widely implemented in large-scale power systems [31]. In the CESA power system, the need for a robust and secure load-shedding scheme is a high priority for system operators. Consequently, adaptive schemes involving central controllers, which would receive data and send commands to relays in the field, are undesirable due to the vulnerability of such communication links to hacking or loss of communication events. To counteract this, local implementation of adaptive load shedding schemes, such as the scheme described in [35], could be effective.

2.3. Semi-Adaptive UFLS Schemes

Semi-adaptive load-shedding schemes monitor both ROCOF and frequency deviation to determine how much load should be shed. These schemes can be viewed as a combination of the traditional and adaptive load shedding schemes [28]. Typically, semi-adaptive schemes calculate the load to be shed in the first stage according to the ROCOF at COI and the frequency deviation. The remaining load is shed at predefined thresholds as in the traditional load-shedding scheme. One such scheme is described in [33], where a power deficit estimation is made using measured frequency and ROCOF. Following the estimated power deficit calculation, 50% of the calculated load is shed in the first shedding step. The remaining load to be shed is distributed equally in fixed thresholds. This method of load shedding reduces the need for continued monitoring and communication by a central controller. A calculation can be carried out in the moments following an event, and the appropriate load-shedding amounts and thresholds issued to relays in one command.

In this section, an overview is given of the three main types of underfrequency load-shedding schemes. The traditional UFLS scheme, in operation in Europe under the name Low-Frequency Demand Disconnection (LFDD) is the subject of analysis in chapter 3 and chapter 4. In Phase 2 of the research presented in this report, some more advanced load-shedding methods are explored, such as those in section 5.5, which operate in a similar manner to the adaptive or semi-adaptive schemes. This investigation into the operation of UFLS schemes provides the basis for the analysis of the existing Dutch frequency defence measures. Understanding the operation of modern UFLS schemes enables improvements to the Dutch LFDD scheme to be developed which exhibit both higher performance and can realistically be implemented given technical and legislative possibilities in the CESA. In the following chapter, the methodology used to analyse the effect of increased penetration of RES on the efficacy of the Dutch LFDD scheme is presented.

3
Dutch Low-Frequency Demand Disconnection Scheme - Modelling Method

In this chapter, the modeling approach for the analysis of the existing Dutch Low-Frequency Demand Disconnection (LFDD) scheme is described. The primary aim during this modeling stage of the project is to create a test network that can provide frequency trajectories to enable analyses of different contingency event sizes and RES penetration levels.

One main objective of the modeling part of this project is to create scenarios in which system inertia is reduced and the largest contingency events possible can be initiated without causing the system to collapse. As this analysis is related to underfrequency defence measures only, all simulations are created to simulate loss of generation events and the subsequent effect on the frequency of the test network. In section 3.1 the power system modelling and scripting software used in this research are outlined. Section 3.2 describes the test grid network used in all simulations. The addition of inverter-based resources and the creation of different system operating scenarios is discussed in section 3.3. Calculations of system inertia in each operating scenario and metrics to represent penetration of non-synchronous generation are outlined in section 2.1. The method used to simulate cascading loss of generation events on the test network is presented in section 3.5. A detailed description of the grid code requirements for the Dutch LFDD scheme and subsequent development of similar schemes for the purpose of this analysis is provided in section 3.6. Finally, an outline of the simulation parameters used throughout this research is given in section 3.7.

3.1. Software

Modelling and simulations in this analysis are performed using DIgSILENT PowerFactory 2022 SP4. Powerfactory is an established software used in power systems analysis for generation, transmission, and distribution systems. This software enables a wide range of power system studies such as RMS simulation, load flow calculation, contingency analysis, and protection coordination studies. In this thesis, numerous scenarios are presented with different contingency event sizes and renewable generation penetration levels. RMS simulations, load flow analysis and short circuit analysis are the primary tools utilised in this research.

Contingency event modelling, generation of operating scenarios, parameter selection for RMS simulation, and definition of export variables are carried out in Power Factory software. Commands to initiate RMS simulation, select study cases, select operating scenarios, and export results to csv files are completed through Python scripts added to the PowerFactory library. Calculations on exported results and plotting of frequency, load shedding amount, and ROCOF trajectories are performed in Python.

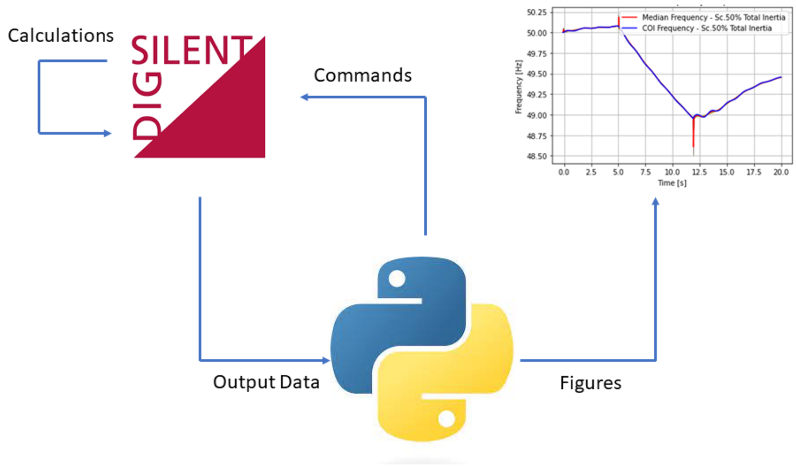

Figure 3.1: Diagram outlining the relationship between modelling and scripting software used in this project.

3.2. Network Model

Grid modelling and simulations for this project were performed on the New England 39 Bus template network available in PowerFactory. As this analysis is aimed at applications in continental Europe, the frequency is set to 50Hz for all simulations.

The 39 Bus test grid is used to perform simulations for this research due to its size and resulting ability to replicate frequency events comparable to those seen in real, utility-scale, power systems. In addition, there is sufficient documentation available regarding network components, particularly control systems for synchronous generators.

The 39 Bus test network, shown in Figure 3.2 is based on a power network in the New England area of the United States. The network consists of 10 synchronous generators, 39 busbars, 12 transformers, and 19 loads. There is no non-synchronous generation present in the standard 39 Bus network. The nominal voltage level is 345kV, however, the system also contains buses at voltage levels of 138kV, 230kV, and 16.5kV. Synchronous generator controls, load voltage dependencies, and transformer tap changer settings have been taken at the default values present in the PowerFactory 39 Bus template network.

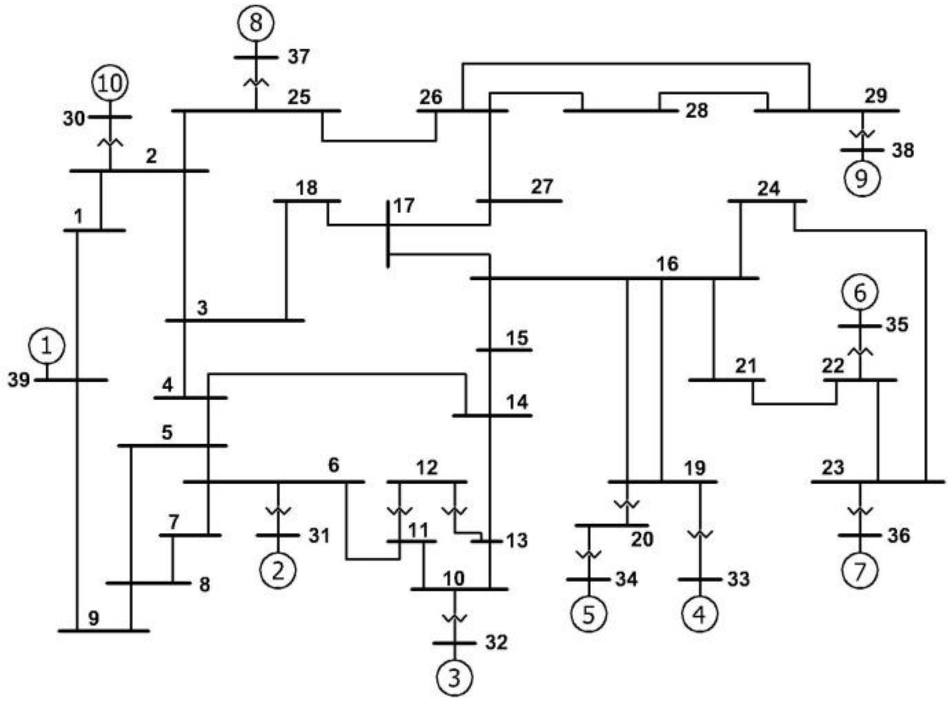

Figure 3.2: An illustration of 39 Bus test Network used in this research [36].

3.3. Renewable Energy Penetration Scenarios

Seven different operating scenarios were created for the analyses. In each sequentially higher RES penetration scenario, one extra synchronous generator is replaced by a non-synchronous generator, as shown in Table 3.1. As the penetration of non-synchronous generation, referred to here as System Non-Synchronous Penetration (SNSP), increases, total system inertia decreases. Frequency deviation and the performance of the LFDD scheme in all scenarios are evaluated based on a series of generation loss contingency events.

Table 3.1: Breakdown of operating scenarios used in this project combined with associated inertia values.

Scenario	Total Active Sync Gens	Total Active RES Gens	SNSP	Total System Inertia - H [s]	Starting Time - T [s]
Full sync Gen	10	0	0%	4.77	9.54
Scenario 1	9	1	9%	4.62	9.25
Scenario 2	8	2	20%	4.45	8.90
Scenario 3	7	3	33%	4.24	8.48
Scenario 4	6	4	43%	4.08	8.16
Scenario 5	5	5	53%	3.87	7.73
Scenario 6	4	6	66%	3.61	7.22

3.3.1. Non-synchronous Generators

WECC type 4B template generators are used to replace the synchronous generators in this model. These advanced models are selected as they are established templates for use in power systems modelling and are often applied in industrial and academic applications as they provide realistic dynamic performance under a wide array of operating conditions. There is ample available documentation on controls and protection for these template generators, including active power response, undervoltage and underfrequency protection.

The six wind generators added to the model and their operating parameters are presented in Table 3.2. The power balance on the network was maintained for each scenario by matching the active power dispatch and MVA rating of the WECC template generators with the synchronous generator being replaced. No changes were made to other wind generator functions such as protection, electrical control, or the generator-converter model.

Table 3.2: Operating parameters and corresponding penetration of non-synchronous generation for wind turbine templates added to 39 Bus test network.

Non-Sync Gen Name	Associated Bus No.	1 unit Active Power Dispatch (MW)	1 unit rated Power (MVA)	No. Inverters	Total Rated Power (MVA)	Total Active Power Dispatch (MW)	Disconnected Sync Gen	Total SNSP
Wind 01	25	56	60	10	600	560	Gen 08	9%
Wind 02	19	64	68	10	680	640	Gen 04	20%
Wind 03	29	104	104	8	832	832	Gen 09	33%
Wind 04	23	95	100	6	600	570	Gen 07	43%
Wind 05	21	65	68	10	680	650	Gen 06	53%
Wind 06	2	80	82	10	820	800	Gen 10	66%

As shown in Figure 3.3, the WECC template includes a transformer which is used to step up the voltage from the local Wind Turbine bus (10kV, 16.5kV or 66kV) to the network bus voltage (345kV).

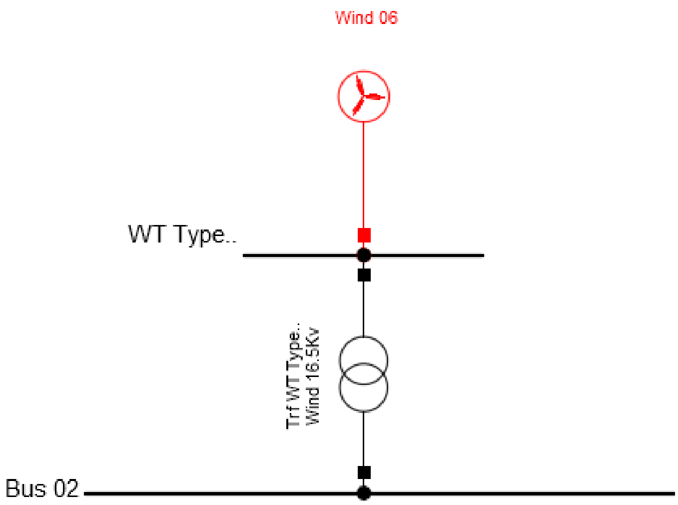

Figure 3.3: WECC Wind Turbine Template Model

The primary criteria in modelling of transformers for a non-synchronous generation was to ensure the transformer ratings were sufficient to transfer the necessary power to the transmission grid. In order to model the system more efficiently, one transformer type was utilised for each LV voltage range with the number of transformers in parallel being varied to reach a total power capacity sufficient for each wind generator. Transformer ratings, bus voltages, and numbers in parallel are shown in Table 3.3.

Table 3.3: Operating parameters of transformers used in the connection of wind generators to transmission network.

Name	LV-Side Voltage	HV-Side Substation	HV-Side Voltage	Snom MVA	No. in Parallel	Stotal MVA
Trf WT 01	10kV	Bus 25	345kV	120	8	960
Trf WT 02	66kV	Bus 19	345kV	120	6	720
Trf WT 03	66kV	Bus 29	345kV	120	8	960
Trf WT 04	66kV	Bus 23	345kV	120	8	960
Trf WT 05	66kV	Bus 21	345kV	120	7	840
Trf WT 06	16.5kV	Bus 02	345kV	100	10	1000

3.3.2. Reactive Power Compensation

There is no reactive power contribution from the non-synchronous generation which is added to the network. Consequently, there is a reactive power deficit on the network which results in voltage collapse on the system following some contingency events. This phenomenon, as expected, becomes more apparent in simulations with higher penetrations of non-synchronous generation. In some cases, the voltage remains stable for steady state conditions with no contingency events but would fail when a contingency was added to the dynamic RMS simulation.

To restore the reactive power balance to the network, a series of capacitors and inductors are added. This reactive power compensation is added in a step-by-step manner through running simulations and observing the buses at which voltage collapse would occur. Table 3.4 displays the bus names and magnitude of reactive power compensation added at each. It is important to note that not all capacitors or inductors are active in each scenario; they are switched on or off depending on the stability of the solver and the proximity of the steady state frequency to the nominal 50Hz value. The addition of capacitors is performed to improve initial condition voltages and improve convergence. Their introduction will generally not have a meaningful impact on frequency dynamics, i.e., the focus of this thesis.

Table 3.4: Location and magnitude of reactive power compensation add to model to improve convergence of solver.

Bus Name	Qmax MVar
WT Type 4B LV	50
Bus 20	75
Bus 04	25
Bus 17	100
Bus 14	50
Bus 04	100
Bus 39	200
Bus 03	80
WT Type 4B LV(1)	100
Bus 32	150
Bus 11	150
Bus 21	50
Bus 23	150
Bus 28	20
Bus 06	60

3.4. Inertia & SNSP

To quantify the penetration of renewable energy on the network, the System Non-Synchronous Penetration (SNSP) is used [15]. This parameter was introduced by the Irish Transmission System Operator, Eirgrid, and is used to represent the amount of non-synchronous generation on the system at any instant. SNSP is given by Equation 3.1 where the total non-synchronous generation is expressed as a percentage of the total load on the network.

$$SNSP = \frac{Non - SyncGen}{TotalLoad} \tag{3.1}$$

It is important to note that this index is relative to the load present on the 39 Bus test grid and does not take into account the load associated with G01, and the connection to the rest of the transmission system. In a system with synchronous condensers and large amounts of import/export, the equation would need to be altered to reflect these exchanges. As there are no synchronous condensers in this system, the SNSP parameter is taken as an effective method of highlighting the amount of non-synchronous generation active on the grid in each operating scenario.

The second parameter used to quantify the variation between scenarios is the system inertia. As mentioned in subsection 1.2.1, system inertia is directly related to the ability of the system to withstand disturbances in the immediate aftermath of a contingency event. The introduction of more non-synchronous generation reduces the total inertia available on the grid and as a result, the impact of disturbances is expected to be higher.

To account for the presence of non-synchronous generation in the inertia calculation for each scenario, the $H^{\text{gen}}_{\text{synch}}$ parameter is used based on the 2020 ENTSO-E paper on inertia and ROCOF [11]. The inertia calculation is calculated according to Equation 3.2.

$$H^{gen}_{synch} = \frac{\sum_{i=1}^{n} H_i.S_{G,i}}{P_{LOAD} + 10000} \tag{3.2}$$

In this test system, generator G01 represents the connection to the wider transmission grid and as such has the highest MVA rating of all synchronous generators on the grid. The inclusion of this generator in the inertia calculation requires the addition of a load equal to the rated power of G01 to correctly model the expected loads on the wider transmission grid also. To achieve this, an additional 10000 MVA is added to P_{Load} in the denominator of Equation 3.2.

The inertia in each scenario is calculated separately based on the number of active synchronous generators in that scenario. As this research is not focused on emergency actions following islanding, G01 is active in all scenarios and therefore the inertia remains above 3s in all scenarios. Lower inertia values could be achieved by disconnecting G01 and simulating an islanding scenario on the 39 Bus system. This scenario would require further research into reactive power compensation and RES modelling in order for the system to maintain stability. However, this is not in the scope of this thesis and will not be discussed here.

3.5. Contingency Events

The frequency deviation and performance of the existing LFDD scheme were analysed in response to various contingency events. The purpose of the simulated contingency events was to create a power deficit on the test network which would result in a sufficient frequency deviation to cause the underfrequency protection to operate.

Contingency events were created by sequentially turning on static loads connected to Bus 39 of the system. Each load has an active power demand of 500MW and a time delay of 300ms was used between switching of sequential loads. The loads are connected at Bus 39 as this is the point of connection of G01, which represents the connection from the 39 Bus network to the rest of the transmission grid. Switching on loads sequentially at this bus simulates the sequential loss of generation at a distant point in the network, resulting in an active power deficit on the test network.

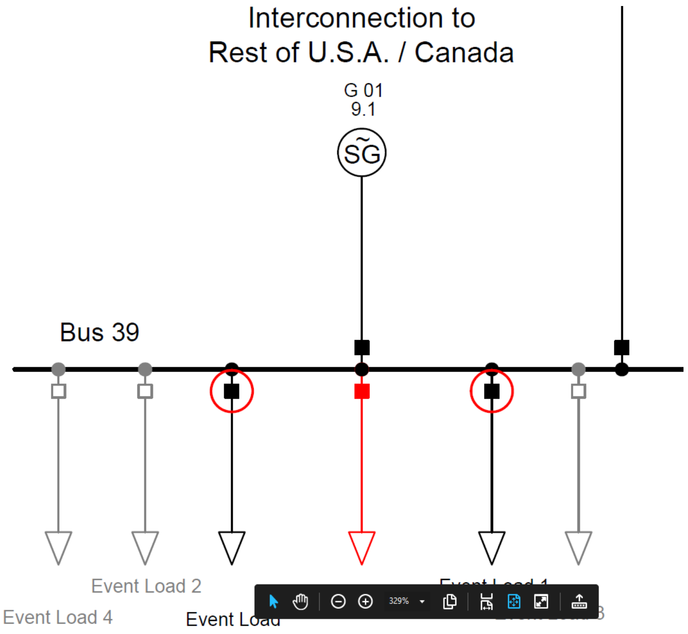

Figure 3.4: Diagram of contingency event loads added to bus 39 of test network

Three contingency event sizes were used in the analysis of the existing Dutch LFDD scheme. These events were of magnitude 500MW, 1000MW and 1500MW respectively. The size of these events is sufficient to study the intended frequency dynamics while preserving numerical convergence of the model in all cases.

3.6. LFDD Scheme

In this section, the process of developing the LFDD schemes for the use in this research is outlined. A description of the Dutch grid code requirements in relating to LFDD is given in subsection 3.6.1. The generation of example LFDD schemes for the 39 Bus test network based on the Dutch grid code requirements is then provided in subsection 3.6.2.

3.6.1. LFDD Scheme - Grid Code Requirements

As mentioned in section 1.3, this research is completed in collaboration with Dutch distribution system operator (DSO) Alliander. Modelling of the Low Frequency Demand Disconnection scheme in PowerFactory was completed based on information gathered from the Alliander network protection scheme and the European grid code for underfrequency protection [23].

The LFDD scheme for Alliander network operates based on six pre-defined thresholds, each containing a distinct load amount and frequency setpoint. The loads assigned to these threshold settings are spread across the HV/MV substations in which LFDD protection is available. LFDD relays are present at the MV side of the HV/MV transfer which connects the substation to the wider transmission grid. In some locations, LFDD relays are present on the outgoing MV feeders rather than the MV incoming supply. Frequency protection relays placed at the outgoing feeders from a substation allow LFDD actions to disconnect specific MV loads instead of the entire substation, increasing flexibility of the scheme. It has been made clear that future plans exist to include LFDD protection at the outgoing MV feeders in all LFDD substations. The addition of LFDD relays to outgoing feeders of all substations is relevant when developing improvements to the existing LFDD methods, as described in chapter 6.

The six thresholds that comprise the LFDD scheme are designed to each contain 7.5% of the peak system load, leading to a cumulative total load shedding amount of 45%, in line with EU grid code requirements. It is not possible to include exactly 7.5% peak load in each threshold due to the constraints related to the amount of load present at each substation, however, continued efforts are being made to optimise load selection to achieve this 7.5% for each threshold. The estimated amount of load in each threshold is based entirely on yearly average power usage at that substation.

Parameter	Values SA Continental Europe	Values SA Nordic	Values SA Great Britain	Values SA Ireland	Measuring Unit
Demand disconnection starting mandatory level: Frequency	49	48,7 – 48,8	48,8	48,85	Hz
Demand disconnection starting mandatory level: Demand to be disconnected	5	5	5	6	% of the Total Load at national level
Demand disconnection final mandatory level: Frequency	48	48	48	48,5	Hz
Demand disconnection final mandatory level: Cumulative Demand to be disconnected	45	30	50	60	% of the Total Load at national level
Implementation range	± 7	± 10	± 10	± 7	% of the Total Load at national level, for a given Frequency
Minimum number of steps to reach the final mandatory level	6	2	4	6	Number of steps
Maximum Demand disconnection for each step	10	15	10	12	% of the Total Load at national level, for a given step

Figure 3.5: European Grid code requirements for the design of LFDD scheme.

The Dutch LFDD scheme includes six load-shedding steps, one step for each load threshold. The first shedding step begins at a frequency threshold of 49Hz with each subsequent step separated by a margin of 0.2Hz. The final shedding step occurs at 48Hz. Each shedding step is triggered as soon as the frequency breaches the associated threshold. A maximum time delay of 300ms is allowed in the EU grid code for measurement, communication, and circuit breaker opening time. In the Dutch scheme, the aim is to maintain this delay at a maximum of 150ms.

Two blocking criteria are also associated with the Dutch LFDD scheme. To account for distributed generation, a substation cannot be considered for inclusion in the LFDD scheme if this station is feeding energy back to the transmission grid more than 20% of the year. In conjunction with this, an under-voltage inhibit element must be active on all LFDD relays to prevent operation should the voltage drop below 70% of Vnom, to ensure the relay only operates during a true contingency event.

3.6.2. Modelling of Dutch LFDD Scheme

As shown in Table 3.5 all loads were organised based on the percentage of total system demand. Similarly to the current Dutch scheme, the loads were organised into six threshold settings, each to be disconnected when the frequency breaches a certain threshold. In the analysis of the existing LFDD scheme, two separate LFDD schemes were generated based on the same criteria described above. Load active powers, load threshold settings and frequency settings for both schemes are presented in Table 3.5.

Table 3.5: Breakdown of loads and frequency thresholds in the two traditional LFDD schemes used in this analysis.

Load No.	Active Power (MW)	% of total Power	Trap Setting Set 1	Trap Frequency (Hz)	Trap Setting Set 2	Trap Frequency (Hz)
3	322	5.3	Trap 4	48.4		
4	500	8.2	Trap 3	48.6	Trap 6	48
7	233.8	3.8			Trap 4	48.4
8	522	8.6	Trap 1	49	Trap 3	48.6
12	7.5	0.1	Trap 5	48.2		
15	320	5.2	Trap 5	48.2		
16	329	5.4	Trap 4	48.4	Trap 5	48.2
18	158	2.6	Trap 2	48.8	Trap 5	48.2
20	628	10.3				
21	274	4.5				
23	247.5	4.1			Trap 4	48.4
24	308.6	5.1	Trap 6	48		
25	224	3.7			Trap 2	48.8
26	139	2.3			Trap 1	49
27	281	4.6			Trap 1	49
28	206	3.4			Trap 2	48.8
29	283.5	4.6	Trap 2	48.8		
31	9.2	0.2				
39	1104	18.1				
Total	6097.1					

In accordance with the existing Dutch LFDD scheme, the loads were divided in an attempt to create six equal threshold settings, each one shedding approximately 7.5% of the total load. The total load curtailment is close to 45%, in accordance with EU regulations. The only criteria involved in load selection was active power rating. As is the case in the Dutch LFDD scheme, no weight is given to any other parameters such as system strength at load-shedding locations. Similarly to the situation on the Dutch grid, it was not possible to maintain exactly 7.5% load in each threshold, instead the focus was maintained on achieving a total curtailment close to 45% of peak system load.

Table 3.6: Traditional LFDD Schemes developed based on DUtch grid code requirements.

Trap No.	% of Total	Load
	LFDD Scheme 1	**LFDD Scheme 2**
Trap 1	8.6	6.9
Trap 2	7.2	7.1
Trap 3	8.2	8.6
Trap 4	10.0	7.9
Trap 5	5.4	8.0
Trap 6	5.1	8.2
Total	45.1	46.6

3.7. RMS Simulation

In this research, RMS simulations were used to analyse the response of the 39 Bus system to a variety of contingency events under various operating conditions. In all cases, the total simulation time was 20 seconds with the system remaining in steady state operation for 5 seconds before the first event load switching action is completed.

The step size used in calculations was 0.01 seconds. The network was represented as a balanced system, resulting in one output value for voltage or current represented by the positive sequence value.

Simulations were automated using Python software and were carried out for all non-synchronous generation penetration scenarios and contingency event sizes. Results were exported to .csv files and collated into representative figures using Python to enable a concise representation of system behaviour.

In this chapter, the modelling methodology is described for phase 1 of this project which is focused on analysing the performance of the existing Dutch LFDD scheme under various RES penetration scenarios. The test network, event sizes, and RES penetration scenarios presented in this chapter are also used in phase 2 of the project, where improvements to LFDD are proposed and investigated. Results and discussion on the effect of contingency event size, renewable energy penetration, and load composition in LFDD schemes on the performance of LFDD in arresting frequency decline following a disturbance are presented in chapter 4.

4 Existing Dutch LFDD Scheme - Results & Analysis

Understanding the effect of increased inverter-based resource (IBR) penetration on the operation of the traditional Dutch LFDD scheme is essential to developing methods to improve LFDD operation for the future power system. In this chapter, the performance of the existing Dutch LFDD scheme is analysed based on a number of contingency event parameters and LFDD scheme operation characteristics. The modelling and development of LFDD schemes for use in the analysis discussed in this chapter are presented in chapter 3.

The selection of an aggregated frequency representation for all simulations is discussed in section 4.1. The effect of RES penetration and contingency event magnitude on frequency decline and ROCOF without an active LFDD is explored in section 4.2. In section 4.3, the effect of RES penetration on LFDD performance and frequency recovery is analysed. The effect of contingency event size for three separate system inertia levels is discussed in section 4.4. Finally, the effect of uncertainty and variability in load demand in LFDD is analysed in section 4.5.

The aim of this analysis is to understand the operation and performance of the existing Dutch LFDD scheme under various contingencies and RES penetrations levels. Following this analysis, it is possible to identify areas in which the current LFDD scheme may be insufficient as power systems become more complex in the future. These areas for improvement, presented in section 4.6 are then used to develop possible strategies to improve LFDD operations for future system conditions. Improvements on existing LFDD measures are discussed in chapter 5.

4.1. Median and COI Frequency

In order to evaluate the frequency of the test network following a contingency event, it is necessary to create an aggregated frequency measurement that will serve as the representative frequency for the whole system. Two possible aggregated frequency metrics were evaluated based on methods described in [37]. These methods were median frequency and centre of inertia (COI) frequency.

The frequency results taken from simulations are the local frequency at each bus in the system. To calculate the median frequency, these results are sorted in ascending order and the middle value in the list is taken for each time step in the simulation. This simple method is useful as it is not severely skewed by potential outlier frequency measurements at individual buses.

The centre of inertia (COI) frequency is an aggregated frequency measurement that is based on the weighted sum of rotor speeds of the active synchronous generators in the network. The sum is weighted based on the inertia time constant of the synchronous gens. The formula to calculate COI frequency is presented in Equation 4.1 [37].

$$f_{coi} = \frac{\sum_{i=1}^{N} I_i.s_i}{\sum_{i=1}^{N} I_i} \tag{4.1}$$

In the above equation, I_i and s_i represent the inertia time constant and the rotational speed of each generator respectively. As there is a different number of synchronous generators in each scenario, the calculation of COI frequency in each scenario is different. Consequently, it was decided to use two different RES penetration scenarios to compare the frequency calculations using median and COI values, one with low RES penetration (SNSP 9%) and one with high RES penetration (SNSP 66%).

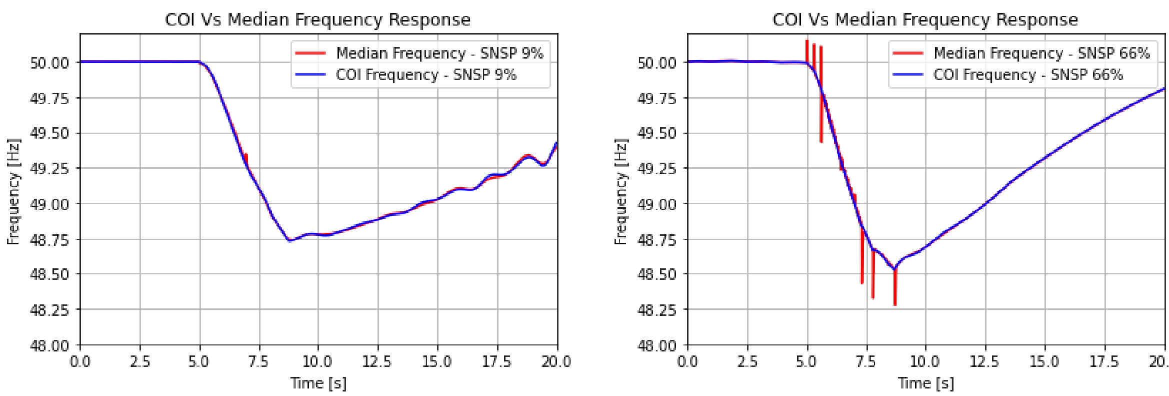

(a) Frequency Plot - COI Vs Median - SNSP 9%.

(b) Frequency Plot - COI Vs Median - SNSP 66%.

Figure 4.1: Frequency Plot - Comparison of frequency trajectory using median and COI frequency.

As shown in Figure 4.1, the median and COI frequency measurements appear to match both for low and high RES penetration scenarios. It can be seen that the median frequency displays spikes during switching events at the instance of the contingency event and during LFDD switching operations. It was decided to use COI frequency as the representative frequency in this study as this is an industry-standard parameter and provides a smoother curve for evaluation. All further frequency plots in this report are based on COI frequency. Simulation results also indicate that median frequency becomes a less representative metric for aggregated frequency as RES penetration increases. It is evident from the figure that spikes in median frequency, which occur at the instance of switching events, are more exaggerated in the plot based on the SNSP 66% scenario.

4.2. Effect of RES Penetration and Contingency Event Size on Frequency and ROCOF

In this section, the effect of changes in contingency size and system inertia on frequency trajectory and ROCOF are explored. The test network setup for these simulations is described in section 3.2. Simulations presented in this section were carried out with no load-shedding schemes active to understand the thresholds for system recovery without emergency restoration actions. In Figure 4.2, the effect of increased RES penetration and changes in contingency size on frequency deviation is shown. Minimum frequency and ROCOF values for all inertia levels and contingency event sizes are shown in Table 4.1.

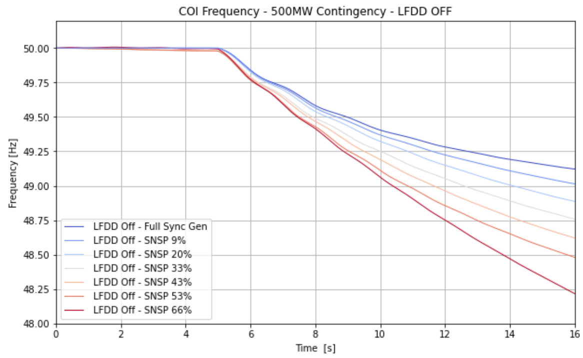

(a) Frequency Plot - 500MW Contingency Event - LFDD OFF.

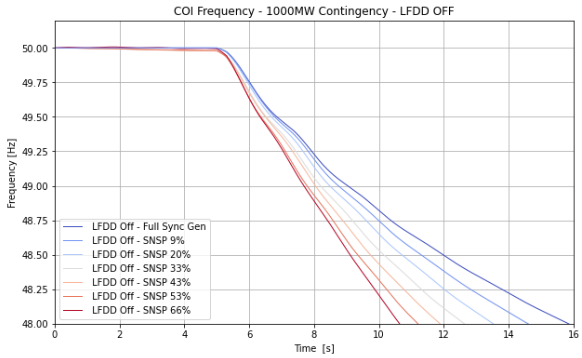

(b) Frequency Plot - 1000MW Contingency Event - LFDD OFF.

Figure 4.2: Frequency Plot - Analysis of effect of contingency event size and RES penetration level on ROCOF and frequency decline.

Table 4.1: Frequency and ROCOF table - No LFDD Active.

Event Size	500MW		1000MW	
Scenario	Min Frequency [Hz]	Min ROCOF [Hz/s]	Min Frequency [Hz]	Min ROCOF [Hz/s]
Full Sync Gen	49.029	-0.210	47.607	-0.371
SNSP 9%	48.877	-0.212	47.429	-0.373
SNSP 20%	48.713	-0.222	47.208	-0.396
SNSP 33%	48.572	-0.237	47.123	-0.463
SNSP 43%	48.407	-0.240	46.901	-0.422
SNSP 53%	48.246	-0.305	46.697	-0.469
SNSP 66%	47.770	-0.264	45.770	-0.484

It can be seen that higher RES penetration results in a greater frequency deviation and a higher rate of change of frequency. In Figure 4.2a, the graph showing frequency deviation for a contingency event of 500MW, the minimum frequency in fully synchronous generation scenario is 48.6Hz while this value drops to 48.1Hz for the scenario with 66% SNSP. Similarly, the minimum ROCOF value is increased as RES penetration is increased, this can pose a potential danger to synchronous machines connected to the network which may disconnect if ROCOF breaches a threshold typically in the range of 1-2Hz/s.

In Figure 4.2b results are shown for a contingency event size of 1000MW. It can be seen from Table 4.1 that the minimum ROCOF is now -0.484Hz/s in scenario SNSP 66% which is almost double the ROCOF magnitude seen in the same scenario for an event size of 500MW. This increase in ROCOF due to a larger contingency event size can be seen for all simulated scenarios. Based on the above graphs, it can be concluded that increased RES penetration on the grid could result in higher ROCOF, and greater frequency deviation in the future. It can also be seen that the effect of higher contingency size on frequency deviation and ROCOF magnitude increases as RES penetration increases. The ROCOF increases by 76% between the two events in the Full Sync Gen scenario while the ROCOF increases by 83% in the SNSP 66% scenario. These results indicate that there is potential for larger contingency events to cause more harm to network stability if the RES penetration is higher and the corresponding grid inertia is lower.

4.3. Effect of RES Penetration on LFDD Performance

The effect of increased RES penetration and reduced system inertia on the performance of the traditional Dutch LFDD is analysed in this section. The generation of the various system operating scenarios used in this analysis are described in section 3.3. The main parameters used in evaluation of the LFDD performance are the frequency nadir and load shedding amount required to restore the frequency to nominal levels following a contingency event.

In Figure 4.3 the response of the network with LFDD active is shown for a contingency event of 1000MW. The load shedding amount in each renewable energy penetration scenario is also presented. Load shedding amount is dependent on the minimum frequency value seen in each system configuration.

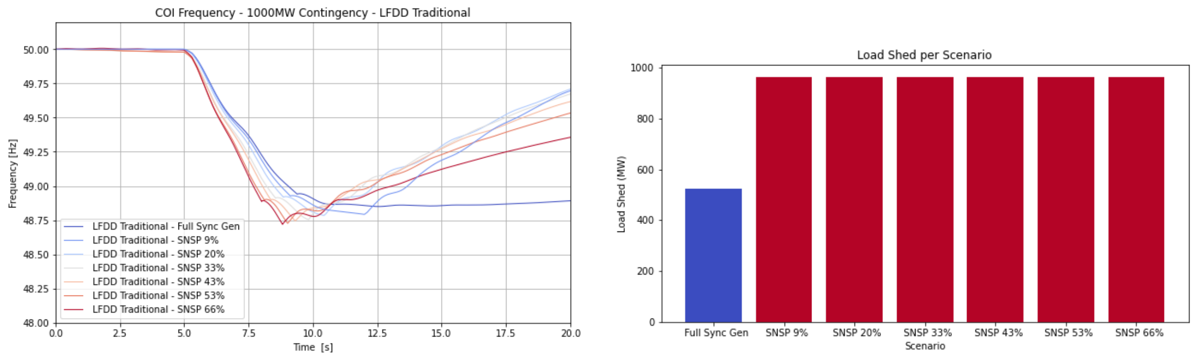

(a) Frequency Plot - 1000MW Contingency Event - LFDD Traditional **(b)** Bar Chart - Load Shedding amount per scenario - 1000MW event

Figure 4.3: Frequency Plot and load shedding amount for 1000MW contingency event with traditional LFDD.

The effect of lower system inertia can be seen in the difference in load shedding amount between fully synchronous generation and the remaining operating scenarios. In these lower inertia scenarios, the frequency nadir is deeper, causing more load to be shed. This is illustrated in the bar plot in Figure 4.3b. The result of breaching the second LFDD threshold of 48.8Hz and shedding an extra 7.5% of peak load is a more rapid return towards the nominal frequency, evident in Figure 4.3a .

In scenarios with lower system inertia, earlier activation of the LFDD scheme can be seen than in scenarios with more synchronous generation active. This is understandable due to the increased ROCOF also seen in low inertia scenarios. Scenarios with SNSP greater than 20% see trap 2 breached in 9s. The same threshold is breached almost two seconds later in the scenario with 9% SNSP.

Frequency trajectory and load shedding amounts for a contingency event of 1500MW are displayed in Figure 4.4.

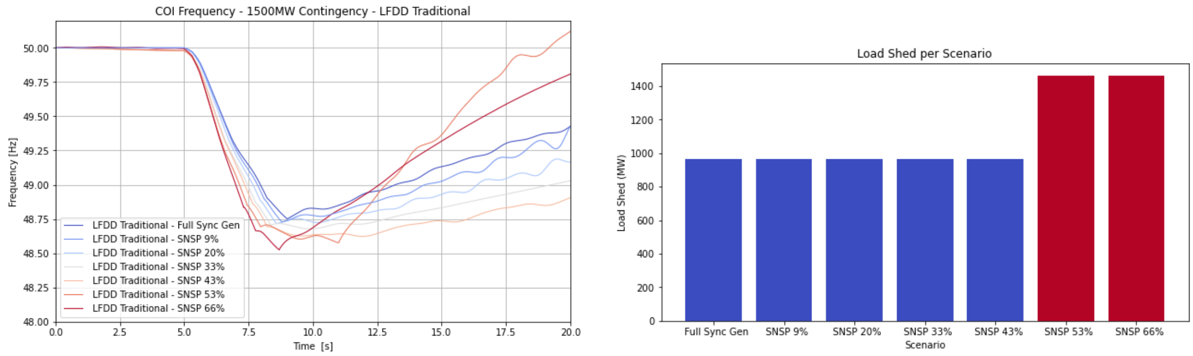

(a) Frequency Plot - 1500MW Contingency Event - LFDD Traditional.

(b) Bar Chart - Load Shedding amount per scenario - 1000MW event.

Figure 4.4: Frequency Plot and load shedding amount for 1500MW contingency event with traditional LFDD.

Increased load shedding due to reduced system inertia is only seen in the two highest RES penetration scenarios for an event of this magnitude. This highlights that the effect of increased RES penetration on LFDD performance may differ based on contingency event size. It is clear that frequency decline is arrested for all scenarios following activation of the LFDD scheme as the frequency begins to return towards nominal values.

It is important to note that shedding more load for the same contingency event could result in overshoot of frequency as the system recovers. This is apparent in Figure 4.4a as the slope of the frequency for the SNSP 66% and SNSP 53% scenarios does not appear to lessen as the frequency reaches 50Hz. The graphs above also highlight the effect of the fixed thresholds used in the traditional LFDD scheme. In some cases, the frequency breaches the 48.6 Hz threshold of trap 3 by a small margin and still the full 7.5% of load in this threshold is shed. It is possible that the system could recover without shedding the whole of the added 7.5% total load in trap 3 during an event such as this.

4.4. Effect of Contingency size on LFDD Performance

The effect of contingency event size on the performance of the existing LFDD scheme was analysed for varying levels of system inertia. In Figure 4.5, results for the Full Sync Gen, SNSP 33%, and SNSP 66% scenarios are presented. It can be seen that a higher contingency size results in higher ROCOF for all scenarios. This may be useful for future schemes in which ROCOF could be used to estimate the power imbalance and thus the expected frequency deviation in the system. The inconsistency in the rate of frequency recovery post LFDD actions for various contingency sizes and RES penetration levels can be seen in the Figure 4.5.

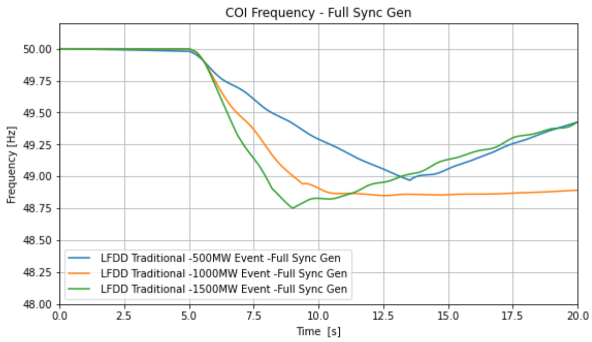

(a) Frequency Trajectory following different contingency event sizes - Full Sync Gen scenario.

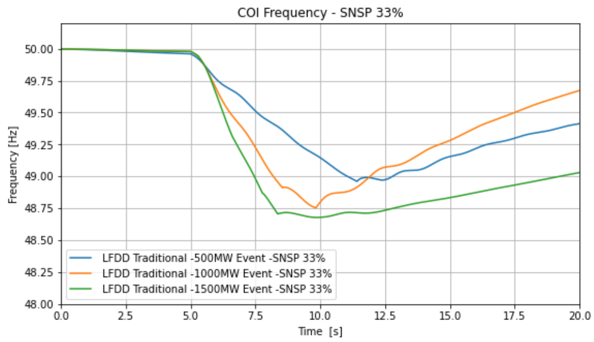

(b) Frequency Trajectory following different contingency event sizes - SNSP 33% scenario.

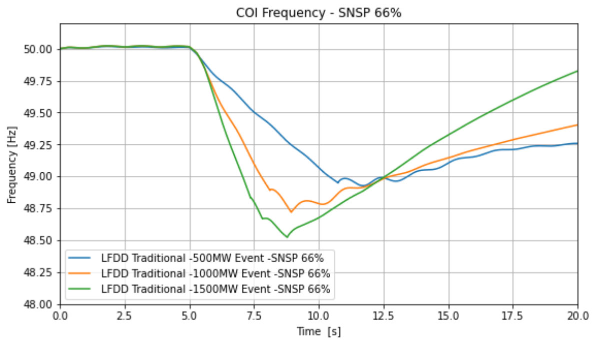

(c) Frequency Trajectory following different contingency event sizes - SNSP 66% scenario.

Figure 4.5: Frequency plots to illustrat the effect of contingency event size on performance of LFDD at different RES penetration and system inertia levels.

Limitations of the LFDD scheme which could be caused by the fixed thresholds for shedding can be seen in all presented scenarios. In the Full Sync Gen scenario, during the 1000MW contingency event, only one LFDD threshold is breached while the frequency comes within 0.05Hz of breaching a second threshold. The frequency decline is successfully stopped, however the system exhibits a slow recovery and the frequency is still below 49Hz at the end of the 20 second simulation.

In the SNSP 33% scenario, the recovery of frequency following LFDD actions is faster for the 1000MW contingency in comparison to the other two event sizes. This is in contrast to the response to the same event size seen for the Full Sync Gen scenario. In the SNSP 33% simulation, it is possible that the load shedding amount was higher than needed to arrest frequency decline and consequently the frequency recovers quickly while showing characteristic of potential overshoot due to the steep recovery slope.

In the 66% SNSP scenario, following the 1500MW contingency event, the frequency drops slightly below 48.6Hz, triggering trap 3 to shed its 7.5% load. In this simulation, it is possible that more load than necessary has been shed and there is a risk of frequency overshoot due to a surplus in supply as primary response of generators takes effect. It may be possible to arrest the frequency decline and restore stability to the system without shedding the total 7.5% load in trap 3.

Table 4.2: Minimum ROCOF and frequency values for all RES penetration scenarios in response to three different contingency events.

Event Size	500MW		1000MW		1500MW	
Scenario	**Min Frequency [Hz]**	**Min RoCoF [Hz/s]**	**Min Frequency [Hz]**	**Min RoCoF [Hz/s]**	**Min Frequency [Hz]**	**Min RoCoF [Hz/s]**
Full Sync Gen	49.029	-0.210	48.850	-0.371	48.752	-0.471
SNSP 9%	48.983	-0.212	48.792	-0.373	48.728	-0.571
SNSP 20%	48.976	-0.222	48.785	-0.396	48.716	-0.511
SNSP 33%	48.970	-0.237	48.754	-0.463	48.678	-0.564
SNSP 43%	48.963	-0.240	48.744	-0.422	48.626	-0.577
SNSP 53%	48.957	-0.305	48.727	-0.469	48.576	-0.628
SNSP 66%	48.931	-0.264	48.719	-0.484	48.524	-0.688

It has been shown in this section that the performance of traditional LFDD can vary largely depending on the contingency event size and the associated minimum frequency value. In some cases, a slow frequency recovery can be seen if the event size is such that the frequency nadir sits just above an LFDD frequency threshold. Conversely, if the minimum frequency value for an event is just below an LFDD frequency threshold, overshedding can occur due to the requirement to shed all 7.5% peak load once a given frequency threshold is breached.

4.5. Effect of Real-Time Load Demand on LFDD Performance

As discussed in chapter 3, in the existing Dutch LFDD scheme, loads are randomly allocated into one of six thresholds with the only selection criteria being the availability of LFDD relays and the aim to create six thresholds, each containing 7.5% of the total load. The yearly average power of each load group is used to estimate the total load contained in each threshold. Due to the characteristics of a real-world power network, it is not possible in practice to keep exactly 7.5% total load in each threshold. However, the requirement to shed 45% total load combining all thresholds is adhered to. No consideration is given to the physical or electrical location of loads in each trap threshold.

The aim of the analysis in this section is to investigate the effect of slight variations of load percentage in LFDD thresholds on the overall performance of the LFDD scheme. As loads are assigned to threshold settings based on yearly average power, it is probable that at the instance of a given contingency event, the actual power demand of a given load could be higher or lower than the average value and therefore the actual load shedding amount may be different to the predicted value.

As described in section 3.6, two distinct LFDD schemes were developed based on the Dutch grid code requirements, each with slightly different load distribution to simulate the case where the actual load in a given threshold is not equal to the predicted 7.5%. The primary differences between the two schemes are that Scheme 1 contains 8.5% total load in threshold 1 and Scheme 2 contains 6.9% of the total load in threshold 1. Both schemes shed a similar amount in threshold 2, with the total accumulated load shed after threshold 2 (48.8 Hz) being greater for scheme 1.

The effect of random load allocation and uncertainty regarding exact load size was analysed for all scenarios. Results are presented for the SNSP 9%, SNSP 43%, and SNSP 66% scenarios in Figure 4.6. The schemes exhibit different behaviour, particularly in the rate of frequency recovery, depending on the magnitude of frequency deviation. When comparing the frequency trajectory for events at the same inertia level, it is assumed the primary factor affecting the difference in frequency deviation is the load-shedding amount in each threshold.

Table 4.3: Minimum ROCOF and frequency values at three RES penetration levels for three distinct LFDD schemes.

	SNSP 9%		SNSP 43%		SNSP 66%	
Scenario	**Min Frequency [Hz]**	**Min RoCoF [Hz/s]**	**Min Frequency [Hz]**	**Min RoCoF [Hz/s]**	**Min Frequency [Hz]**	**Min RoCoF [Hz/s]**
LFDD Set 1	48.728	-0.475	48.627	-0.577	48.526	-0.662
LFDD Set 2	48.590	-0.475	48.552	-0.577	48.523	-0.662
LFDD Off	46.547	-0.571	46.059	-0.561	45.125	-0.688

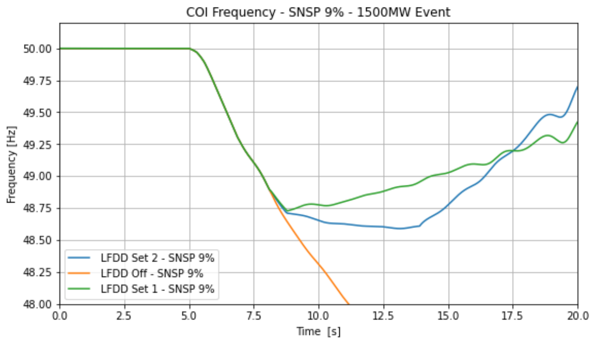

(a) Frequency trajectory for 1500MW event based on three distinct LFDD schemes - Scenario SNSP 9%.

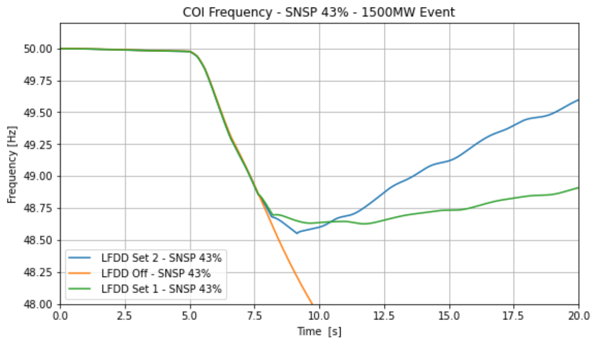

(b) Frequency trajectory for 1500MW event based on three distinct LFDD schemes - Scenario SNSP 9%.

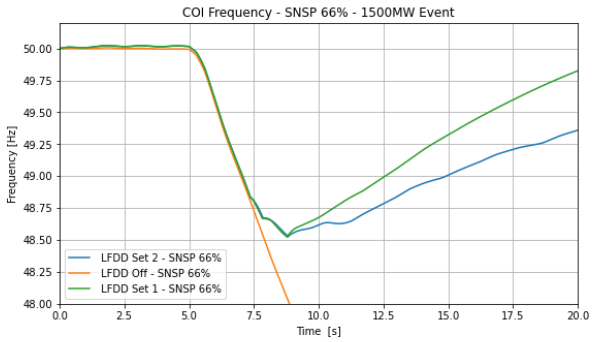

(c) Frequency trajectory for 1500MW event based on three distinct LFDD schemes - Scenario SNSP 9%.

Figure 4.6: Frequency plots for 1500MW Contingency event. Comparison of three different LFDD Schemes.

In the SNSP 9% scenario, Scheme 1 exhibits a slower frequency recovery than Scheme 2. This is due to the higher amount of load being shed in trap 1 for the first scheme. In Full Sync Gen scenario, Scheme 1 only sheds load from trap 1 (8.6% total) while scheme 2 sheds load from traps 1 and 2 (15% total). Although the difference in load in trap 1 is 1.7% for these schemes, the effect on frequency recovery can be noticed, particularly should the frequency nadir fall close to a trap threshold frequency.

In the SNSP 66% scenario, both Schemes trip loads in trap 1 and trap 2. In this case, Scheme 1 exhibits a more rapid frequency recovery than Scheme 2 due to the higher cumulative amount of load being shed. In this simulation, the effect of lower system inertia results in the frequency breaching the trap 2 thresholds for both schemes.

4.6. Overall assessment of existing Dutch LFDD Scheme

In this chapter, the effect of lower system inertia and higher ROCOF on the performance of the existing LFDD scheme in the Netherlands is investigated. This scheme is analysed based on RES penetration level, contingency event size, and the effect of uncertainty and random load allocation in LFDD bus selection criteria.

It can be seen that traditional LFDD is effective in arresting frequency decline and restoring balance to the system for all inertia levels and contingency event sizes. Although the existing LFDD scheme does successfully stop frequency decline for this test network, several areas for improvement have been identified in relation to load bus selection and the ability of the LFDD scheme to adapt to lower inertia scenarios.

The following areas for improvement are identified in relation to the existing Dutch LFDD scheme:

- **Load Selection Criteria - Real-time Power Demand:** Selection of loads for individual thresholds is based solely on yearly active power usage. This criterion is limiting as no attention is given to variation in load demand throughout the year. Similarly, the only criterion regarding distributed generation is a requirement not to include locations that feed power back to the transmission grid more than 20% of the year. Considering the expected increase in DER generation in the future power system, this requirement may lead to disconnections of DERs and insufficient overall power being shed.

- **Fixed Frequency Thresholds:** The fixed nature of the existing LFDD scheme is a limiting factor in enabling the scheme to adapt to changes in inertia level or contingency event size. Such a simple discrete scheme with 7.5% load in each trap threshold is vulnerable to over or under shedding when the frequency nadir is close to frequency threshold values for a particular trap setting. In the future power system, as ROCOF and frequency deviation escalate due to reduced inertia, a more intelligent LFDD scheme may be required to provide an adequate response to all event scenarios.

- **Static Scheme:** As the power network becomes more fluid in configuration with increased IBR penetration and bi-directional power flows that vary throughout the year, the response of the system to LFDD could vary in comparison to the traditional system. Due to topology changes in the system, the locations of strong and weak points in the network may vary as the level of synchronous generation changes and fault levels vary throughout the year. Maintaining one fixed LFDD scheme that does not adapt to changes in power flow, network strength, distributed generation, or system topology could result in wide variations in the effectiveness of this scheme in responding to contingency events.

- **Delayed response - 49Hz Threshold:** The existing LFDD scheme in the Netherlands is a purely reactive scheme designed as a last resort mechanism to arrest frequency decline and prevent blackouts. As the power system changes and the impact of disturbances increases, it may be beneficial to include proactive measures which activate before the frequency has dropped to the 49Hz threshold. The result of these proactive measures could be a reduced frequency deviation and accelerated frequency recovery even for the most severe events during instances of low system inertia.

In this chapter, performance analysis has been completed on the existing Dutch LFDD scheme based on the methodology outlined in chapter 4. It is clear that this scheme is hindered by its inability to shed the optimal amount of load for all contingency event sizes and RES penetration scenarios. Furthermore, no consideration is given to parameters that can be expected to vary dynamically in future power systems such as active DER generation and network strength at LFDD locations. This analysis, in conjunction with the literature research presented in chapter 2 is used to develop ideas for improvement to existing LFDD measures, described in chapter 5, which would enhance performance in systems with higher concentration of IBRs and lower system inertia. In the following chapters, the justification, modelling methodology, and results for all proposed LFDD improvements are presented.

5

Proposed Improvements to LFDD - Methodology

The analysis of the performance of the existing Dutch LFDD scheme under various non-synchronous generation penetration levels and contingency event sizes highlighted a number of areas for possible improvement. These areas for improvement are described in detail in section 4.6. An overview of the two project stages is presented in Figure 5.1. In phase 1, the areas for improvement identified in the existing LFDD scheme are shown. In phase 2, the potential improvements and alternative methods to this scheme that are investigated are outlined.

This chapter is focused on the methodology used to model and investigate each of the proposed areas for improvement to LFDD. In all cases, the grid network and contingency event sizes used in analysis were the same as those used in the analysis of the existing LFDD scheme and described in chapter 3. Modelling of improvements was focused on generating simulations that would give an impression of the relative benefits, if any, associated with the proposed changes to LFDD in comparison with the traditional Dutch scheme.

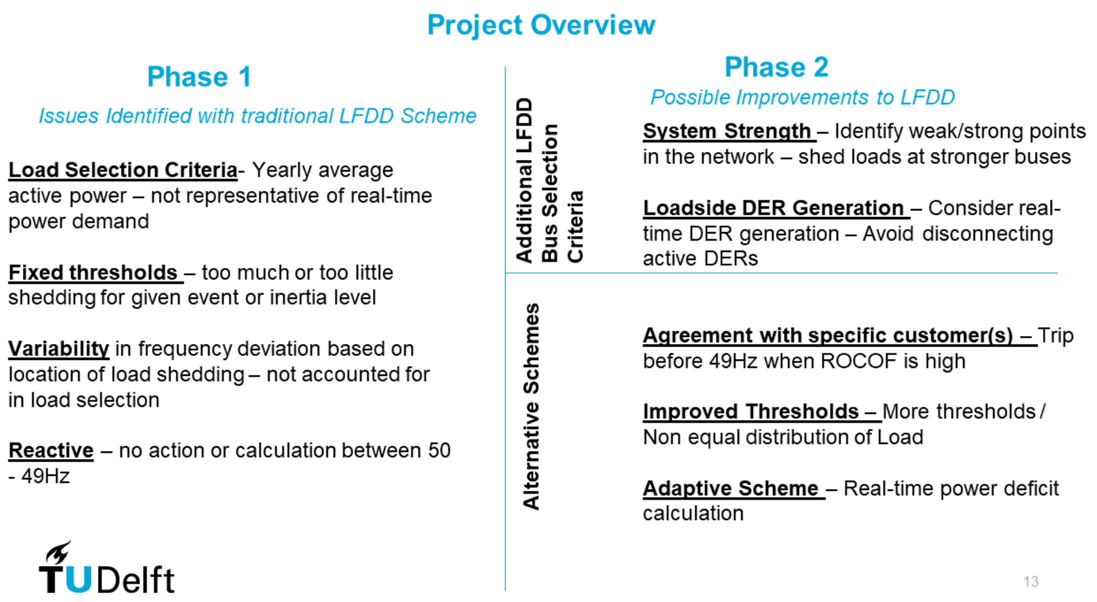

Figure 5.1: Project overview.

As detailed in Figure 5.1 five methods for improvement to existing LFDD measures have been proposed. Firstly, the methodology for studying the proposed improvements to LFDD load selection criteria is defined. In section 5.1, the methodology for investigating the effect of disconnecting active DER generation during LFDD is described. In section 5.2, the method for investigating the effect of including network strength under different system configurations as an added parameter in LFDD load bus selection is discussed. Secondly, the modelling and analysis method for investigating proposed alternative load-shedding mechanisms is described. The process of investigating the effect of varied load distribution in LFDD trap thresholds is described in section 5.3. Modelling and investigation of proactive ROCOF based disconnection of specific consumers is outlined in section 5.4. The development and testing of a simple adaptive load shedding scheme based on real-time power deficit estimation is described in section 5.5.

5.1. Load Selection Criteria - Active DER Generation

In order to analyse the effect on system dynamics of disconnecting active distributed energy resources (DERs) during LFDD, six DER units were added to the test grid network. A standard DER model template, available in PowerFactory software, was used to model the distributed generation units.

As shown in Figure 5.2, DER units were connected to the test network through a transformer. The nominal voltage of the DER units is 10kV. The transformer is used to connect all DERs to the transmission network at a bus voltage of 345kV. As the amount of DER generation was varied in different simulations, the transformer MVA rating was adapted to be suitable for the associated DER in each scenario.

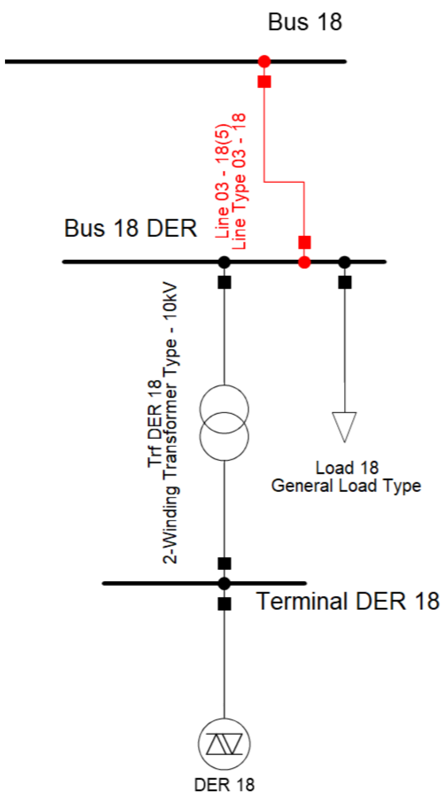

Figure 5.2: Schematic of DER added to Power Factory model

The aim of this section of analysis is to understand the effect of unintentionally disconnecting active DER generation during LFDD switching operations. Therefore, six DER units were added to the model at the bus locations that were already included in the LFDD scheme. The LFDD scheme used for these simulations is a traditional LFDD scheme based on the Dutch grid code.

The active power output of the DER was varied between 25%, 50%, and 75% of the load connected at the same bus, as outlined in Table 5.1. Simulations were carried out for various contingency event sizes to assess the impact of disconnecting active DERs on the performance of the LFDD scheme. Each simulation (a combination of a certain contingency event size and DER generation percentage) was carried out for all RES penetration scenarios. Thus allowing the effect of reduced inertia on system resilience to tripping DERs to be examined.

Table 5.1: Active power rating values for various DER generation levels.

Bus No.	Load Active Power (MW)	DER Active Power 25% Load (MW)	DER Active Power 50% Load (MW)	DER Active Power 75% Load (MW)
3	322	80.5	161.0	241.5
4	500	125.0	250.0	375.0
8	522	130.5	261.0	391.5
16	329	82.3	164.5	246.8
18	158	39.5	79.0	118.5
29	283.5	70.9	141.8	212.6
Total	2114.5	528.6	1057.3	1585.9

In order to maintain the power balance on the network with the addition of the new generation units, it was necessary to reduce the active power dispatch of some synchronous generators. It was decided to reduce the active power dispatch of generators G01, G03, and G05 to compensate for the DER generators in all RES penetration scenarios, as shown in Table 5.2. The reason these generators were selected for reduced power dispatch is they are active in all scenarios and therefore the composition of the model is changed as little as possible for each RES penetration level.

Table 5.2: Altered Power of Synchronous Generators to account for added DER generation.

Sync Gen Name	Active Power Dispatch DER 25% (MW)	Active Power Dispatch DER 50% (MW)	Active Power Dispatch DER 75% (MW)
G01	823.8	647.6	407.5
G03	473.8	297.58	61.5
G05	165.9	77.79	54

The DER generation percentage was not increased beyond 75% as the aim of these simulations is to understand the effect of tripping a DER which may not be producing more energy than the associated load. In this situation, the associated substation would not be feeding power back to the transmission grid. It is possible that a location such as this would not feed power back to the transmission grid more than 20% of the year and therefore could realistically be included in an LFDD scheme.

The focus of this analysis is to understand the effect of tripping active DERs on the frequency decline and recovery following a contingency event and LFDD activation, therefore, frequency trajectory is the primary variable used in the analysis of this section.

5.2. Load Selection Criteria - Network Strength

The ability of power system equipment to operate in a stable fashion and the capacity of the entire network to withstand and recover from disturbances is influenced by the "strength" of the electrical system. [38]. Short-circuit power (also referred to as fault level) at a certain point in the network is the fault current that would flow in the event of a short circuit at that location. Short-circuit power can be calculated based on the minimum or maximum fault current that would flow for a given location in a particular network configuration [38].

In recent years, fault levels have been used as an indication of system strength, particularly in systems with a higher penetration of IBRs. Higher fault levels correspond to a "stronger system". Lower fault levels indicate a "weak" system which is associated with a high sensitivity of voltage magnitude and phase angle to changes in active and reactive power flow.

During a contingency event, power flows in a network can change rapidly due to sudden changes in loading conditions. This phenomenon could also be seen during the load-switching operations of LFDD. Consequently, it was decided to investigate the effect of system strength at locations where LFDD takes place to understand whether this parameter could be useful when deciding what locations should be included in an LFDD scheme for a particular network configuration.

5.2.1. Modelling - System Strength

Minimum short-circuit power is a common parameter used in industry to assess system strength at a given location. Therefore, this parameter was used as the metric for system strength at each bus in the test network. Minimum short circuit power was calculated for each bus, according to the IEC60909 standard, and the results were used to develop LFDD schemes with network strength as a load selection criterion. To understand the effect of RES penetration on system strength, particularly the location of the strongest and weakest buses in the network, minimum short circuit power calculations were completed for all RES penetration scenarios.

The effect of system strength at LFDD load shedding locations on the performance of LFDD was analysed for two RES penetration scenarios: Full Sync Gen and SNSP 66%. Following the short circuit calculation mentioned above, load buses were ranked in descending order based on system strength. Two traditional LFDD schemes (7.5% peak load in each threshold setting) were developed based on the system strength calculations. One scheme was designed to include the loads at the strongest buses in the earliest LFDD threshold settings. The second scheme was designed to include the loads connected to the weakest buses in the network in the early LFDD threshold settings. Two schemes are shown in Table 5.3 where the network strength calculations were completed for the fully synchronous generation scenario.

Table 5.3: Description of two LFDD schemes generated using network strength results from Full Synchronous Generation Scenario.

Load No.	Active Power (MW)	% of total Power	Bus SC Power - Full sync (MVA)	% of total SC Power	LFDD weak buses	LFDD strong buses
3	322	5.3	7358.7	4.7	Trap 6	Trap 3
4	500	8.2	6929.8	4.4	Trap 5	Trap 4
7	233.8	3.8	5838.4	3.7		Trap 5
8	522	8.6	6050.8	3.8	Trap 3	
12	7.5	0.1	2838.1	1.8		Trap 6
15	320	5.2	6341.3	4.0		
16	329	5.4	8916.6	5.6		Trap 1
18	158	2.6	6392.4	4.0	Trap 4	Trap 1
20	628	10.3	5049.3	3.2		
21	274	4.5	6016.6	3.8		Trap 5
23	247.5	4.1	6194.2	3.9		Trap 2
24	308.6	5.1	6570.4	4.2	Trap 4	Trap 6
25	224	3.7	7031.7	4.5		Trap 2
26	139	2.3	5275.3	3.3	Trap 2	Trap 3
27	281	4.6	5014.7	3.2	Trap 1	
28	206	3.4	3446.7	2.2	Trap 1	
29	283.5	4.6	4531.2	2.9	Trap 2	
31	9.2	0.2	5833.5	3.7		Trap 6
39	1104	18.1	52263.0	33.1		
Total	6097.1		157892.7		44.6	47.6

As mentioned previously, the effect of network strength at load-shedding locations on LFDD performance was also analysed based on system strength during high a RES penetration scenario. The LFDD schemes developed for the SNSP 66% scenarios are outlined in Table 5.4.

Table 5.4: Description of two LFDD schemes generated using network strength results from SNSP 66% scenario.

Load No.	Active Power (MW)	% of total Power	Bus SC Power SNSP 66% (MVA)	% of total SC Power	LFDD Weak Buses	LFDD Strong Buses
3	322	5.28	4189.2	3.7		
4	500	8.20	5185.5	4.5	Trap 6	Trap 1
7	233.8	3.83	5168.1	4.5	Trap 5	Trap 3
8	522	8.56	5359.2	4.7		Trap 2
12	7.5	0.12	2624.7	2.3	Trap 4	Trap 6
15	320	5.25	3840.5	3.4		Trap 6
16	329	5.40	4075.2	3.6		Trap 4
18	158	2.59	3691.3	3.2	Trap 4	
20	628	10.30	3417.1	3.0		
21	274	4.49	2798.6	2.4	Trap 5	Trap 5
23	247.5	4.06	2270.3	2.0	Trap 2	
24	308.6	5.06	3333	2.9	Trap 3	
25	224	3.67	3014.2	2.6	Trap 2	Trap 3
26	139	2.28	2512.6	2.2	Trap 3	Trap 4
27	281	4.61	2780.4	2.4	Trap 4	
28	206	3.38	1440.7	1.3	Trap 1	Trap 5
29	283.5	4.65	1403.6	1.2	Trap 1	
31	9.2	0.15	5609.1	4.9		
39	1104	18.11	51630.9	45.2		
Total	6097.1		114344.2			

The goal behind this method of modelling the LFDD schemes is to assess whether system strength calculations carried out for commonly used network topologies could be useful in selecting locations for LFDD to promote a more robust response to contingency events, particularly in scenarios with high RES penetration. The analysis in this section was carried out for contingency event sizes of 500MW, 1000MW and 1500MW for both RES penetration levels.

5.3. Alternative Load Distribution in LFDD

As discussed in chapter 4, the fixed nature of the traditional Dutch LFDD scheme combined with the requirement to maintain 7.5% peak load in each of the six thresholds can result in sub-optimal performance in response to certain contingency events. As the scheme does not incorporate an adaption based on event size or inertia level, it is clear that an optimal response cannot be ensured for all event sizes and system inertia levels.

In this section, the possibility of developing a series of fixed LFDD schemes is investigated. These schemes could have a non-equal distribution of load in the trap thresholds and may also include more trap settings than the 6 thresholds required by the Dutch grid code. The aim of this section of analysis is to understand whether one LFDD scheme could be chosen from a selection of schemes, with different compositions and load distributions, based on the predicted level of rotational inertia present at a given instance. In this mode of operation, it is possible that the performance of the LFDD would be improved as the overall defence of the network would become more adaptive and would no longer be constrained to one single LFDD scheme option.

5.3.1. Modelling of Alternative LFDD Schemes

To investigate the effect of different distributions of load on LFDD performance, three distinct LFDD schemes were developed. As shown in Table 5.5, The LFDD schemes vary in terms of load distribution, trap frequency setting, and number of trap thresholds. The purpose of this analysis is to understand whether improved performance in terms of frequency deviation and load shedding amount can be found for certain inertia levels by varying the LFDD scheme in comparison to the traditional Dutch scheme described in chapter 3. Each LFDD scheme is designed to shed a total of 45% load and the max load in one trap threshold is maintained at 10% peak load to align with European grid code requirements.

In Scheme 1 – more load is distributed in thresholds 1 and 2 (10% each), with the remaining load distributed evenly among the remaining thresholds. The number of load thresholds and associated frequency settings are maintained in line with the traditional Dutch scheme, 6 trap settings separated by 0.2Hz, beginning at 49Hz.

In Scheme 2 – less load is distributed in thresholds 1 and 2 (5% each) with the remaining load distributed evenly among the 4 remaining thresholds. The number of load thresholds and associated frequency settings are maintained in line with the traditional Dutch scheme, 6 threshold settings separated by 0.2Hz, beginning at 49Hz.

In Scheme 3 – 9 load thresholds are included in the scheme, each containing 5% peak load. As there are more load thresholds in this scheme, the frequency thresholds settings are spaced closer together, typically 0.1Hz or 0.15Hz apart.

Table 5.5: Load allocation and frequency threshold settings for alternative LFDD schemes.

Load No.	Active Power (MW)	Alternate Scheme 1	Frequency Threshold [Hz]	Alternate Scheme 2	Frequency Threshold [Hz]	Alternate Scheme 3	Frequency Threshold [Hz]
3	322	Trap 2	48.8	Trap 1	49	Trap 5	48.5
4	500	Trap 3	48.6				
7	233.8	Trap 4	48.4	Trap 6	48		
8	522			Trap 4	48.4		
12	7.5						
15	320	Trap 2	48.7	Trap 5	48.2	Trap 4	48.65
16	329	Trap 1	49			Trap 3	48.8
18	158	Trap 1	49				
20	628						
21	274	Trap 4	48.4	Trap 2	48.8	Trap 6	48.4
23	247.5			Trap 6	48	Trap 8	48.1
24	308.6	Trap 5	48.2			Trap 1	49
25	224	Trap 1	49	Trap 3	48.6	Trap 9	48
26	139	Trap 6	48			Trap 9	48
27	281			Trap 3	48.6	Trap 2	48.9
28	206						
29	283.5			Trap 5	48.2	Trap 7	48.25
31	9.2						
39	1104						

Performance of each of the three LFDD schemes was analysed in response to three contingency event sizes, 500MW, 1000MW, and 1500MW generation loss. Each simulation was carried out for all inertia levels and the results were compared between the three new schemes and also between the new schemes and the existing Dutch LFDD scheme.

The concept behind this analysis is to understand whether certain LFDD scheme types are more suitable for particular inertia levels. If this is the case, it is possible that a number of LFDD schemes could be developed and selected for operation based on the predicted inertia level. If a contingency event were to occur, the previously selected LFDD scheme for that time period would then activate to mitigate the frequency deviation as effectively as possible.

5.4. Proactive - ROCOF Based Disconnection before 49Hz

As mentioned in section 1.3, one aspect of this project is to investigate the possibility of taking action to arrest frequency deviation before the frequency has reached the 49Hz threshold to activate LFDD. As the existing Continental Europe Synchronous Area (CESA) network does not regularly experience major frequency deviations, any additional measures which would activate before 49Hz should ideally only activate in cases where the frequency deviation is expected to be severe. In cases where the standard LFDD scheme is expected to be sufficient to allow the system to recover, no additional load-shedding actions should take place before 49Hz.

In the European grid code [23], it is mentioned that agreements can be made with specific consumers to disconnect before the frequency reaches 49Hz. In this case, it is also possible to implement a protection scheme that functions based on a ROCOF threshold and not the typical frequency threshold that is used in LFDD.

It was decided to investigate the possibility of disconnecting particular consumers by applying a ROCOF-based protection relay with definite time characteristics at certain load buses. The effect of disconnecting a specific consumer (or consumers) based on ROCOF was analysed under three criteria. 1. Load size 2. ROCOF Threshold 3. Definite time delay.

5.4.1. Modelling of ROCOF-based Disconnection

The protection relay used for ROCOF-based disconnection is the standard F81R df/dt relay available in PowerFactory software. In each simulation case, one load, which is not already included in the LFDD scheme, is selected for additional ROCOF protection. The selected loads and varied ROCOF relay parameters are presented in Table 5.6.

Table 5.6: Parameters which are varied during investigation of ROCOF-based relay for disconnections before 49Hz.

ROCOF Threshold [Hz/s]	Load Size % of Peak	Time Delay [s]
0.2 - 0.5	2.3 - 4.6	0.5 - 3

In order to avoid voltage collapse and maintain numerical stability in the simulation solver, the maximum amount of load disconnected by the ROCOF relay was 4.6%. Shedding higher load amounts using the ROCOF-based protection caused numerical instability due to voltage fluctuations in the simulation which could not be solved within the time constraints of this research.

Performance of LFDD in combination with each ROCOF relay setting configuration was analysed in response to the two most severe contingencies in this analysis: 1000MW and 1500MW. Each simulation was carried out for all inertia levels and the results were compared between different ROCOF relay settings and the existing Dutch LFDD scheme.

5.5. Adaptive Load Shedding Scheme

Adaptive underfrequency load shedding schemes are designed to disconnect the appropriate amount of load to provide the desired frequency recovery response for all contingency event sizes and system inertia levels. These schemes typically make a real-time decision regarding where and how much load should be shed to provide the ideal frequency response.

It was decided to develop a simple, representative adaptive scheme for this project to compare the results of the fixed schemes described in the previous sections and an adaptive scheme that has no fixed thresholds or load-shedding amounts.

Should the results of the adaptive scheme show a sufficient improvement in performance relative to the traditional LFDD scheme, proposals could be made for further research into this area to develop an adaptive scheme that could be implemented in a practical manner given the operational constraints of existing power systems.

A flowchart of the simulation methodology for the adaptive load shedding scheme developed in this project is presented in Figure 5.3

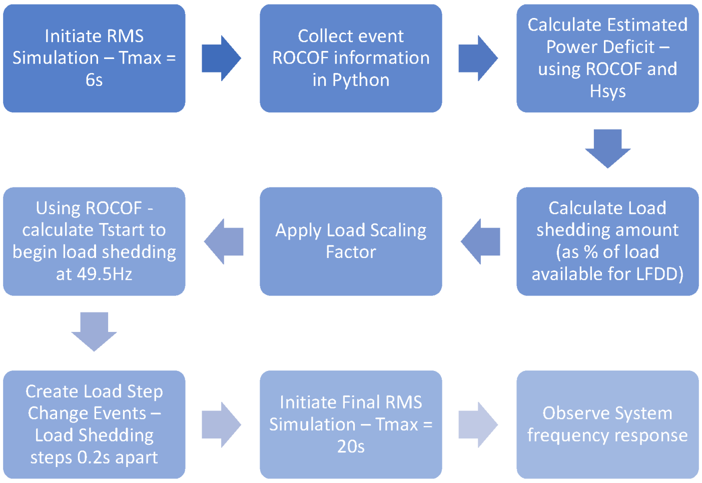

Figure 5.3: Flowchart of operation of Adaptive UFLS scheme.

5.5.1. Operation of Adaptive Scheme

In order to generate the inputs for the adaptive scheme calculations, a RMS simulation is carried out in PowerFactory environment. The frequency results of this simulation are then transferred to Python where the max COI ROCOF is estimated and combined with the system inertia (known in advance offline) to estimate the power deficit.

Once the power deficit has been calculated, the max ROCOF is used to calculate the time to begin load-shedding events for the adaptive scheme. The time is calculated according to Equation 5.6, where the aim is to begin shedding loads at 49.5Hz.

The load shedding is assumed to be evenly distributed across all loads which are included in the traditional LFDD scheme, such that the max possible load to be shed is still 45% of peak load. The load shedding is simulated by defining events that cause a step change in the active power of the chosen load by a certain scale factor. This method of shedding load is designed to simulate a situation where LFDD relays are present on the outgoing MV feeders from substations and the possibility to curtail a certain percentage of the load at a substation is available.

Following the definition of the load scaling events in Python, a second RMS simulation with the same inertia level and contingency size is carried out in Power Factory, the only difference is in this second simulation, the adaptive scheme is active and the traditional LFDD relays are switched off. The frequency deviation is measured and exported to be compared with the results from the traditional LFDD scheme.

Although this method does not specifically use a “real-time” calculation as it requires two separate RMS simulations, it is assumed that in a controller or relay, the possibility to implement a real-time calculation based on the ROCOF at a certain moment following the event is reasonable. The real-time online calculation was not implemented in PowerFactory for this research due to the time constraints of the project and a higher focus on generating representative results to allow comparison with the other improvement methods. Should this adaptive scheme be investigated further, it is possible that an integrated adaptive relay model in PowerFactory could be implemented to calculate the power deficit online during a simulation and not in Python software.

5.5.2. Power Deficit Estimation

The adaptive scheme functions based on a real-time power deficit estimation. Once the power deficit has been estimated, a decision on the load shedding amount can be made based on any user-defined scaling criteria.

The power deficit calculation used in this adaptive scheme is based on a 1992 paper by Anderson et al which estimated power deficit according to Equation 5.1 [33]. As this equation is developed for a 60Hz frequency system in North America, the equation is adapted for the 50Hz IEEE network resulting in the final Equation 5.2.

$$P_{step}(p.u.) = \frac{2.H.m_0}{60} \tag{5.1}$$

In this power deficit estimation, it is assumed that the inertia (H) of the system can be estimated with reasonable accuracy on the grid. As a result, this calculation is used assuming that the inertia level at any given moment on the grid is known with reasonable accuracy and could be fed to a controller or relay for power deficit estimation.

$$P_{imb}(MW) = (\frac{2.H^{gen}_{sync}.\frac{df}{dt}max}{50}).(P_{load} + 10000) \tag{5.2}$$

The only other external input to the calculation is the ROCOF which is taken from simulation data. In order to create a representative adaptive scheme, the centre of inertia ROCOF is calculated for the systems and this value is used to estimate power deficit.

5.5.3. Load Shedding Amount

Following the calculation of power deficit, a decision is made on the amount of load to be shed for the given event. First, the calculated imbalance must be expressed as a percentage of the available load to be shed, in this case the max shedding amount has been set to 45% of peak load to remain in line with European guidelines. This parameter is stated as the imbalance factor Λ and is calculated using Equation 5.3.

$$\Lambda = \frac{P_{imb}}{P_{LFDD}} \tag{5.3}$$

In order to create load-shedding events, a percentage step load change is assigned to each load included in the LFDD scheme. To assess the effect of shedding different amounts of load during different inertia levels, the final load shedding factor is calculated by multiplying the imbalance factor by a further scaling factor as shown in Equation 5.4. If the load scaling factor, α, is set to 100%, the total load shedding will be equal to the calculated power deficit. The calculated load-shedding factor is applied to all loads in the LFDD scheme. The adaptive scheme was analysed by shedding 50%, 75%, and 100% of the estimated power deficit for each contingency event and inertia level.

$$F_{shed} = \Lambda * \alpha \tag{5.4}$$

The total sum of load shedding in MW can be calculated by multiplying the total load available for LFDD by the load shedding factor, as shown in Equation 5.5

$$P_{shed} = P_{LFDD}.F_{shed} \tag{5.5}$$

5.5.4. Load Shedding Start Time

Based on literature research on typical adaptive load shedding schemes, it was decided to begin load shedding actions at a frequency of 49.5Hz for this adaptive load shedding scheme. However, as load-shedding actions were modelled as step changes in load for this research, it was necessary to calculate a start time for load-shedding actions as it was not possible to input a frequency threshold as the activation parameter for the step change event. The start time for load shedding action was calculated based on the maximum ROCOF for each particular event according to Equation 5.6.

$$T_{start} = 5.6 + \frac{50 - 49.5}{\frac{df}{dt}max} \tag{5.6}$$

As discussed in section 3.5, contingency events in the simulations for this research begin at a time of 5 seconds with the final generation loss event occurring at a time of 5.6s in the simulation. To coordinate the first load-shedding step of the adaptive scheme with a frequency value of 49.5Hz, it is assumed that frequency decline begins at a time of 5.6s. Therefore, 5.6 seconds are added in the calculation for T_{start} to give the correct time instant for load shedding to begin in the simulation.

In this chapter, the modelling methodology for proposed improvements to the existing Dutch LFDD scheme is outlined. Five total methods to improve the performance of LFDD have been proposed. Proposed improvements can be categorised into two sections. The first category contains improvements to LFDD load bus selection criteria. Here the method used to analyse the effect of including active DER generation and system strength at LFDD load-shedding locations is described. The second category relates to alternative load-shedding methods outside of the existing Dutch LFDD scheme. In this section, fixed LFDD schemes with alternative load distributions, proactive ROCOF-based disconnection before 49Hz and an adaptive load-shedding scheme are outlined. The performance of all proposed improvements was analysed for a variety of contingency event sizes and system inertia levels, results of these simulations are presented in chapter 6.

6 Proposed Improvements to LFDD - Results & Analysis

In this chapter, the results for phase two of this research are presented. Results for each potential improvement described in chapter 5 are presented and discussed. The purpose of this chapter is to highlight areas where the frequency response is improved in comparison to the traditional LFDD scheme and to identify areas that could be useful for the future, warranting further investigation.

Firstly, possible improvements to load selection criteria for the traditional Dutch LFDD scheme are presented. Section 6.1 describes the potential effect of including data of real-time distributed energy resource (DER) generation as an added criterion for load bus selection in a traditional LFDD scheme. A similar analysis is completed in section 6.2 where the benefits of adding network strength as a load bus selection criterion are explored.

Secondly, alternative load-shedding mechanisms, outside of the traditional Dutch LFDD scheme, are explored. Non-equal distribution of load in LFDD thresholds and the possibility to select one of multiple schemes depending on inertial level are explored as a possible alternative to the fixed, equally distributed, LFDD scheme currently in use in section 6.3. The effects of including proactive ROCOF-based disconnection of specific consumers at frequencies higher than 49Hz are described in section 6.4. Possible benefits of an adaptive load shedding scheme are analysed in section 6.5 including the effect of real-time power deficit estimation, initializing load shedding actions before 49Hz, and the possibility to scale load shedding amount based on estimated imbalance and inertia level.

6.1. Load Selection Criteria - DER Generation

In this section, the effect of unintentionally disconnecting active distributed generation on the performance of LFDD is analysed. The modelling strategy for this section is outlined in section 5.1. The purpose of this analysis is to understand the potential negative impact on LFDD performance should an LFDD relay activate and disconnect a substation that has active DER generation at that instant. If the impact of disconnecting active DER generation is severe, it may be prudent to include real-time DER generation as an added criterion in selecting LFDD load-shedding locations. As outlined in subsection 3.6.1, there is a requirement that a substation not be considered for LFDD if this substation is feeding energy back to the transmission grid more than 20% of the year. Considering the expected increase in distributed generation on the European power system in the near future, there is a possibility that locations that do not fall under this rule may have high active distributed generation at the instance a severe under-frequency event occurs.

Results for a 1000MW contingency event with the traditional Dutch LFDD scheme are presented in Figure 6.1. The frequency plots are presented for the case with no DER generation and results are displayed for all RES penetration levels. It can be seen that frequency recovery is achieved for all scenarios as the LFDD scheme sheds sufficient load to allow system recovery to take place.

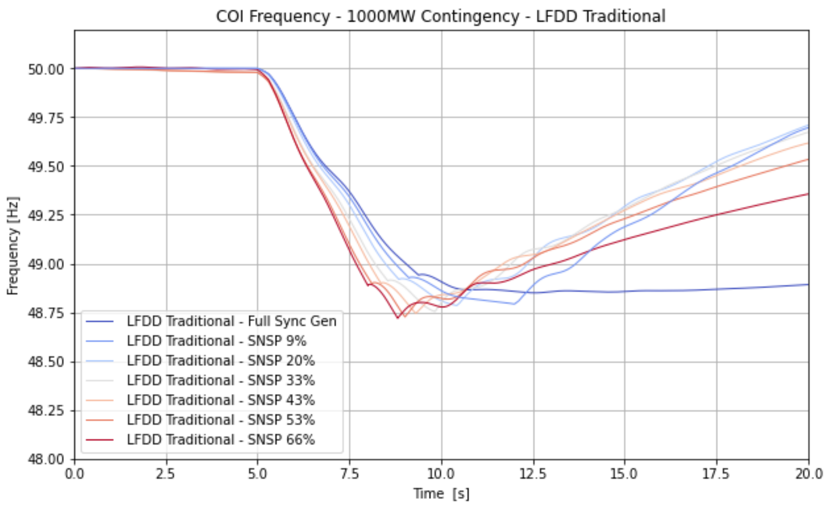

Figure 6.1: Frequency Plot - 1000 MW Contingency - Traditional LFDD

The effect of shedding different amounts of active DER generation on LFDD performance is presented in Figure 6.2. DER generation is varied between 25%, 50%, and 75% of the active power of the load connected at the same bus. As all DERs are connected at buses that are included in the LFDD scheme, should LFDD switching operations take place, one or more DERs will be disconnected at the same time as the corresponding load. Frequency plots are presented for each RES penetration scenario and DER generation level.

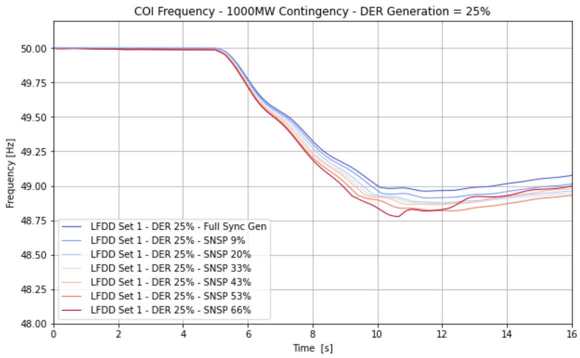

(a) Frequency Plot - 1000 MW Contingency - DER Generation 25%.

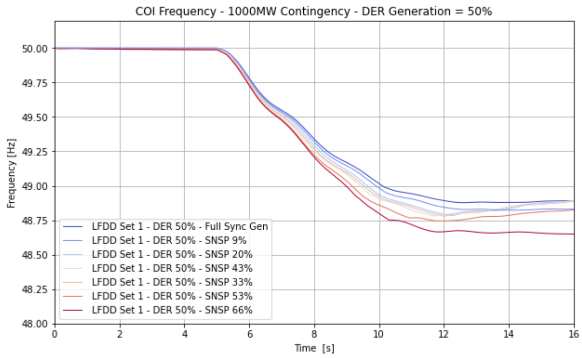

(b) Frequency Plot - 1000 MW Contingency - DER Generation 50%.

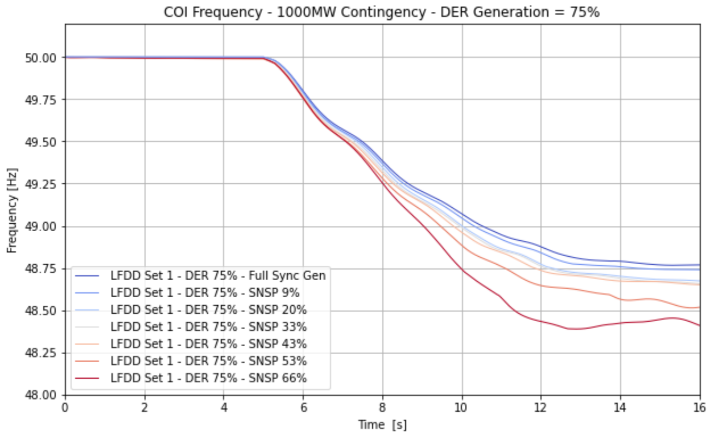

(c) Frequency Plot - 1000 MW Contingency - DER Generation 75%.

Figure 6.2: Frequency Plot - 1000MW Contingency - DER Generation 50% & 75%.

It can be seen in Figure 6.2a that a small percentage of DER generation (25% of the associated load) can have an effect on the restoration of system frequency following LFDD. Disconnecting active DER generation prevents the power balance from being effectively restored as the LFDD scheme is not disconnecting the pre-estimated amount of load. The effect of a small amount of active DER generation being disconnected can be seen as the frequency in all scenarios is slower to recover towards nominal values than in the case of no DER generation.

Increasing the DER generation to 50% of the associated load results in further degradation of LFDD performance as shown in Figure 6.2b. In this case, the power balance is not restored and therefore the system frequency does not recover within the simulation time frame. The sensitivity of a system with higher RES penetration levels to shedding active DER disconnection is evident as the frequency plot for the SNSP 66% case displays a continued downward trend following LFDD activation while the frequency decline is successfully halted in higher inertia scenarios for the same event.

Substantial degradation of LFDD performance, particularly in scenarios with higher RES penetration can be seen in Figure 6.2c which shows the effect of DER generation at 75% of the associated load. In this case, the frequency nadir is lower for all scenarios and the LFDD scheme is ineffective in restoring power balance to the system. In this case, due to the high level of active DER generation being disconnected, the LFDD scheme does not restore the power balance. Consequently, further loss of generation and possible blackouts could occur on the network.

The effect of disconnecting active DER generation during a larger 1500MW contingency was also investigated. Figure 6.2c presents the frequency trajectory for all scenarios with no active DER generation. The frequency plots for two DER generation levels 50% and 75% are presented in Figure 6.3.

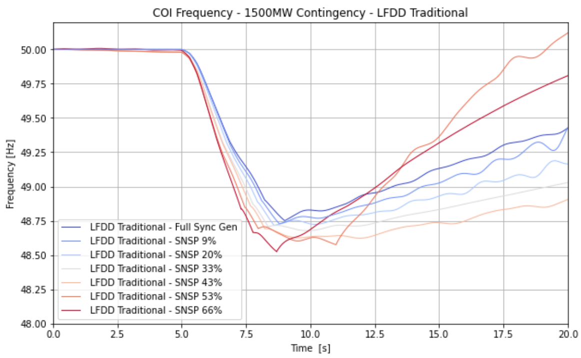

(a) Frequency Plot - 1500 MW Contingency - Traditional LFDD

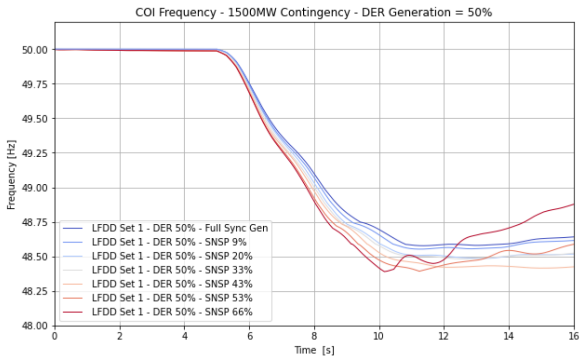

(b) Frequency Plot - 1500 MW Contingency - DER Generation 50%

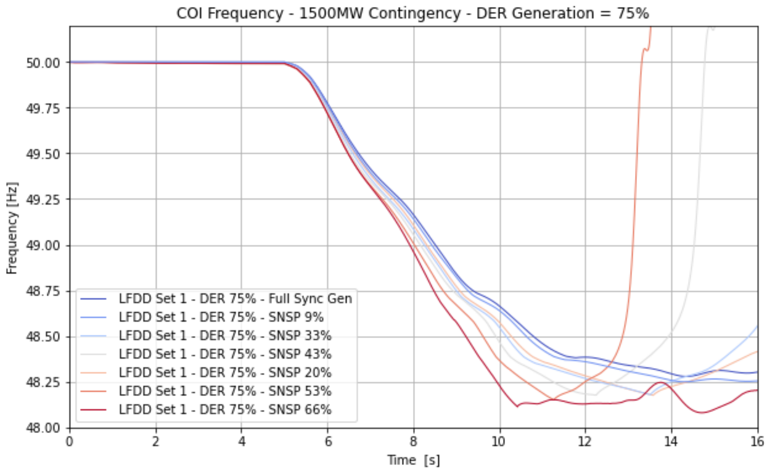

(c) Frequency Plot - 1500 MW Contingency - DER Generation 75%

Figure 6.3: Frequency Plot - 1500MW Contingency - DER Generation 50% & 75%

The effect of unintentionally disconnecting DER generation on LFDD performance becomes more severe as the size of the contingency is increased. In Figure 6.3b, it can be seen that the frequency drops below 48.5Hz for numerous RES penetration scenarios. This increased frequency deviation is significant in comparison to the case with no DER generation where the 48.5Hz threshold is not breached in any scenario. A DER generation level of 75% causes the system to split in low inertia scenarios following the LFDD actions as shown in Figure 6.3c. These figures highlight the potential for cascading disconnections and system collapse caused by unintentional shedding of active DER generation.

It is clear that the unintentional disconnection of active DERs could have a detrimental effect on the performance of LFDD in arresting frequency decline and restoring system frequency to nominal values. Including real-time or predicted data regarding DER generation levels at LFDD substations as a criterion for LFDD bus selection could avoid this phenomenon and ensure that LFDD actions restore power balance as effectively as possible for all levels of system inertia and DER penetration. Further details on the benefits and challenges associated with this proposed improvement to LFDD are presented in section 7.2.

6.2. Load Selection Criteria - System Strength

In this section, the effect of system strength, represented by minimum short circuit power, at LFDD load shedding buses on LFDD performance and system recovery is analysed. The methodology for this analysis is described in section 5.2. In future power systems, network topology can be expected to change frequently as power flow becomes increasingly bi-directional and increased penetration of distributed generators is observed. As a result, system strength at locations selected for LFDD could change based on the system topology or level of inverter-based generation active at that instant. Understanding the potential benefits of shedding load at locations with higher voltage and frequency stability could be beneficial in developing the most robust LFDD actions possible for the future power system. The purpose of this analysis is to investigate whether system strength at locations selected for LFDD has an effect on the performance of LFDD in arresting frequency decline or the ability of the system to recover following the disconnection of loads and restoration of power balance.

6.2.1. Short Circuit Analysis

Minimum short circuit powers for each load bus at each renewable energy penetration level are presented in Table 6.1. These values are calculated based on the IEC60909 standard with contribution from asynchronous machines included in the calculation. The results were used to rank the possible buses available for LFDD in terms of system strength. Following the ranking of the buses, LFDD schemes could then be developed based on system strength at different inertia levels.

It can be seen from the table that fault levels at all buses are highest in the fully synchronous generation scenario. This is due to the highest number of synchronous generators being active in this scenario leading to the highest available short circuit currents. As the penetration of inverter-based generation increases, replacing synchronous generation, the fault levels reduce and the system can be viewed as becoming weaker and more susceptible to voltage and frequency instability.

Table 6.1: Minimum Short Circuit Power Results.

	Min SC Power (MVA)						
	Full Sync Gen	**SNSP 9%**	**SNSP 20%**	**SNSP 33%**	**SNSP 43%**	**SNSP 53%**	**SNSP 66%**
Bus 01	5512.7	5421.9	5412.7	5360.9	5348.8	5307.1	4853.8
Bus 02	8817	7542.5	7438.1	6870	6752.8	6375.3	3754.2
Bus 03	7358.7	6901.9	6713	6288.9	6102.8	5535.2	4189.2
Bus 04	6929.8	6787.6	6645.2	6460.6	6316.7	5864.2	5185.5
Bus 05	7208.3	7129.5	7036.4	6924.9	6827.8	6511.1	6051.6
Bus 06	7484.1	7408.7	7315.7	7207	7109.9	6792.3	6342.7
Bus 07	5838.4	5795.4	5743.2	5681	5625.6	5441.6	5168.1
Bus 08	6050.8	6006.2	5952.7	5888.4	5831.6	5642.8	5359.2
Bus 09	5396.8	5388.2	5379.7	5368.1	5358.7	5326.1	5264.8
Bus 10	6977.1	6914.5	6817.1	6718.8	6618.6	6293.2	5903.6
Bus 11	6752.1	6692.3	6605.6	6513.9	6424.1	6130.9	5759.1
Bus 12	2838.1	2826.6	2808.6	2790.1	2770.9	2706.5	2624.7
Bus 13	6488.7	6424.9	6319.4	6217.3	6110	5765	5376.2
Bus 14	6709.5	6612.5	6434.1	6276.7	6103.1	5569.5	5051.6
Bus 15	6341.3	6245.6	5815.7	5598.5	5236.7	4279.1	3840.5
Bus 16	8916.6	8720.4	7631.5	7187	6407.8	4659.3	4075.2
Bus 17	7465.4	7181.8	6691	6032.5	5639	4600.3	3853.5
Bus 18	6392.4	6133.7	5862.4	5425	5181.5	4484.3	3691.3
Bus 19	6967	6929.4	4382.1	4291.9	4115.2	3601.5	3380.1
Bus 20	5049.3	5037	3990	3943.1	3848.8	3554.4	3417.1
Bus 21	6016.6	5959.3	5612.7	5455.5	4753	3062.2	2798.6
Bus 22	6790.3	6750.9	6505.7	6390.7	5085.5	2543.6	2359
Bus 23	6194.2	6161.6	5958.3	5862.4	4070.9	2440.8	2270.3
Bus 24	6570.4	6475.6	5921.5	5680.8	5030.7	3713.8	3333
Bus 25	7031.7	5147.4	5090.5	4542.5	4474.6	4253.9	3014.2
Bus 26	5275.3	4904.3	4819.9	3331	3256.5	3022.2	2512.6
Bus 27	5014.7	4783	4645.2	3772.3	3650	3281.6	2780.4
Bus 28	3446.7	3377.1	3360.3	1677.1	1658	1595.1	1440.7
Bus 29	4531.2	4449.1	4429.3	1627	1609	1549.7	1403.6
Bus 31	5833.5	5820.3	5803.7	5783.9	5765.9	5704.2	5609.1
Bus 39	52263	52194.9	52179.1	52128.9	52109.5	52042.4	51630.9

Changing network topology by adding IBRs to the system and deactivating certain synchronous generators also changes the location of the stronger and weaker points on the network. In the Full Sync Gen scenario, Bus 02 has a min SC power of 8817 MVA, the third highest fault level in the system. In the SNSP 66% scenario, this bus has a fault level of 3754.2 MVA which places it lower on the list of buses in terms of system strength. This scenario-dependent variation in the location of the strongest and weakest points in the network could have an effect on LFDD performance as choosing to shed load at a certain bus that has a high fault level in one topology may be counter-productive in a different configuration where the relative strength at that bus is much lower.

6.2.2. System Strength and LFDD Performance - Fully Synchronous Generation

As discussed in section 5.2, two sets of LFDD schemes were generated using the system strength, calculated in the fully synchronous generation scenario, as an added input to LFDD load selection criteria. One scheme focused on disconnecting loads at the strongest buses first, the second scheme focused on disconnecting loads at the weakest buses first.

An RMS simulation based on a 1000MW contingency event was carried out to assess the performance of these two contrasting LFDD schemes. Frequency plots for simulations of all RES penetration scenarios are shown in Figure 6.4. It can be seen by comparing the two subfigures and by observing the minimum frequency values shown in Table 6.2, that frequency nadir is not largely affected by the network strength at LFDD load shedding locations. This explains that including system strength as a selection criteria has little effect on the ability of LFDD to reduce the frequency nadir following an event. It is anticipated that the frequency nadir is more likely to be affected by the load shedding amount, which is equal for both schemes in this analysis.

Table 6.2: Frequency Table - Load Shed at Strong Vs Weak Buses - SC calculations from Full sync Gen scenario

Scenario	Strong Buses		Weak Buses	
	Min Frequency [Hz]	Min RoCoF [Hz/s]	Min Frequency [Hz]	Min RoCoF [Hz/s]
Full Sync Gen	48.876	-0.370	48.868	-0.370
SNSP 20%	48.792	-0.375	48.799	-0.399
SNSP 9%	48.777	-0.399	48.788	-0.375
SNSP 33%	48.769	-0.427	48.760	-0.427
SNSP 43%	48.749	-0.434	48.743	-0.434
SNSP 53%	48.730	-0.479	48.724	-0.479
SNSP 66%	48.724	-0.475	48.719	-0.478

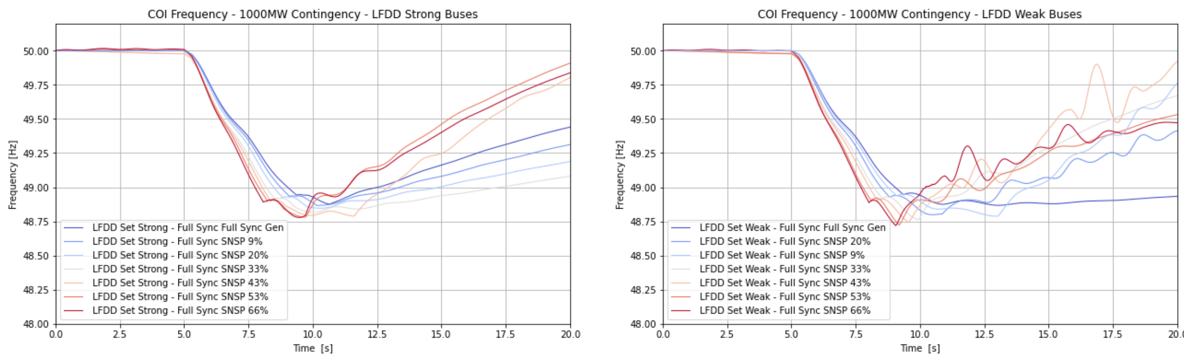

(a) Frequency Plot - 1000 MW Contingency - Strong Buses.

(b) Frequency Plot - 1000 MW Contingency - Weak Buses.

Figure 6.4: Frequency Plot - 1000 MW Contingency - LFDD at Strong Vs Weak Buses - SC Calculations at Full Sync Gen.

The primary difference in the performance of the two LFDD schemes shown in Figure 6.4 is evident in the response of the system after LFDD actions have restored power balance and the system begins to recover. In the seconds following the activation of LFDD, the frequency plots in Figure 6.4b show more frequency oscillations than those in Figure 6.4a. This could be caused by the LFDD activating at locations where the system is more vulnerable to voltage and frequency instability following switching events when the loads are disconnected at weaker buses. As a result, it is possible that adding a selection criterion to LFDD load allocation to prioritise shedding loads at locations with higher fault levels may allow the system to achieve a more stable recovery and avoid possible cascading events. Therefore, this could help to prevent potential frequency and voltage instability as the system recovers from a large contingency.

6.2.3. Network Strength and LFDD Performance - SNSP 66%

The effect of network strength at LFDD load shedding locations on the stability of the system was also analysed for two shedding schemes developed based on system strength in a high RES penetration scenario. In this case, the SNSP 66% system configuration was chosen. The effect of shedding loads at weaker or stronger buses, based on system strength calculations completed for SNSP 66%, was analysed for contingency events of 1000MW and 1500MW. Frequency plots for all simulations are presented in Figure 6.5 and Figure 6.6.

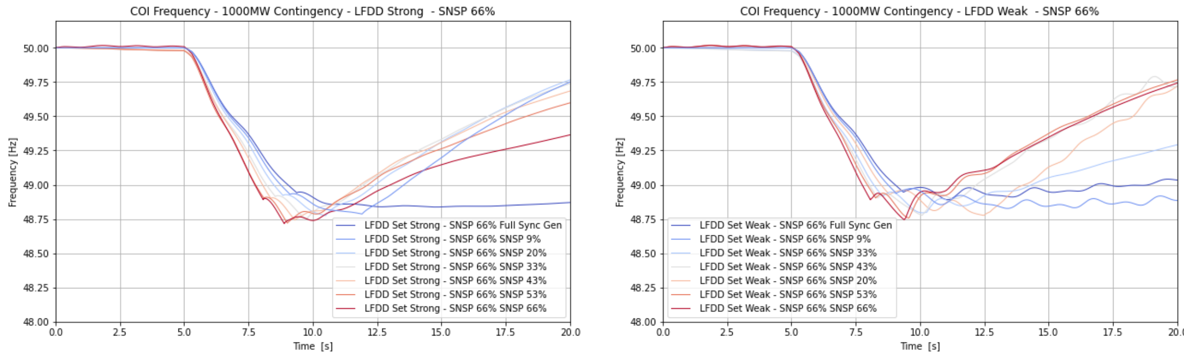

(a) Frequency Plot - 1000 MW Contingency - Strong Buses - SC Calculations at SNSP 66%.

(b) Frequency Plot - 1000 MW Contingency - Weak Buses - SC Calculations at SNSP 66%.

Figure 6.5: Frequency Plot - 1000 MW Contingency - LFDD at Strong vs Weak Buses - SC Calculations at SNSP 66%.

The expected increase in oscillations in the frequency response when shedding loads at weaker buses can be seen for the 1000MW event in Figure 6.5. Shedding loads at locations with higher network strength provides a smoother frequency recovery at all inertia levels even though the LFDD scheme was based on system strength calculations at the lowest inertia level. Although there are more oscillations in the frequency response, the frequency decline is still effectively halted when shedding load at weaker buses during this particular contingency event.

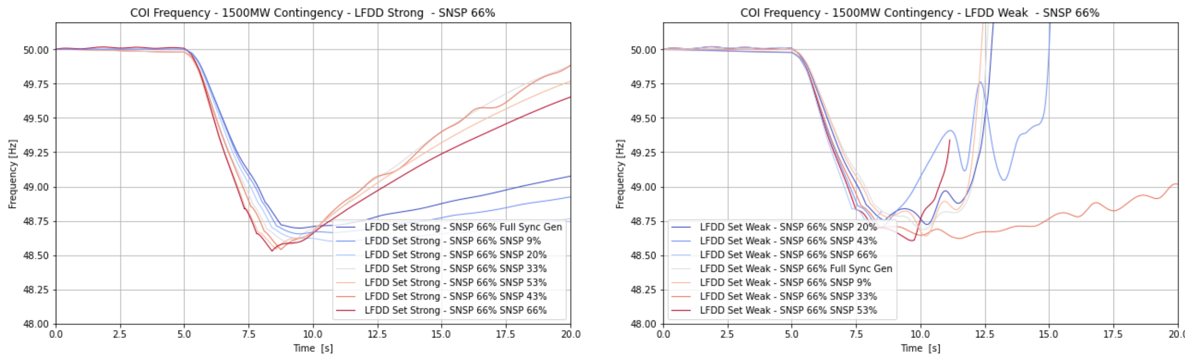

(a) Frequency Plot - 1500 MW Contingency - Strong Buses - SC Calculations at SNSP 66%.

(b) Frequency Plot - 1500 MW Contingency - Weak Buses - SC Calculations at SNSP 66%.

Figure 6.6: Frequency Plot - 1500 MW Contingency - SC Calculations at SNSP 66%.

Increasing the contingency event size exaggerates the effect of system strength on the frequency recovery immediately after LFDD load-shedding actions. As shown in Figure 6.6b, system splitting occurs in almost all RES scenarios when the loads are shed at locations with low system strength. This is highlighted by the drastic increase in COI frequency on the plot as the system is now no longer one synchronised area and therefore the calculation of COI frequency is not representative. Conversely, it can be seen in Figure 6.6a that shedding load at locations where network strength is higher can ensure a more stable response on this network and avoid the system splitting events.

It can be seen from the results presented in this section that shedding loads at stronger buses during LFDD actions can ensure a more stable frequency and voltage profile following LFDD. As expected, fewer frequency oscillations are observed during high inertia scenarios for all LFDD schemes and contingency event magnitudes. This suggests that accounting for system strength at LFDD locations is more important for lower inertia scenarios where the system is more vulnerable. It is possible that giving priority to shedding load at the strongest buses based on calculations of system strength at the lowest inertia level could ensure a more stable response for the largest array of contingency event sizes and system inertia levels. Further details on the benefits and challenges related to the inclusion of system strength as an LFDD load selection criterion are presented in section 7.1.

6.3. Alternative Load Distribution in LFDD

In this section, the effect of altering the distribution of load in the thresholds of a traditional, fixed, LFDD scheme is investigated. As discussed in subsection 3.6.1, the traditional Dutch LFDD scheme requires 7.5% of the peak system load in each of the six threshold settings that comprise the scheme. In this section, the effect of placing more or less load in the beginning traps of the scheme is analysed. The effect of increasing the number of trap thresholds while maintaining the same total load-shedding amount is also investigated. The steps taken to develop these alternate LFDD schemes are described in section 5.3.

The purpose of this analysis is to understand if it is beneficial to develop a number of LFDD schemes with different load distributions. The purpose of these schemes would be to enable the system operator to choose between pre-defined options for LFDD based on a prediction of the inertia level in the system at any given time. A selection between LFDD schemes could potentially be made based on real-time ROCOF measurements to select the most appropriate scheme based on the severity of each individual event.

6.3.1. Alternative Scheme 1 - Front Loading

As described in section 5.3, alternative scheme 1 consists of 10% of peak load in each of the first two thresholds with the remainder of the load evenly distributed among the remaining 4 thresholds. Frequency thresholds are maintained the same as in the traditional Dutch LFDD scheme, beginning at 49Hz and ending at 48Hz with 0.2Hz gap between thresholds.

The performance of this alternate scheme was compared with the traditional dutch LFDD scheme in response to a large contingency event of 1500MW. Frequency plots for both schemes and all inertia levels are presented in Figure 6.7. Minimum frequency and ROCOF values for simulations with both schemes are presented in Table 6.3.

Table 6.3: Minimum frequency and ROCOF values - comparison between traditional LFDD scheme and Alternate scheme 1 for an event size of 1500MW.

Scenario	Original LFDD Scheme		Alternate LFDD Scheme	
	Min Frequency [Hz]	Min RoCoF [Hz/s]	Min Frequency [Hz]	Min RoCoF [Hz/s]
Full Sync Gen	48.752	-0.471	48.749	-0.471
SNSP 9%	48.728	-0.571	48.745	-0.571
SNSP 20%	48.716	-0.511	48.706	-0.511
SNSP 33%	48.678	-0.564	48.675	-0.564
SNSP 43%	48.623	-0.561	48.667	-0.561
SNSP 53%	48.576	-0.628	48.657	-0.628
SNSP 66%	48.524	-0.688	48.681	-0.688

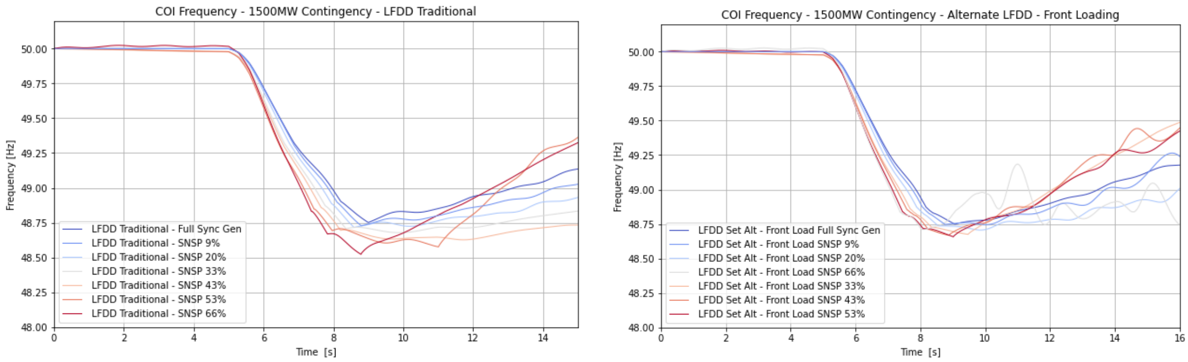

(a) Frequency Plot - 1500 MW Contingency - Traditional LFDD. **(b)** Frequency Plot - 1500 MW Contingency - Alternative Scheme 1.

Figure 6.7: Frequency Plot - 1500 MW Contingency - Comparison between traditional, evenly distributed, load selection for LFDD and an alternative scheme with increased load in trap 1 & 2.

Plots presented in Figure 6.7 and minimum frequency values shown in Table 6.3 suggest that the alternative load shedding scheme is more effective at arresting the frequency decline than the traditional scheme, particularly in higher SNSP scenarios. In the two network scenarios with highest RES penetration, the alternate LFDD scheme prevents the frequency from breaching 48.6Hz and breaching trap 3 of the LFDD scheme. The total load shed by the alternate scheme in these simulations is 20% of peak load. By comparison, the traditional scheme does not prevent trap 3 from being breached and as a result, 22.5% of peak load is shed in response to the same event. In this case, the alternate scheme has shed less load and still halted frequency decline at a higher value.

It can be seen from the figure and table that the effect of placing more load in the early trap settings is less evident in high inertia scenarios. This could be caused by reduced sensitivity of the system to changes in load due to the presence of more active synchronous generators. In scenario SNSP 9%, SNSP 20% and SNSP 33%, the alternate scheme sheds more load (20%) compared to the traditional scheme (15%) without a large change in frequency nadir or system recovery time.

It is possible that including more than 10% of peak load in the early trap thresholds would further improve the response on the system, particularly in lower inertia scenarios. This has not been investigated in this project as all alternate schemes were designed to comply with the existing EU grid code. This EU grid code requires no more than 10% peak load be included in any one trap setting.

6.3.2. Alternative Scheme 2 - End Loading

In contrast to the scheme described in subsection 6.3.1, the second alternative LFDD scheme is based on the inclusion of less load in the first two thresholds compared with the existing Dutch LFDD scheme. Alternative scheme 2 consists of 5% peak load in traps 1 & 2 with the remaining load evenly distributed throughout the remaining traps. The purpose of this scheme is to avoid over shedding during smaller contingency events or when the system inertia is high and the system has the inherent capacity to recover from frequency excursions without extra load shedding.

The performance of the second alternative LFDD scheme in response to a 1000MW contingency event is displayed in Figure 6.8b. Frequency trajectory plots for all RES penetration scenarios are shown for both the traditional LFDD scheme with 7.5% load in each trap and the alternative scheme described in this section. Minimum frequency and ROCOF values for both LFDD schemes in response to the 1000MW event are shown in Table 6.4.

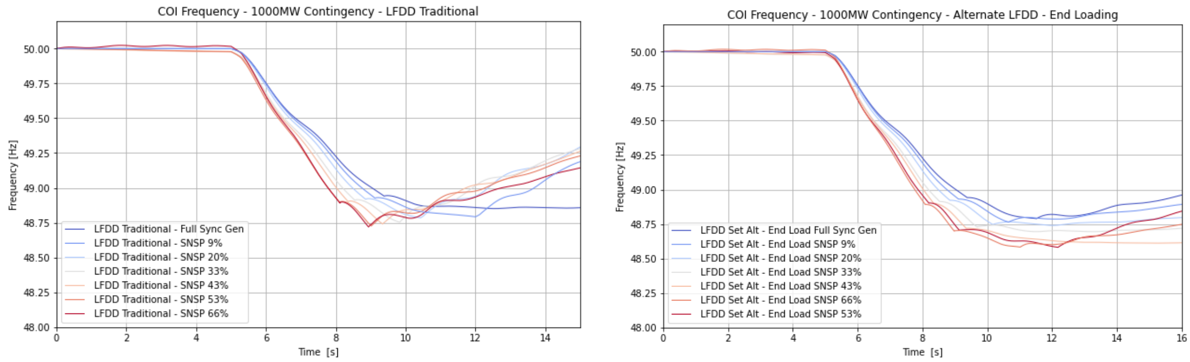

(a) Frequency Plot - 1000 MW Contingency - Traditional LFDD.

(b) Frequency Plot - 1000 MW Contingency - Alternative Scheme 2.

Figure 6.8: Frequency Plot - 1000 MW Contingency - Comparison between traditional, evenly distributed, load selection for LFDD and an alternative scheme with reduced load in trap 1 & 2.

Table 6.4: Comparison of minimum frequency and ROCOF values for traditional LFDD and Alternative scheme 2 - Contingency size = 1000MW.

Scenario	Original LFDD Scheme		Alternate LFDD Scheme 2	
	Min Frequency [Hz]	**Min RoCoF [Hz/s]**	**Min Frequency [Hz]**	**Min RoCoF [Hz/s]**
Full Sync Gen	48.850	-0.371	48.789	-0.369
SNSP 9%	48.792	-0.373	48.764	-0.375
SNSP 20%	48.785	-0.396	48.740	-0.398
SNSP 33%	48.754	-0.463	48.695	-0.429
SNSP 43%	48.744	-0.422	48.611	-0.427
SNSP 53%	48.727	-0.469	48.582	-0.479
SNSP 66%	48.719	-0.484	48.581	-0.471

Results presented in Table 6.4 highlight the similarity between the minimum frequency values for both schemes during high inertia scenarios. Scenarios SNSP 9%, 20%, and 33% display little difference in the frequency nadir between the traditional and alternate LFDD schemes despite the traditional scheme shedding 7.5% peak load and the alternate scheme shedding 5%. The potential challenge of shedding less load in the beginning trap thresholds can be seen in the higher SNSP scenarios where the frequency trajectory is lower in comparison with the traditional LFDD scheme.

Shedding less load in the first two thresholds, during low inertia scenarios, is not sufficient to stop the frequency decline, and therefore a third threshold of 48.6Hz is breached in the two highest SNSP scenarios. The result of this is a cumulative shedding of 15% peak load, equal to the amount shed by the traditional scheme. Due to the lower frequency nadir using the alternative scheme, it is evident that alternative scheme 2 is not as effective as the traditional scheme during low inertia instances with medium to high contingency event sizes on this network. However, in scenarios with high inertia, alternate scheme 2 achieves the same frequency nadir as the traditional LFDD scheme while shedding 33% less load.

Frequency response of the system to a smaller 500MW event is presented in Figure 6.9. In this plot, alternative scheme 2 is again compared with the traditional Dutch LFDD. Table 6.5 contains minimum frequency and ROCOF values for both simulations.

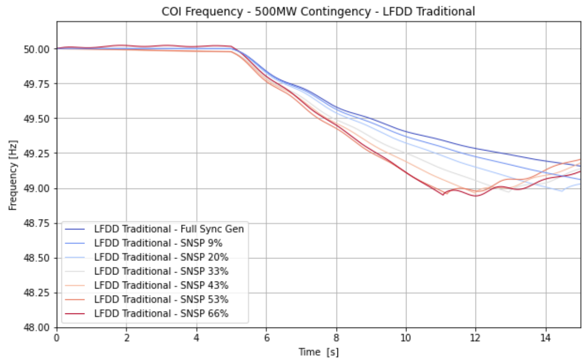

(a) Frequency Plot - 500 MW Contingency - Traditional LFDD.

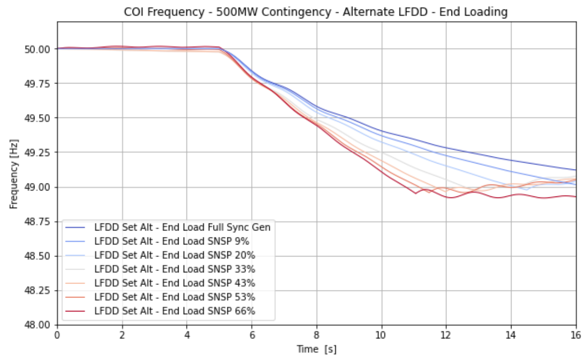

(b) Frequency Plot - 500 MW Contingency - Alternative Scheme 2.

Figure 6.9: Frequency Plot - 500 MW Contingency - Comparison between traditional, evenly distributed, load selection for LFDD and an alternative scheme with reduced load in trap 1 & 2.

Table 6.5: Comparison of minimum frequency and ROCOF values for traditional LFDD and Alternative scheme 2 - Contingency size = 500MW.

Scenario	**Original LFDD Scheme**		**Alternate LFDD Scheme 2**	
	Min Frequency [Hz]	**Min RoCoF [Hz/s]**	**Min Frequency [Hz]**	**Min RoCoF [Hz/s]**
Full Sync Gen	49.029	-0.210	49.027	-0.209
SNSP 9%	48.983	-0.212	48.983	-0.213
SNSP 20%	48.976	-0.222	48.976	-0.223
SNSP 33%	48.970	-0.237	48.969	-0.239
SNSP 43%	48.963	-0.240	48.962	-0.241
SNSP 53%	48.957	-0.253	48.956	-0.253
SNSP 66%	48.931	-0.264	48.915	-0.258

Minimum frequency values shown in Table 6.5 show that the alternative scheme is effective in limiting frequency decline for all inertia levels during this 500MW contingency event. Due to the smaller event size, less load can be shed in the early trap thresholds and the system is still able to recover. The system is also capable of avoiding overshoot associated with shedding excess load. Although the alternative scheme is effective in arresting the frequency decline, the recovery of the frequency towards nominal levels is slower in all scenarios than the recovery using the traditional LFDD scheme. This is to be expected as less load has been shed with the alternate scheme. Secondary and tertiary control measures, not included for analysis in this project, could be used to accelerate the frequency recovery using the alternate scheme.

6.3.3. Alternative Scheme 3 - Increased Number of Thresholds

As discussed in chapter 4, the effect of maintaining 7.5% peak load in each trap threshold poses a risk of over shedding or under shedding following LFDD actions. This is particularly evident in cases where the minimum frequency falls very close to the frequency setting of a particular load threshold. Increasing the number of thresholds, and reducing the amount of load in each, could allow LFDD actions to shed total load amounts closer to the optimal value for a particular event.

In this section, the performance of an alternative, fixed, LFDD scheme based on 9 thresholds (instead of 6 in the traditional scheme) is compared with the traditional Dutch LFDD scheme for contingency events of 1000MW and 1500MW. A comparison of the frequency trajectory between the alternative and traditional LFDD schemes for a contingency event of 1000MW is presented in Figure 6.10. Minimum frequency and ROCOF values for both schemes for this contingency are presented in Table 6.6.

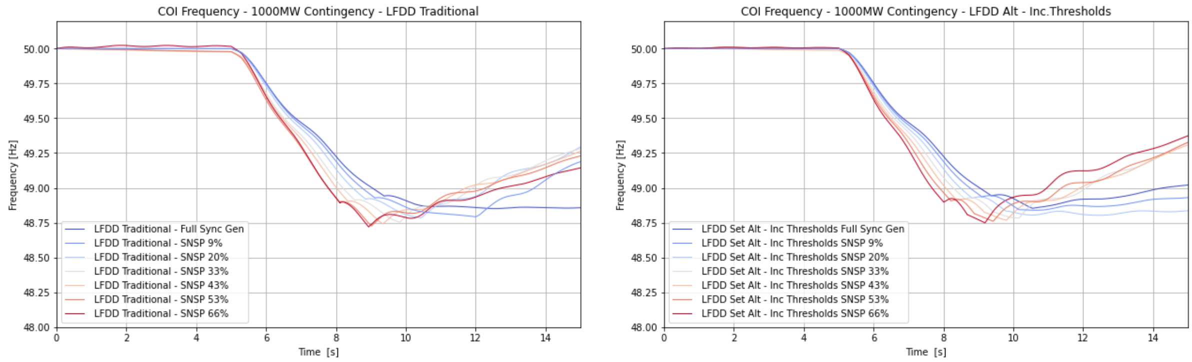

(a) Frequency Plot - 1000 MW Contingency - Traditional LFDD.

(b) Frequency Plot - 1000 MW Contingency - Alternative Scheme 3.

Figure 6.10: Frequency Plot - 1000 MW Contingency - Comparison between traditional, evenly distributed, load selection for LFDD and an alternative scheme with an increased number of trap threshold settings.

Table 6.6: Comparison of minimum frequency and ROCOF values for traditional LFDD and Alternative scheme 3 - Contingency size = 1000MW.

	Original LFDD Scheme		**Alternative LFDD Scheme 3**	
Scenario	**Min Frequency [Hz]**	**Min RoCoF [Hz/s]**	**Min Frequency [Hz]**	**Min RoCoF [Hz/s]**
Full Sync Gen	48.850	-0.371	48.853	-0.371
SNSP 9%	48.792	-0.373	48.839	-0.381
SNSP 20%	48.785	-0.396	48.803	-0.398
SNSP 33%	48.754	-0.463	48.783	-0.428
SNSP 43%	48.744	-0.422	48.767	-0.442
SNSP 53%	48.727	-0.469	48.760	-0.478
SNSP 66%	48.719	-0.484	48.749	-0.502

It can be seen from the plots on Figure 6.10 that the frequency trajectory of all RES penetration scenarios is quite similar for both schemes. The frequency response with the alternative scheme displays slightly more oscillations, this may be attributed to the smaller frequency gap between thresholds and the higher number of switching actions occurring in a shorter length of time.

In terms of load shedding amount, in the SNSP 9% scenario, the less total load is shed using the alternative scheme while the frequency deviation is still arrested at a higher value than achieved using the traditional scheme. This is similar to the effect of alternative Scheme 1, when less load is shed in higher inertia situations to allow the system to recover naturally. In Alternative Scheme 3, the load shedding actions to shed this lesser amount of load occur at 49Hz and 48.9Hz, therefore the system begins to react to the contingency sooner than would be achieved with the traditional scheme.

Based on the values in Table 6.6, it can be seen that the frequency nadir in higher RES penetration scenarios is consistently higher than the case with the traditional scheme. This may be attributed to the effect of disconnecting more load earlier, in a similar manner to Alternative Scheme 1. In the higher inertia scenarios for the 1000MW event, the load-shedding amounts are the same for both schemes, however, as load-shedding actions occur more quickly for the alternative scheme, the frequency deviation is halted at a higher value.

A comparison between the frequency trajectory for the traditional LFDD scheme and Alternative Scheme 3 in response to a 1500MW contingency is presented in Figure 6.11. Corresponding minimum frequency and ROCOF values are presented in Table 6.7

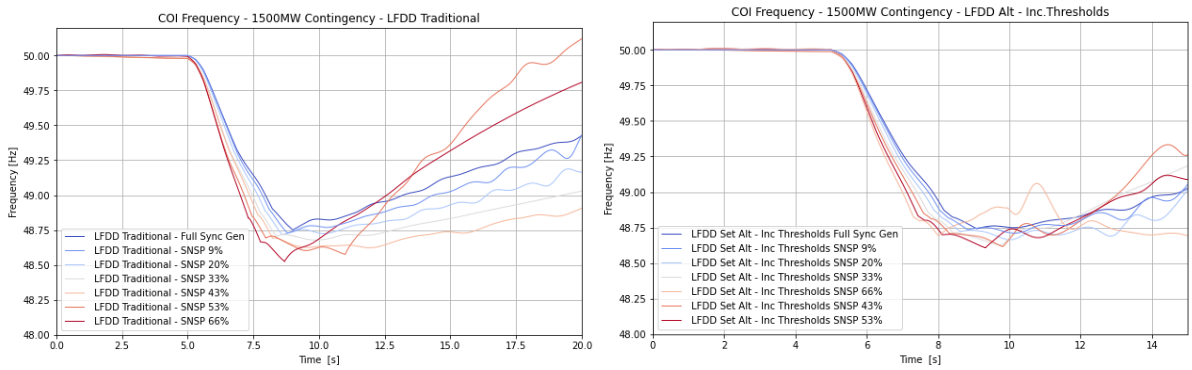

(a) Frequency Plot - 1500 MW Contingency - Traditional LFDD. **(b)** Frequency Plot - 1500 MW Contingency - Alternative Scheme 3.

Figure 6.11: Frequency Plot - 1500 MW Contingency - Comparison between traditional, evenly distributed, load selection for LFDD and an alternative scheme with an increased number of trap threshold settings.

Table 6.7: Comparison between minimum ROCOF and Frequency values for the original Dutch LFDD scheme and alternative scheme 3, for all RES penetration scenarios.

Scenario	Original LFDD Scheme		Alternate LFDD Scheme 3	
	Min Frequency [Hz]	**Min RoCoF [Hz/s]**	**Min Frequency [Hz]**	**Min RoCoF [Hz/s]**
Full Sync Gen	48.752	-0.471	48.741	-0.476
SNSP 9%	48.728	-0.571	48.711	-0.489
SNSP 20%	48.716	-0.511	48.664	-0.517
SNSP 33%	48.678	-0.564	48.626	-0.571
SNSP 43%	48.626	-0.577	48.616	-0.588
SNSP 53%	48.576	-0.628	48.607	-0.646
SNSP 66%	48.524	-0.688	48.625	-0.690

The effect of an increased number of load shedding events on the stability of the frequency response can be seen in Figure 6.11b. The frequency plots, particularly in lower inertia scenarios display more oscillations than those generated using the traditional LFDD scheme. This may be caused by an increased number of switching events, due to the smaller frequency gap between thresholds, occurring as the frequency declines following the 1500MW event.

The effect of including more load thresholds, with less load in each, can be seen by observing the frequency recovery in the lower inertia scenarios. In the plots generated using traditional LFDD, the frequency recovers rapidly and shows signs of overshoot following LFDD actions, In the case of SNSP 53% and SNSP 66% the total load shedding amount is 22.5% using traditional LFDD. It can be seen from the plots in Figure 6.11b that the frequency recovery is slower and the plot shows a more shallow increase towards nominal values following LFDD. In the same scenarios, using the alternative scheme, the total load shedding amount is 20% of peak load while the frequency decline is halted at a higher value than in the case of traditional LFDD.

It is clear from these graphs that including more thresholds, which have smaller amounts of load in each, allow the LFDD actions to shed load amounts closer to the ideal value for each contingency and inertia level. An increased number of threshold settings, with a smaller gap between each, allows the frequency deviation to be arrested at a higher value as defence actions are triggered earlier than in the case of traditional LFDD. However, as seen from some post-disturbance frequency oscillations, it is possible that including more threshold settings could affect the stability of the frequency recovery as an increased number of switching actions are taking place in a shorter amount of time.

6.4. Proactive ROCOF-Based Disconnection before 49Hz

In this section, the effect of proactively disconnecting a pre-determined consumer using ROCOF-based protection is analysed. The modelling steps to complete this analysis are described in section 5.4. The aim of this proactive disconnection is to take action before the frequency has reached the 49Hz threshold for the initialization of LFDD. Firstly, one possible use case is presented to compare the effect of proactive tripping vs traditional LFDD.

Next, the effect of changing the settings of the relay used in proactive disconnection is analysed to understand how the relay could be tuned to system operator requirements. The settings of the ROCOF-based protection are analysed under three criteria. 1. Load size. 2. ROCOF Threshold 3. Definite time delay.

6.4.1. Proactive ROCOF-based Disconnection vs Traditional LFDD

In this section, a comparison is made between the frequency response of the system with an added ROCOF-based relay which would disconnect a specified consumer before 49Hz, and the traditional LFDD scheme without the added ROCOF relay. As the goal behind the use of the added ROCOF relay is to improve system response under severe event conditions, simulations are presented for the 1500MW contingency event in Figure 6.12. Table 6.8 shows the minimum frequency and ROCOF values for all RES penetration levels. Also included in the table is the trip time at which the ROCOF-based protection activates. In all simulations presented in this section, the ROCOF relay is set with a ROCOF threshold of 0.5Hz/s and a definite time delay of 0.5s. The ROCOF protection is added to load 27, which is equal to 4.6% of the peak load on the system.

Table 6.8: Minimum frequency and ROCOF values for 1500MW contingency - comparison between traditional LFDD scheme and LFDD with added ROCOF based protection.

	Traditional LFDD		With ROCOF Relay		
Scenario	**Min Frequency [Hz]**	**Min RoCoF [Hz/s]**	**Min Frequency [Hz]**	**Min RoCoF [Hz/s]**	**ROCOF Relay Trip Time**
Full Sync Gen	48.752	-0.471	48.750	-0.471	No Trip
SNSP 9%	48.728	-0.493	48.728	-0.493	No Trip
SNSP 20%	48.716	-0.511	48.716	-0.511	No Trip
SNSP 33%	48.678	-0.564	48.733	-0.560	6.44s
SNSP 43%	48.623	-0.561	48.711	-0.561	6.43s
SNSP 53%	48.576	-0.628	48.736	-0.626	6.17s
SNSP 66%	48.524	-0.671	48.702	-0.671	6.2s

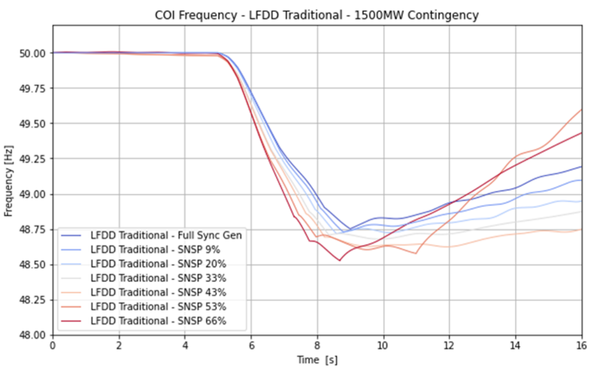

(a) Traditional LFDD - 1500MW Contingency.

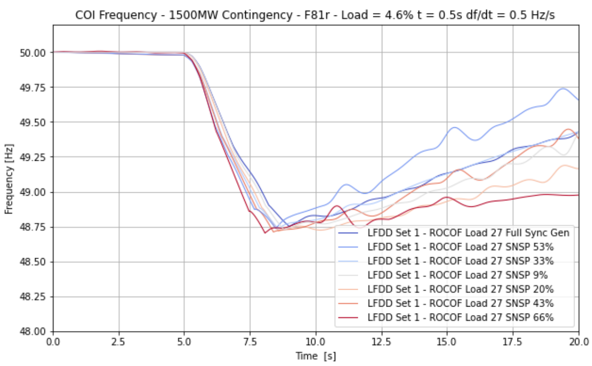

(b) Proactive ROCOF-Based Disconnection Active - 1500MW Contingency.

Figure 6.12: Frequency Plot - 1500MW Contingency - Comparison of frequency deviation using traditional LFDD with and without proactive ROCOF-based disconnection.

In Figure 6.12a, the expected frequency trajectory based on the traditional LFDD scheme is observed.

The most severe frequency decline is seen in the highest RES penetration scenarios and therefore more load is shed in these scenarios to achieve system recovery. In Figure 6.12b, the scenarios are not arranged in the same order. During plotting, the legend is automatically ordered based on minimum frequency, the scenario at the bottom of the legend is the plot with the lowest frequency nadir. As this suggests, when the ROCOF-based protection is activated, the frequency decline is halted more rapidly than when there is no proactive load shedding, resulting in the minimum frequency value being higher for some scenarios in which the ROCOF relay activates, despite having less inertia on the system.

It can be seen from Table 6.8 that the ROCOF relay is activated in the four scenarios with the lowest inertia level. This is expected as these are the scenarios with higher ROCOF. In these simulatinos, the ROCOF relay was set with a threshold of 0.5Hz/s, a value which is not seen in the high inertia scenarios for an event of this magnitude. Due to the settings applied to the ROCOF based protection relay, the added load shedding is only activated in the scenarios where the ROCOF is most severe. In the scenarios where the ROCOF value experienced by the system is lower, the traditional LFDD scheme acts as normal and the system recovery is as expected. This suggests that proactive ROCOF-based protection could be useful in avoiding over-shedding when traditional LFDD is sufficient to restore the frequency. In addition, using ROCOF-based protection, more load can be shed proactively in situations where a more severe frequency deviation is expected, due to low system inertia or high contingency event size. Oscillations induced by proactive disconnection of loads can be seen in all plots in Figure 6.13. To minimise this effect and maintain a smooth frequency trajectory, ROCOF-based protection relays should be placed at locations in the network where system strength is high, in a similar manner as described in section 6.2.

6.4.2. Effect of Changing ROCOF Threshold

In this section, the effect of changing the ROCOF threshold setting on the ROCOF protection relay is explored. To focus on the effect of changing this parameter, the load size and definite time delay parameters are kept constant for all simulations in this section. In practice, the ROCOF threshold setting could be chosen based on simulations carried out on a network model or based on historical data from real events. In either case, it is possible to choose a ROCOF value that enables the relay to act only when severe frequency deviation is expected.

Frequency plots of the system response to a 1000MW event for three distinct ROCOF threshold settings are displayed in Figure 6.13. Details regarding tripping of the ROCOF-based protection and associated trip time for each threshold setting are shown in Table 6.9.

Table 6.9: Comparison of trip times of ROCOF-based relay for various RES penetration levels and ROCOF threshold values.

Scenario	**Trip Time**		
	df/dt = 0.2Hz/s	**df/dt = 0.3Hz/s**	**df/dt = 0.4Hz/s**
Full Sync Gen	6.45	No Trip	No Trip
SNSP 9%	6.30	No Trip	No Trip
SNSP 20%	6.30	6.61	No Trip
SNSP 33%	6.30	6.55	No Trip
SNSP 43%	6.30	6.53	No Trip
SNSP 53%	6.30	6.47	No Trip
SNSP 66%	6.30	6.30	No Trip

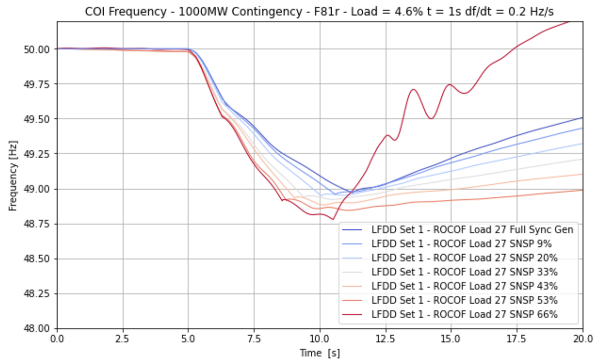

(a) ROCOF Threshold = 0.2Hz/s.

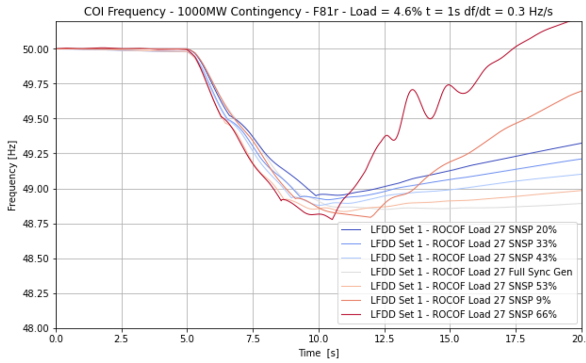

(b) ROCOF Threshold = 0.3Hz/s.

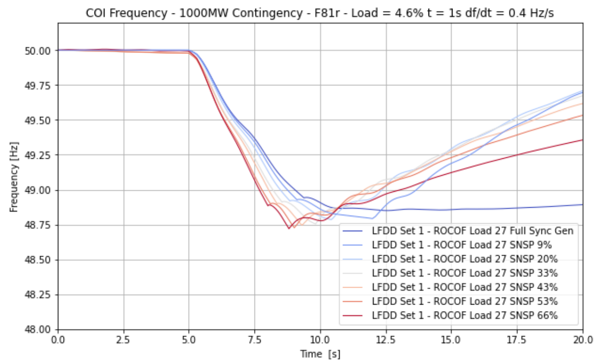

(c) ROCOF Threshold = 0.4Hz/s.

Figure 6.13: Frequency plot for 1000MW Contingency event. Comparison of frequency trajectories based on three different ROCOF threshold settings for ROCOF relay.

Using a lower ROCOF threshold value, such as the 0.2Hz/s value shown in the plots of Figure 6.13a, results in the ROCOF-based protection activating in all scenarios and shedding extra load before 49Hz. It can be seen in Table 6.9 that the trip time for all scenarios outside the full sync gen scenario is the same for this low threshold. This could be because the ROCOF in response to this event reached 0.2Hz/s quickly regardless of inertia level.

Increasing the ROCOF threshold to 0.3Hz/s results in the ROCOF-based protection remaining inactive in the two highest inertia scenarios. It can be seen from the frequency plots in Figure 6.13b that the frequency decline is still effectively halted in scenarios where the ROCOF relay does not activate. In this configuration, the frequency nadir of the lower inertia scenarios is higher than that of the high inertia scenarios due to the difference in load shedding amount.

Increasing the ROCOF threshold to 0.4Hz/s results in no activation of the ROCOF relay for this event, regardless of inertia level. In this scenario, the traditional LFDD scheme acts as normal to enable the system to recover. It can be seen from the plots that the frequency nadir is lowest in this scenario as there is no proactive disconnection before the frequency breaches the 49Hz threshold. However, they are still able to effectively recover front the event, highlighting that proactive disconnection may not be required for this particular event size.

6.4.3. Effect of Changing Load Size for ROCOF Disconnection

In this section, the effect of changing the size of the load which is proactively disconnected from the overall LFDD performance is analysed. In a practical application, the ideal load amount to be disconnected could be computed based on simulations of a network and the required value could be reached by adding ROCOF-based protection to specific consumers until the total cumulative shedding amount is reached.

The ROCOF-based protection was applied at three separate loads which comprised 2.3%, 3.7%, and 4.6% of the total load respectively as outlined in table 5.6. Simulations were carried out for an event size of 1000MW with the ROCOF threshold set at 0.3Hz/s and the definite time delay fixed at 1 second. The frequency plots for each load shedding configuration are shown in Figure 6.14.

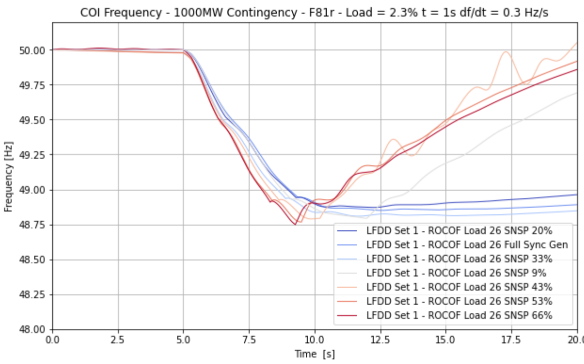

(a) Load Size - 2.3% Peak Load.

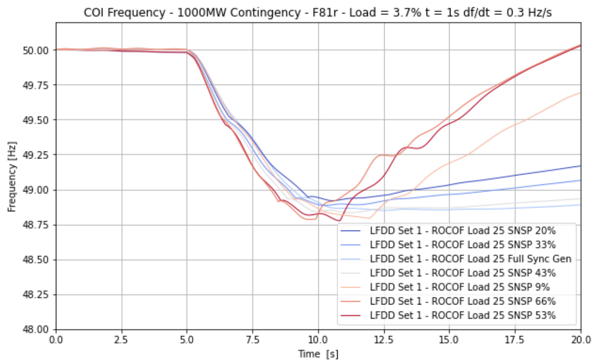

(b) Load Size - 3.7% Peak Load.

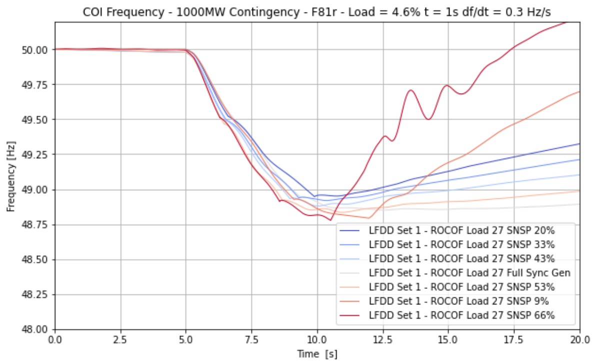

(c) Load Size - 4.6% Peak Load.

Figure 6.14: Frequency plot for 1000MW Contingency event. Comparison of frequency trajectories for three different load amounts to be proactively disconnected by ROCOF relay.

As the contingency event size, ROCOF threshold, and time delay are the same as those in the middle column of Table 6.9, the ROCOF-based protection activates in the same scenarios as in Figure 6.13b. Therefore no change in performance is seen for the SNSP 9% and full sync gen scenarios as the ROCOF-based protection does not activate. Minimum frequency and ROCOF values for these simulations are presented in Table 6.10.

Table 6.10: Effect of load shed by ROCOF-based protection on the minimum frequency and ROCOF values for 1000MW contingency.

	2.3% Peak Load		3.7% Peak Load		4.6% Peak Load	
Scenario	**Min Frequency [Hz]**	**Min ROCOF [Hz/s]**	**Min Frequency [Hz]**	**Min ROCOF [Hz/s]**	**Min Frequency [Hz]**	**Min ROCOF [Hz/s]**
Full Sync Gen	48.849	-0.367	48.849	-0.366	48.850	-0.368
SNSP 9%	48.792	-0.372	48.792	-0.372	48.793	-0.370
SNSP 20%	48.870	-0.395	48.919	-0.394	48.946	-0.392
SNSP 33%	48.808	-0.428	48.885	-0.426	48.919	-0.426
SNSP 43%	48.789	-0.434	48.832	-0.432	48.879	-0.422
SNSP 53%	48.766	-0.473	48.775	-0.477	48.834	-0.469
SNSP 66%	48.748	-0.497	48.784	-0.479	48.777	-0.480

The effect of shedding more or less load using the proactive disconnection is apparent when looking at the frequency nadir and the rate of recovery for each of the cases shown in Figure 6.14. In Figure 6.14c, twice as much load is shed using the ROCOF relay than is shed in Figure 6.14a. As a result, the frequency nadir, particularly in the high inertia scenarios is higher as system recovery is accelerated due to the extra load being shed. It can be seen that shedding extra load using ROCOF protection could potentially result in overshoot and over-frequency complications as the system recovers from a contingency.

It is apparent that the amount of load shedding associated with proactive disconnection should be chosen to assist the system in arresting frequency decline and accelerating system recovery without posing the risk of overshooting and creating instability during system recovery.

6.4.4. Effect of Changing Definite Time Delay

As discussed in section 5.4, the ROCOF protection relay used in this project is the standard F81r relay available in Power Factory. This relay has definite time characteristics meaning that the relay will open the circuit breaker if the ROCOF breaches the threshold value and stays above the threshold for a specified period of time.

The effect of changing the definite time delay of the ROCOF-based protection on frequency trajectory following a 1000MW contingency event is analysed in this section. Figure 6.15 displays the frequency plots for the three separate cases. In all cases, the ROCOF threshold and load shedding amount are kept constant. Details of ROCOF relay tripping and associated trip time for each simulation are presented in Table 6.11

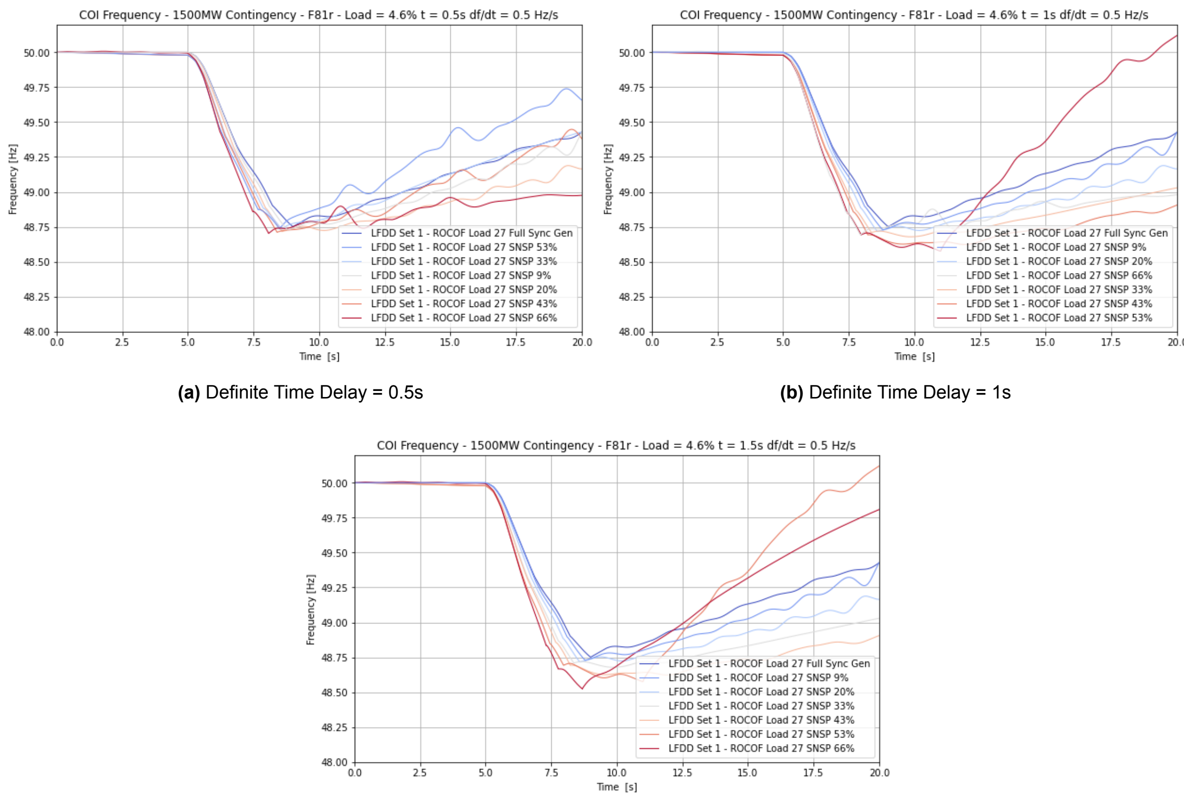

(a) Definite Time Delay = 0.5s

(b) Definite Time Delay = 1s

(c) Definite Time Delay = 1.5s

Figure 6.15: Frequency plot for 1000MW Contingency event. Comparison of three different load amounts to be proactively disconnected by ROCOF relay.

It can be seen from the values in Table 6.11 that a smaller time delay means the ROCOF-based protection is more likely to activate, particularly for lower inertia scenarios. As expected, increasing the definite time delay results in the ROCOF-based protection activating in fewer simulations. If the time delay is increased, it is possible that the ROCOF value still breaches the specified threshold, however, it does not stay above that value for a sufficient length of time to activate the protection relay.

Using this information, a combination of ROCOF and time delay settings could be used to set the ROCOF-based protection to still be sensitive to lower ROCOF values but allow the high inertia systems time to recover independently before shedding the extra load.

Table 6.11: Comparison of ROCOF protection trip times with various definite time settings.

Scenario	ROCOF Relay Trip Time		
	Tdef = 0.5s	Tdef = 1s	Tdef = 1.5s
Full Sync Gen	No Trip	No Trip	No Trip
SNSP 9%	No Trip	No Trip	No Trip
SNSP 20%	No Trip	No Trip	No Trip
SNSP 33%	6.444980	No Trip	No Trip
SNSP 43%	6.431362	No Trip	No Trip
SNSP 53%	6.170811	No Trip	No Trip
SNSP 66%	6.225164	6.779573	No Trip

The results presented in this section highlight the potential performance enhancements associated with the addition of proactive ROCOF-based disconnection of consumers before 49Hz. During severe contingencies, proactively disconnecting specific loads at higher frequencies enables the frequency deviation to be halted at a higher value, relieving stress on the system. Correct tuning of settings applied to ROCOF-based protection can ensure this measure is selective to only act during severe events. This selectivity could be useful in systems with varying amounts of inertia depending on seasonal and daily variations in generation and demand. Further details on the performance improvements associated with this measure, in combination with the associated implementations challenges, are provided in section 7.3.

6.5. Adaptive Scheme

A comparison between the existing Dutch LFDD scheme and an adaptive load shedding scheme is carried out in this section. Using an adaptive scheme to make a real-time estimation of power deficit on the system could allow the load-shedding amount to be tailored to each specific event that occurs in the network. In this section, a simple adaptive scheme is used to make an initial assessment of the benefits of this scheme over a fixed scheme, such as the one currently used in the Netherlands.

As described in section 5.5, the adaptive scheme calculates an estimated power deficit on the system based on ROCOF following an event and using the system inertia at that instant. A decision on the amount of load to shed is made based on the scaling factor applied to the calculated power deficit before assigning the load-shedding actions to the system.

In this analysis, three scaling factors are used in the adaptive scheme to generate three possible responses to a certain event. These factors are 50%, 75%, and 100% and define the percentage of calculated power deficit that the system will shed. In Figure 6.16 frequency plots are shown for a 1000MW contingency event on the system with 9% SNSP at that instant. Results are shown for the adaptive scheme using the three scaling factors. Also shown is the results of the traditional Dutch LFDD scheme for the same event.

The calculated power deficit using the adaptive scheme is presented in Table 6.12. The frequency nadir, minimum ROCOF, and load shed amount are also presented for each adaptive scheme scaling factor and the traditional LFDD scheme in which two trap thresholds are breached. It should be noted that both the legend in the figures for this section and the rows in the tables are ordered based on frequency nadir. In both cases, the scenario with the lowest minimum frequency is placed at the bottom of the list.

This can be used as a quick reference to understand the relative performance of LFDD schemes.

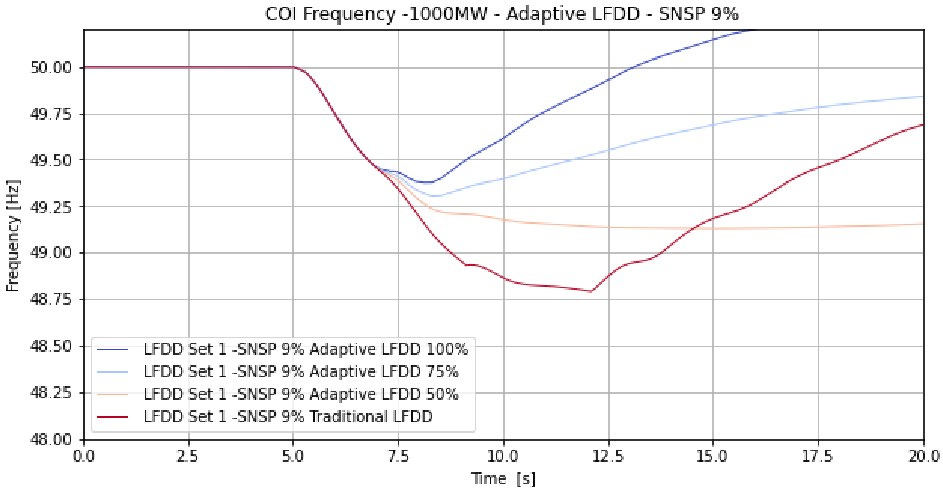

Figure 6.16: Frequency Plot - 1000MW Contingency Event - 9% SNSP - Traditional LFDD Scheme compared with adaptive scheme and with varied load shedding amounts

Table 6.12: Comparison between Adaptive Load Shedding Scheme and Traditional Dutch LFDD Scheme for 1000MW contingency event during SNSP 9% Scenario.

Scenario	Event Size (MW)	Estimated Power Deficit (MW)	Min Frequency [Hz]	Min RoCoF [Hz/s]	Load Shed (MW)
SNSP 9% Adaptive LFDD 100%	1000	1153	49.376	-0.380	1153
SNSP 9% Adaptive LFDD 75%	1000	1153	49.305	-0.380	865
SNSP 9% Adaptive LFDD 50%	1000	1153	49.130	-0.380	577
SNSP 9% Traditional LFDD	1000	N/A	48.790	-0.380	964

It can be seen both in the graph of frequency trajectory and from the minimum frequency results that the adaptive scheme is effective in reducing the frequency nadir in comparison with the traditional LFDD scheme. This effect is expected as the adaptive scheme is designed to begin shedding load when the frequency drops below 49.5Hz while the traditional LFDD does not activate until frequency reaches 49Hz. Shedding 100% of the estimated power deficit is the most effective in arresting frequency decline. Min frequency results in Table 6.12 shows a frequency nadir of 49.38Hz when the scaling factor is 100% versus a nadir of 49.13Hz when the scaling factor is 50%. At this inertia level, all three adaptive scheme iterations show improved performance in comparison to the traditional scheme in reducing the frequency deviation following the contingency event.

At this inertia level, the adaptive scheme calculates an estimated power deficit of 1153MW for an event size of 1000MW. This calculation is considered reasonable for the purpose of this study as a simple equation is used to calculate power deficit on the system. A more accurate power deficit estimation could be achieved by accounting for the effect of IBRs and other system controls in the response of the system, however, this is outside the scope of this project.

It can be seen that the scale factor of 100% results in load shedding greater than the original power imbalance. This is evident in Figure 6.16 as the frequency plot for this scale factor is seen to recover and increase beyond 50Hz, resulting in potential overshoot and over-frequency issues for the system. In the case of this event size and inertia level, it appears that shedding 75% of the estimated load is the most effective response. Using this scale factor, the frequency nadir is just over 0.5Hz higher than that for the traditional scheme while also shedding less load to achieve this response.

A similar comparison as the one shown above was completed for a lower inertia scenario. A simulation based on the same event size, 1000MW, and the same adaptive scheme scaling factors was carried out. Frequency trajectories for the three adaptive scheme simulations and the traditional LFDD are shown in Figure 6.17. Load shedding amounts, minimum frequency and ROCOF values, and the estimated power deficit for the SNSP 66% network configuration are presented in Table 6.13. In both Figure 6.17 and Table 6.13, the scenario with the lowest frequency nadir is shown at the bottom of the legend.

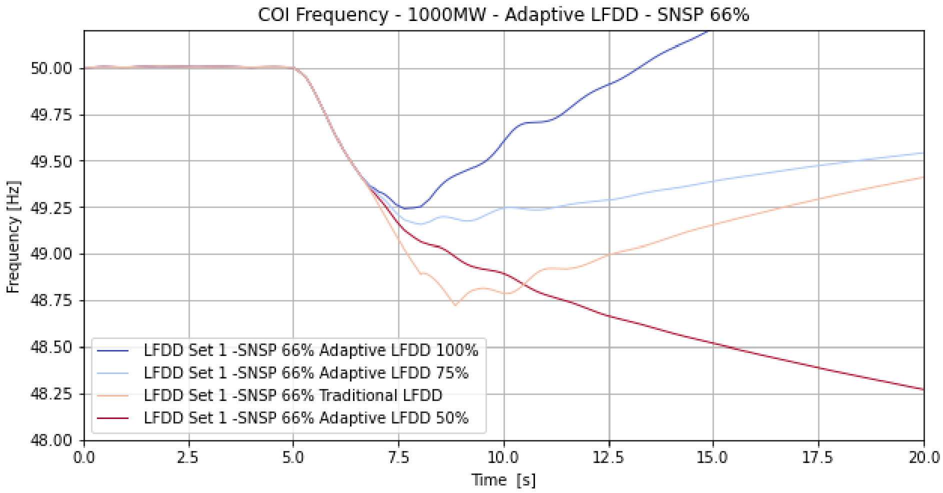

Figure 6.17: Frequency Plot - 1000MW Contingency Event - 66% SNSP - Traditional LFDD Scheme compared with adaptive scheme and with varied load shedding amounts

Table 6.13: Comparison between Adaptive Load Shedding Scheme and Traditional Dutch LFDD Scheme for 1000MW contingency event during SNSP 66% Scenario.

Scenario	Event Size (MW)	Estimated Power Deficit (MW)	Min Frequency [Hz]	Min RoCoF [Hz/s]	Load Shed (MW)
SNSP 66% Adaptive LFDD 100%	1000	1140	49.241	-0.482	1140
SNSP 66% Adaptive LFDD 75%	1000	1140	49.156	-0.482	855
SNSP 66% Traditional LFDD	1000	N/A	48.721	-0.482	964
SNSP 66% Adaptive LFDD 50%	1000	1140	48.271	-0.482	570

In a similar manner to the system with 9% SNSP, in this lower inertia scenario the adaptive scheme is more effective in arresting the frequency decline and maintaining the frequency nadir above 49Hz.

The power deficit is estimated to be 1140MW at this inertia level which is slightly closer to the actual contingency event size than the calculation for the higher inertia system. The overshoot effect of using the adaptive scheme with 100% scaling factor is more pronounced in Figure 6.17, possibly due to the lower system inertia and a higher sensitivity to changes in load on the system.

The primary difference between the response of the adaptive scheme in both inertia levels is the effect of shedding 50% of the estimated power deficit. In the case of higher system inertia, shedding this smaller amount of load can still be effective in arresting the frequency decline and beginning the recovery of the system. In the lower inertia system, shedding 50% of the estimated power deficit is ineffective in stopping the frequency decline and the system does not recover from the contingency event in this scenario as shown in Figure 6.17. The varying responses of the high and low inertia systems suggest that a specific scaling factor could be used to determine the optimum amount of load to be shed based on inertia level.

In this chapter, results are presented and discussed for the performance analysis of the five proposed improvements to the existing Dutch LFDD scheme, outlined in chapter 5. It is clear that all improvements exhibit enhanced performance compared to the existing Dutch LFDD scheme. Results shown in section 5.2 and section 6.1 indicate that improving LFDD load selection criteria by accounting for system strength and active DER generation at LFDD locations reduces oscillations in frequency response following LFDD switching actions and ensures the desired load amount is successfully shed for all operating scenarios. Enhanced performance in halting frequency decline and optimising load shedding amount for all contingency event sizes and RES penetration levels is seen in the three alternative LFDD measures described in section 6.3, section 6.4 and section 6.5. Implementing a range of fixed LFDD schemes, selected in advance based on predicted inertia level, with varying load distribution can provide improved response for all system operating scenarios. Introducing proactive ROCOF based protection in conjunction with the existing LFDD scheme can improve performance for severe contingencies while avoiding unnecessary extra load shedding for smaller disturbances. Implementing an adaptive load shedding scheme with online power deficit estimation can ensure the optimal load shedding amount for each contingency while also enabling shedding to begin at frequencies above 49Hz. A detailed overview of the benefits associated with each improvement method, in combination with the technical, implementation and legislative challenges associated with implementing these proposed improvements is given in chapter 7.

7

Consolidation of LFDD Improvements

In this section, the primary findings for each discussed improvement to traditional LFDD are consolidated. The primary benefits of each method are discussed in conjunction with the associated challenges from a technical, legislative, and implementation perspective.

Improvement	Grid Code Compliance	Complexity	Effect
LFDD Location Selection Criteria – System Strength	Complies with Dutch an EU Grid codes	• Calculation of min SC power for each inertia level. • LFDD scheme adapted to shed load at strongest buses	• Improved system stability following LFDD
LFDD Location Selection Criteria – DER Generation	Complies with Dutch an EU Grid codes	• Predicted DER generation info • Pro-active change to LFDD • Avoid shedding locations with high DER gen	• Avoid negative effect of tripping DERs with high generation. • Ensure LFDD responds as expected.
Proactive Disconnection of Consumer before 49Hz – Based on high ROCOF	Complies with EU Grid code	• Agreements with customers required. • Agreements needed between all TSOs on CES • Tune desired settings for ROCOF relay to trip for severe events.	• Reduce frequency nadir for most severe cases. • Early action promotes faster system recovery.
Alternative Thresholds – Non-equal Load distribution	Complies with EU Grid code	• Possibility of multiple different traditional LFDD schemes • Agreements needed between all TSOs on CES • Change based on inertia level *e.g. – Shed more load in Trap 1&2 when inertia is low*	• Smaller thresholds – reduced over / under shedding. • Possibility of multiple LFDD load distributions to be selected in advance based on inertia level
Adaptive Scheme – Real time Power deficit estimation	Does not currently comply	• Real time power deficit calculation + Load shedding decision • Investigation needed into local control – avoid communication and central controller	• Adaptive scheme – shed ideal amount of load for each event size and inertia level – • Reduce frequency nadir – promote faster system recovery

Figure 7.1: Overview of main points regarding proposed improvements to LFDD.

7.1. Load Selection Criteria: Network Strength

- **Associated Performance Improvements:** Focusing LFDD bus selection on areas with higher fault levels improves voltage and frequency stability following the sudden load changes associated with LFDD switching. Resulting in a more stable trajectory back to nominal frequency and voltage levels.

- **Technical Challenges:** Due to changing topologies and varying inertia levels associated with intermittent renewable energy generation, stronger and weaker locations in the network can vary.

It could be necessary to perform system strength calculations based on a number of commonly used system topologies and generate an LFDD scheme to shed load at the strongest buses for each system configuration. Choosing which LFDD scheme to implement would require forecasted information on the expected topology, possibly a day ahead.

- **Implementation Challenges:** Changing LFDD schemes in real-time (or one day ahead if DER generation forecasts are available) could require extensive communication between TSO's to ensure coordination of protection measures is maintained throughout the European grid.

- **Legislative Challenges:** Changes to LFDD bus locations can be carried out while adhering to the Dutch grid code and maintaining 7.5% peak load in each trap setting. No severe legislative challenges are apparent for this improvement method.

7.2. Load Selection Criteria: Loadside DER Generation

- **Associated Performance Improvements:** Avoiding disconnection of active DERs during LFDD ensures the power balance is restored as efficiently as possible to enable a faster system recovery.

- **Technical Challenges:** Real-time information on expected DER generation at each LFDD location would be required. Alterations to LFDD bus selection would be required based on predicted DER generation. A control algorithm would need to be implemented to automate the LFDD bus selection updates based on the selected time interval.

- **Implementation Challenges:** Changing LFDD schemes in real-time (or one day ahead if DER generation forecasts are available) could require extensive communication between TSO's to ensure coordination of protection measures is maintained throughout the European grid.

- **Legislative Challenges:** Changes to LFDD bus locations can be carried out while adhering to the Dutch grid code and maintaining 7.5% peak load in each trap setting. No severe legislative challenges are apparent for this improvement method.

7.3. Proactive ROCOF-Based Disconnection before 49Hz

- **Associated Performance Improvements:** Reduction of frequency deviation during severe contingency events by proactively disconnecting load before frequency reaches 49Hz. ROCOF Relay settings can be tuned to only activate for severe events, allowing protection to be sensitive to large contingencies or low inertia situations while avoiding over-shedding for small contingencies or when system inertia is high.

- **Technical Challenges:** Detailed investigation and simulations would be required to determine the optimum settings for ROCOF-based protection. It may be necessary to combine a frequency and ROCOF threshold for proactive disconnection to provide proactive protection for situations where ROCOF is low (due to high inertia) but the power imbalance is large and thus a high-frequency deviation is expected.

- **Implementation Challenges:** Specific agreements would be required with consumers to become "Defence Service Providers" to enable disconnection according to specific requirements. Any agreements for disconnection before the action of LFDD would need to be communicated with all European TSO's to ensure coordination throughout the network.

- **Legislative Challenges:** The European grid code does contain legislation to enable consumers to be proactively disconnected based on ROCOF. This is not present in the Dutch grid code, therefore some amendments may be needed to the Dutch grid code to allow these proactive measures to be implemented.

7.4. Alternative Load Distribution in LFDD

- **Associated Performance Improvements:** The availability of multiple traditional LFDD schemes with varying load distribution could improve system response and recovery, particularly as inertia levels in the system are expected to vary in the future. Shedding more or less load in the beginning thresholds can reduce frequency nadir for severe events and low inertia system configurations or avoid over-shedding for smaller events and higher inertia system configurations.

- **Technical Challenges:** Further investigation would be required to determine how many alternate LFDD schemes should be developed and the criteria under which each scheme would be selected. A controller would be required to select between alternate schemes in advance based on forecasted inertia level or in real-time based on ROCOF or a power deficit estimation.

- **Implementation Challenges:** Any changes to LFDD load distribution would need to be communicated with all European TSOs to enable coordination throughout the system. It is possible that some alternate LFDD schemes could be unacceptable due to coordination requirements throughout the CESA grid.

- **Legislative Challenges:** The European grid code provides a percentage range of load to be included in each trap threshold and only specifies the beginning and end frequency for LFDD actions to occur. The Dutch grid code requires 6 trap thresholds, each with 7.5% peak load. Amendments to the Dutch grid code could be required to enable the implementation of alternate LFDD schemes.

7.5. Adaptive Load Shedding

- **Associated Performance Improvements:** Real-time power deficit estimation allows the ideal amount of load to be shed for each specific event and inertia level of the system. The adaptive scheme can enable load shedding to begin at a frequency above 49Hz, thus reducing frequency deviation and accelerating system recovery.

- **Technical Challenges:** An accurate power deficit estimation in a system with high IBRs and active loads would require detailed investigation to ensure the robustness of the LFDD scheme. Implementation of a centrally controlled adaptive scheme would require extensive communication which could make the scheme more vulnerable from a security perspective. Local implementation of adaptive load shedding is complex but could be effective following research and development.

- **Implementation Challenges:** Changing LFDD schemes away from traditional fixed thresholds and moving to an adaptive scheme would require coordination throughout the European network. This would require extensive collaboration between TSOs as well as possible hardware upgrades on LFDD relays installed in the network to enable local implementation of intelligent controls.

- **Legislative Challenges:** There is no legislation currently in the European or Dutch grid code to enable active, real-time power deficit estimation and load shedding before 49Hz. Implementation of an adaptive load-shedding scheme in the European system would require considerable policy and legislative changes.

In this chapter, an overview of the benefits and possible challenges to the implementation of the proposed improvements to LFDD is presented. This overview is used to generate conclusions and recommendations and answer the research questions posed in chapter 1. Conclusions and recommendations for continuation of this research are presented in chapter 8 and chapter 9 respectively.

8 Conclusion

This research was initialized in light of the anticipated increase in inverter-based resources in the Continental European Synchronous Area network and the subsequent reduction in rotational inertia and inherent stability of the power system. As a result of these changes, it is possible that existing system defence measures will be insufficient to arrest frequency decline and avoid cascading loss of generation should a severe contingency event, such as the 2021 system slitting events discussed in section 1.2.4, occur in the future. The purpose of this research is to investigate, firstly, the effect of increased penetration of renewable energy on post-contingency power system dynamics and, subsequently, the corresponding effect on the performance of the existing underfrequency system defence measures. Findings from this initial research phase are then used to develop potential improvements to existing defence measures which should increase system resilience to contingency events and reduce the risk of cascading disconnections and blackouts. To achieve this goal, a test grid network was used in which operating scenarios with increasing penetrations of renewable generation were created. Loss of generation contingency events of different magnitudes were simulated and the corresponding frequency trajectory was observed based on the activation of a variety of load-shedding schemes. To consolidate the findings of this research, the following research questions can be answered:

- *How does the increased penetration of inverter-based resources influence power system frequency trajectory during large-scale disturbances, such as generation loss?*

Higher penetration of inverter-based resources results in less available rotational inertia on the grid. As discussed in section 4.2, increased penetration of RES generation results in higher frequency deviation and greater ROCOF magnitude following a contingency event. As expected, increased contingency size results in higher ROCOF and greater frequency deviation for a given system inertial level. Results indicate that the effect of a larger contingency size on frequency and ROCOF is increased for systems with higher penetration of renewable generation sources. Consequently, the potential for contingency events to cause severe frequency oscillations and deviations beyond the safe threshold is increased as more IBRs are added to the network.

- *To what extent does the increased proliferation of renewable generation affect the efficacy of current frequency defence measures implemented on the grid?*

The primary deficiency associated with the existing Dutch LFDD scheme is the inability to shed the optimal load amount for a given contingency event size and RES penetration level. Incorrect load shedding amount can lead to undesired damages and costs to the system [39]. As discussed in chapter 4, higher RES penetration and lower system inertia result in a deeper frequency nadir following a loss of generation event. Consequently, in lower inertia scenarios, more load is shed by the existing LFDD scheme to arrest frequency decline as more frequency thresholds are breached. The result of this excess load shedding is the potential for frequency to overshoot and create further operational challenges.

Secondly, increased penetration of distributed energy resources on the grid poses the risk of LFDD actions being insufficient to restore power balance and stop frequency decline following an event. Currently, as outlined in subsection 3.6.1, the Dutch LFDD scheme does not account for active DER generation at locations where LFDD load-shedding actions could take place. Results presented in section 6.1 indicate that a DER generation level of 25% of the local load demand at that substation can reduce the efficacy of LFDD in arresting frequency decline. Unintentional disconnection of higher DER generation levels such as 50% or 75% of the associated load can render the LFDD actions ineffective and, in the case of severe contingencies, result in system collapse.

- *What strategies can be adopted to enhance the performance of the existing frequency defence mechanisms in a lower inertia power system?*

Outcomes from this research indicate that adding additional LFDD load selection criteria could enhance the performance in a system with higher penetration of IBRs. As discussed in section 6.2 understanding system strength at LFDD load shedding locations for different system operating scenarios and choosing to shed load at buses with the highest fault levels could reduce oscillations following switching events and improve frequency and voltage stability during system recovery.

Further expanding load selection criteria to include real-time or predicted DER generation levels at buses where LFDD is available, as presented in section 6.1, could ensure adequate load shedding following contingency events in a power system with widespread distributed generation. It is anticipated that the existing condition related to DER generation, in which a substation is exempt from LFDD if it is feeding power back to the transmission system more than 20% of the year, may be insufficient to avoid disconnection of active DER generation in the future power system. It is possible to predict, with reasonable accuracy, the level of renewable generation from wind and solar one day in advance based on weather data and electricity demand patterns. Using this information to avoid LFDD actions at locations where DER generation is high can ensure the desired cumulative load shedding amount is reached in the event of a contingency, therefore effectively restoring power balance to the system.

- *What are some alternative approaches to frequency defence measures that could be implemented outside of existing measures? Do these exhibit enhanced performance within the future power system?*

Alternative approaches to LFDD explored in this thesis include: (i) Additional proactive ROCOF-based disconnection of consumers at frequencies above 49Hz, (ii) Alternative fixed LFDD schemes with non-equal load distributions and (iii) the use of an adaptive load shedding scheme incorporating real-time power deficit estimation. Results indicate that each of the alternative methods shows improved performance in comparison with the existing Dutch LFDD scheme, particularly for a power system with varying inertia levels.

Introducing proactive ROCOF-based disconnection in the manner discussed in subsection 6.4.2 can enable frequency decline to be halted more quickly for severe contingency events by disconnecting a pre-defined amount of load before the frequency reaches 49Hz. Although LFDD actions may still take place, the frequency decline is halted at a higher value than without proactive disconnection. Employing ROCOF-based protection enables a level of selectivity that is not possible with standard frequency thresholds currently in use. During smaller contingency events, disconnection of additional load can be avoided by setting ROCOF relay thresholds to a value only seen during more severe contingencies. This creates an additional protection stage that acts only for the most severe contingency events or during the lowest inertia operating scenarios.

Improved adaptability to the changing system operating conditions in a future power system can be achieved through alteration of the load distribution within the traditional LFDD scheme. Section 6.3

describes the benefits associated with non-equal load distribution in LFDD thresholds. Results indicate that employing a range of LFDD schemes with varied load distribution, which can be selected in advance based on predicted system inertia, can result in more appropriate amounts of load being shed for each contingency. Consequently, the overshedding and undershedding challenges seen with the traditional, evenly distributed, LFDD scheme used in the Netherlands are reduced. During high inertia scenarios, less load can be placed in the early threshold settings as the system has a higher inherent resilience to disturbances. During low inertia scenarios, when the system is more vulnerable, more load can be placed in the early threshold settings to ensure frequency decline is successfully halted before cascading loss of generation occurs.

Outcomes from this research indicate that an adaptive load shedding scheme, such as the one described in section 6.5, can best account for the changing inertia levels and contingency event magnitudes in the future power system. Implementing a real-time power deficit estimation, in conjunction with a load-shedding scaling factor based on system inertia at the moment of an event, can ensure the optimal load-shedding amount is disconnected for all contingencies. Furthermore, as the severity of an event can be known quickly (<500ms) based on ROCOF following an event, load-shedding actions can take place before the frequency has reached 49Hz, ensuring the frequency decline is less severe than it might be using the existing LFDD scheme. As the load shedding amount would be adapted for each specific event, proactive disconnection can take place before 49Hz without the potential for overshoot associated with other non-adaptive methods.

- *Among the proposed enhancements and alternatives to current system defence mechanisms, which solutions are the most applicable for implementation within the Continental European Synchronous Area?*

The addition of ROCOF-based disconnection for specific consumers, known as ”Defence Service Providers” in the European power system, is a promising improvement to the existing LFDD scheme as this measure falls within the existing European grid code. The ability to apply settings to make this defence measure selective and only act for severe contingencies is appropriate for a large network such as the CESA where the transition to a low inertia system will take a number of years these additional measures may not be immediately necessary. The adaptive scheme is the most effective in terms of LFDD performance in a power system with varying levels of rotational inertia. However, the high level of complexity in terms of communication requirements, online calculations, and central control results in this being a difficult scheme to implement in the CESA given the existing grid code requirements and the need for homogeneity in defence measures across all transmission system operators.

The inclusion of system strength at LFDD load shedding locations as an extra load selection criterion could enhance the performance of LFDD without requiring major changes to the operation of the scheme. As described in section 6.2, performing network strength calculations based on the lowest conceivable inertia scenario and choosing to shed load at the strongest locations based on these results could ensure a more stable response to contingency events in all operating scenarios. Currently, in the existing Dutch grid code, there are no requirements for load selection beyond the requirement of 7.5% peak load in each threshold. Choosing to shed loads at the strongest buses can be achieved while still adhering to these existing requirements.

The results of this work successfully answer the research questions posed and highlight the potential effects of increased penetration of IBRs and reduced rotational inertia on the system on the performance of the Dutch emergency load shedding scheme. Proposed improvements to the existing frequency defence measures can be categorised into two main areas: (i) Improvements to load selection criteria for the existing LFDD scheme & (ii) Alternative load shedding schemes to improve performance in low inertia systems. Enhanced performance, including reducing frequency deviation, enabling a stable frequency recovery following switching actions, and ensuring the desired load amount is successfully disconnected are benefits associated with the proposed improvements. Findings indicate that improving load selection criteria by adding parameters such as network strength and active DER generation at load-shedding locations can improve the robustness of the existing Dutch LFDD scheme. Finally, alternative methods such as the addition of proactive ROCOF-based protection, utilising an adaptive load shedding scheme, or developing a range of fixed schemes with varying load distribution can ensure frequency decline is halted successfully for large contingency events while avoiding overshedding for smaller contingencies. Results indicate that improved performance of LFDD can be achieved within the constraints of the existing European grid code while some measures, such as the introduction of an adaptive scheme, would require policy changes and widespread collaboration between TSO's prior to successful implementation. Recommendations for the continuation of the work presented in this report and areas of research related to the practical implementation of proposed improvements are given in chapter 9.

9
Recommendations for Future Work

In this chapter, recommendations for future research into the improvement of load-shedding schemes for critical system conditions in the CESA are presented. The points outlined in this chapter can be used as a basis to build on the research carried out in this project and also as a guide to move towards practical implementation and validation of chosen improvements to LFDD.

9.1. Recommendations: Continuation of Overall Research

- The research in this project could be transferred to a larger, more detailed network model, potentially one that accurately depicts part or all of the CESA. A more detailed model will enable a more realistic representation of the expected frequency trajectory following contingency events in the future European power system, enabling more definitive conclusions to be drawn on the benefits of implementing the various improvements proposed in this thesis. In this more expansive network model, a detailed representation of the active power response of non-synchronous generators could be developed to provide more detail on the behaviour of these units during large-scale contingency events.

- Detailed investigation should be undertaken into the technical and legislative challenges associated with implementing any chosen improvement to LFDD in a real-world power system. Further details are provided in later sections, however, it is important to understand which improvements can most readily be implemented given the technical and legislative constraints in the CESA today. It is possible that research could be divided into two sections, improvements that could be implemented in a short timeframe and improvements that require longer-term technical and legislative developments prior to implementation.

- Detailed modelling of the networks downstream from LFDD substations could provide greater information regarding system response to LFDD switching actions. In this research, downstream networks from LFDD substations are represented as static loads. Detailed modelling of downstream DER generation and dynamic loads could provide further insight into the effect of both disconnections of active DERs and network strength on the overall performance of LFDD defence measures.

9.2. Recommendations: Load Selection Criteria

- As mentioned above, the effect of network strength at LFDD load-shedding substations could be investigated using models containing detailed depictions of the network downstream from LFDD substations. The effect of disconnecting downstream networks with high or low penetration of IBRs on the evolution of overall strength in the system should be considered. In this project, consideration is given only to the ability of the substation bus to withstand frequency and voltage oscillations following switching actions. Consideration should be given to the evolution of overall system strength as load-shedding actions take place.

- To implement additional selection criteria in the existing LFDD algorithm for load bus selection is a technical challenge that requires further investigation. Resources could be dedicated to understanding the requirements needed to expand the functionality of the existing LFDD scheme to include system strength. Initially, system strength calculations from one chosen inertia level could be utilised. If successful, this could be expanded to include the adaption of LFDD load bus selection, one or two days in advance, based on system strength calculations for the predicted network operating state.

- Implementing a selection criterion to avoid disconnecting active DER generation during LFDD actions requires detailed information regarding predicted DER generation on the grid. It could be beneficial to investigate the availability of real-time DER generation data and how this can be implemented in an LFDD scheme to avoid selecting feeders with active DER generations for shedding. It is anticipated that it will be possible to avoid disconnection of large-scale MV DER generation in future scenarios as LFDD relays are in the process of being applied to outgoing feeders at LFDD substations. Therefore it would be useful to quantify the voltage level and DER plant size at which the ability to exclude this DER from the LFDD scheme stops. In doing so, the stability risks associated with disconnecting active DERs can be properly quantified.

9.3. Recommendations: Alternative LFDD Measures

- Research should be carried out into the practical and legislative requirements to employ a range of LFDD schemes with alternative load distributions. Functionalities such as remote updates of LFDD relays and forecasting of system inertia should be investigated to determine whether switching between a range of schemes is a viable option given the existing European grid code and the technical capabilities of system components.

- Detailed modelling of a wider range of contingency event sizes and associated frequency trajectories should be carried out on a model of the Dutch system. This analysis could provide estimates of the ROCOF values that define severe events in which proactive disconnection of consumers before 49Hz would be required. This would enable the determination of settings that could be applied to ROCOF-based protection relays. In conjunction with this, information could be gathered on the amount of load which should be associated with proactive disconnection to ensure this measure will be effective should they be implemented in the CESA.

- Research could be undertaken into the inclusion of frequency threshold settings in combination with ROCOF threshold settings for relays associated with proactive disconnection. The addition of frequency thresholds would be useful in the event of a large contingency happening during a high inertia operating scenario. In this case, the measured ROCOF may not be high enough to trip the proactive disconnection but, due to the amount of generation loss, the frequency deviation may still breach desired thresholds. It may be useful to employ additional threshold settings or investigate the possibility of estimating power deficit and using this value to issue trip commands to proactive disconnection relays.

- Local implementation of an adaptive load shedding scheme, such as the one described in [35], could provide a promising pathway to introducing more intelligent load shedding schemes to the CESA. Research into this could be completed by implementing an integrated relay model in Powerfactory which can perform real-time power deficit estimation based on local frequency measurements and subsequently make a calculation on load shedding amount. As the use of central controllers and complex communication is undesirable for emergency defence measures in a large-scale power system, local implementation of adaptive schemes could enable a sophisticated load-shedding scheme without diminishing security and robustness.

References

[1] WORLD METEOROLOGICAL ORGANIZATION. *Global Annual to Decadal Climate Update*. Tech. rep. 2022.

[2] K. Calvin et al. *IPCC, 2023: Climate Change 2023: Synthesis Report. Contribution of Working Groups I, II and III to the Sixth Assessment Report of the Intergovernmental Panel on Climate Change [Core Writing Team, H. Lee and J. Romero (eds.)]. IPCC, Geneva, Switzerland.* Tech. rep. Intergovernmental Panel on Climate Change, July 2023. DOI: `10.59327/IPCC/AR6-9789291691647`. URL: `https://www.ipcc.ch/report/ar6/syr/`.

[3] International Energy Agency. *Renewable Energy Market Update - June 2023*. Tech. rep. 2023. URL: `www.iea.org/t&c/`.

[4] Q. Li et al. *Analyzing the inertia of power grid systems comprising diverse conventional and renewable energy sources*. Nov. 2022. DOI: `10.1016/j.egyr.2022.11.022`.

[5] Iea. *Renewables 2022*. Tech. rep. 2022. URL: `www.iea.org`.

[6] Entso-e. *Completing the map – Power system needs in 2030 and 2040*. Tech. rep. 2021.

[7] ENTSO - E. *Frequency Stability Evaluation Criteria for the Synchronous Zone of Continental Europe-Requirements and impacting factors-RG-CE System Protection & Dynamics Sub Group*. Tech. rep. 2016.

[8] N. Hatziargyriou et al. "Definition and Classification of Power System Stability – Revisited and Extended". In: *IEEE Transactions on Power Systems* 36.4 (2021), pp. 3271–3281. DOI: `10.1109/TPWRS.2020.3041774`.

[9] F. Milano et al. "Foundations and Challenges of Low-Inertia Systems (Invited Paper)". In: *2018 Power Systems Computation Conference (PSCC)*. 2018, pp. 1–25. DOI: `10.23919/PSCC.2018.8450880`.

[10] R. W. Kenyon et al. "Stability and control of power systems with high penetrations of inverter-based resources: An accessible review of current knowledge and open questions". In: *Solar Energy* 210 (Nov. 2020), pp. 149–168. ISSN: 0038092X. DOI: `10.1016/j.solener.2020.05.053`.

[11] ENTSO-E. *Inertia and Rate of Change of Frequency (RoCoF)*. Tech. rep. 2020.

[12] ENTSO-E. *High Penetration of Power Electronic Interfaced Power Sources and the Potential Contribution of Grid Forming Converters*. 2020. URL: `www.entsoe.eu`.

[13] P. Anderson and A. Fouad. *POWER SYSTEM CONTROL AND STABILITY, 2ND ED*. IEEE Press power engineering series. Wiley India Pvt. Limited, 2008. ISBN: 9788126518180. URL: `https://books.google.nl/books?id=2BXOzA34qBkC`.

[14] D. Nouti, F. Ponci, and A. Monti. "Heterogeneous inertia estimation for power systems with high penetration of converter-interfaced generation". In: *Energies* 14.16 (Aug. 2021). ISSN: 19961073. DOI: `10.3390/en14165047`.

[15] CIGRE. *Impact of High Penetration of Inverter-based Generation on System Inertia of networks*. 2021. ISBN: 9782858735563.

[16] O. J. Ayamolowo, P. Manditereza, and K. Kusakana. "An overview of inertia requirement in modern renewable energy sourced grid: challenges and way forward". In: *Journal of Electrical Systems and Information Technology* 9.1 (Dec. 2022). DOI: `10.1186/s43067-022-00053-2`.

[17] Netbeheer Nederland. *Power-Generating Modules compliance verification Power-Generating Modules type B, C and D according to NC RfG and Netcode elektriciteit*. Tech. rep.

[18] A. Boričić, J. L. R. Torres, and M. Popov. "System Strength: Classification, Evaluation Methods, and Emerging Challenges in IBR-dominated Grids". In: *2022 IEEE PES Innovative Smart Grid Technologies - Asia (ISGT Asia)*. 2022, pp. 185–189. DOI: `10.1109/ISGTAsia54193.2022.10003499`.

[19] M. G. Dozein et al. “System Strength and Weak Grids: Fundamentals, Challenges, and Mitigation Strategies”. In: *2018 Australasian Universities Power Engineering Conference (AUPEC)*. 2018, pp. 1–7. DOI: 10.1109/AUPEC.2018.8757997.

[20] O. Gomis-Bellmunt et al. “Steady-state impedance mapping in grids with power electronics: What is grid strength in modern power systems?” In: *International Journal of Electrical Power and Energy Systems* 136 (Mar. 2022). ISSN: 01420615. DOI: 10.1016/j.ijepes.2021.107635.

[21] A. Borićič, J. L. R. Torres, and M. Popov. “Beyond SCR in Weak Grids: Analytical Evaluation of Voltage Stability and Excess System Strength”. In: *2023 International Conference on Future Energy Solutions (FES)*. 2023, pp. 1–6. DOI: 10.1109/FES57669.2023.10183286.

[22] A. Ketabi and M. H. Fini. “An Underfrequency Load Shedding Scheme for Hybrid and Multiarea Power Systems”. In: *IEEE Transactions on Smart Grid* 6.1 (2015), pp. 82–91. DOI: 10.1109/TSG.2014.2349999.

[23] ENTSO-E. *ENTSO-E Network Code on Emergency and Restoration*. Tech. rep. 2015.

[24] D. Sodin et al. “Proving a concept of flexible under-frequency load shedding with hardware-in-the-loop testing”. In: *Energies* 13.14 (July 2020). ISSN: 19961073. DOI: 10.3390/en13143607.

[25] ENTSO-E. *ENTSO-E Interim Report – Continental Europe Synchronous Area Separation on 8 January 2021*. Tech. rep. 2021.

[26] ENTSO-E. *» Continental Europe Synchronous Area Separation on 24 July 2021 About ENTSO-E*. Tech. rep.

[27] S. Saha, M. I. Saleem, and T. K. Roy. “Impact of high penetration of renewable energy sources on grid frequency behaviour”. In: *International Journal of Electrical Power and Energy Systems* 145 (Feb. 2023). ISSN: 01420615. DOI: 10.1016/j.ijepes.2022.108701.

[28] C. Li et al. “Continuous Under-Frequency Load Shedding Scheme for Power System Adaptive Frequency Control”. In: *IEEE Transactions on Power Systems* 35.2 (Mar. 2020), pp. 950–961. ISSN: 15580679. DOI: 10.1109/TPWRS.2019.2943150.

[29] X. Wu et al. “Adaptive Under-Frequency Load Shedding Control Strategy of Power Systems With Wind Turbines and UHVDC Participating in Frequency Regulation”. In: *Frontiers in Energy Research* 10 (May 2022). ISSN: 2296598X. DOI: 10.3389/fenrg.2022.875785.

[30] U. Rudez and R. Mihalic. *RoCoF-based Improvement of Conventional Under-Frequency Load Shedding; RoCoF-based Improvement of Conventional Under-Frequency Load Shedding*. Tech. rep. 2019.

[31] M. Abedini, M. Sanaye-Pasand, and S. Azizi. “Adaptive load shedding scheme to preserve the power system stability following large disturbances”. In: *IET Generation, Transmission and Distribution* 8.12 (Dec. 2014), pp. 2124–2133. ISSN: 17518695. DOI: 10.1049/iet-gtd.2013.0937.

[32] P. Sorensen and V. Trovato. *Review of defence plans in europe: current status, strengths and opportunities*. Tech. rep. 2016. URL: https://www.researchgate.net/publication/303997007.

[33] P. M. Anderson and M. Mirheydar. “An adaptive method for setting underfrequency load shedding relays”. In: *IEEE Transactions on Power Systems* 7.2 (1992), pp. 647–655. ISSN: 15580679. DOI: 10.1109/59.141770.

[34] J. A. Laghari et al. “Application of computational intelligence techniques for load shedding in power systems: A review”. In: *Energy Conversion and Management* 75 (2013), pp. 130–140. ISSN: 01968904. DOI: 10.1016/j.enconman.2013.06.010.

[35] M. Sun et al. “Underfrequency Load Shedding Using Locally Estimated RoCoF of the Center of Inertia”. In: *IEEE Transactions on Power Systems* 36.5 (Sept. 2021), pp. 4212–4222. ISSN: 15580679. DOI: 10.1109/TPWRS.2021.3061914.

[36] J. C. Cepeda et al. “Probabilistic approach-based PMU placement for real-time power system vulnerability assessment”. In: *IEEE PES Innovative Smart Grid Technologies Conference Europe*. 2012. ISBN: 9781467325974. DOI: 10.1109/ISGTEurope.2012.6465671.

[37] S. You et al. *Calculate Center-of-Inertia Frequency and System RoCoF Using PMU Data*. Tech. rep. 2020. URL: http://fnetpublic.utk.edu/tabledisplay.html.

[38] CIGRE. “Innovation in the Power Systems Industry Towards System Strength”. In: (2021). ISSN: 2426-1335. URL: http://www.cigre.org/Menu-links/.

[39] V. Terzija. “Adaptive underfrequency load shedding based on the magnitude of the disturbance estimation”. In: *IEEE Transactions on Power Systems* 21.3 (2006), pp. 1260–1266. DOI: 10.1109/TPWRS.2006.879315.